İSTANBUL TECHNICAL UNIVERSITY ★ INSTITUTE OF SCIENCE AND TECHNOLOGY

NETWORK PARAMETERS AND SWELLING PROPERTIES OF POLY(N-ISOPROPYLACRYLAMIDE)/MONTMORILLONITE NANOCOMPOSITE HYDROGELS

M.Sc. Thesis by
Deniz TOPUZ, B.Sc.

Department: **Polymer Science and Technology**

Programme: **Polymer Science and Technology**

JANUARY 2008

İSTANBUL TECHNICAL UNIVERSITY ★ INSTITUTE OF SCIENCE AND TECHNOLOGY

NETWORK PARAMETERS AND SWELLING PROPERTIES OF POLY(N-ISOPROPYLACRYLAMIDE)/MONTMORILLONITE NANOCOMPOSITE HYDROGELS

M.Sc. Thesis by

Deniz TOPUZ, B.Sc.

515061009

Date of submission: 24 December 2007

Date of defence examination: 31 January 2008

Supervisor (Chairman) : Prof. Dr. Candan ERBİL (ITU)

Members of the Examining Committee: Prof. Dr. F. Seniha GÜNER (ITU)

Assos. Prof. Dr. B. Filiz ŞENKAL (ITU)

JANUARY 2008

İSTANBUL TEKNİK ÜNİVERSİTESİ ★ FEN BİLİMLERİ ENSTİTÜSÜ

POLİ(N-İZOPROPİLAKRİLAMİD)/ MONTMORİLLONİT NANOKOMPOZİT HİDROJELLERİNİN AĞ PARAMETRELERİ VE ŞİŞME ÖZELLİKLERİ

YÜKSEK LİSANS TEZİ

Kim. Deniz TOPUZ

515061009

Tezin Enstitüye Verildiği Tarih : 24 Aralık 2007
Tezin Savunulduğu Tarih : 31 Ocak 2008

Tez Danışmanı : Prof. Dr. Candan Erbil (İ.T.Ü.)

Diğer Jüri Üyeleri: Prof.Dr. F.Seniha Güner (İ.T.Ü.)

Doç.Dr. B. Filiz ŞENKAL (İ.T.Ü.)

OCAK 2008

ACKNOWLEDGEMENTS

First of all, I would like to thank my advisor Prof. Dr. Candan Erbil for her continuous support and trust. It was a pleasure to study under her supervision. I have gained a new vision for future during my master study.

I would like to thank Prof. Dr. Nurseli Uyanık for accessing me to utilize the infrastructure in her laboratory.

I would like to thank Assoc. Prof. Bahriye Filiz Şenkal for her contributions and I also thank to Argun Talat Gökçeören, whose advice and support gave me a whole new direction.

I am glad to have friends; Erdem Yavuz, Bülent Eriman and Şebnem Ş. Tayyar, who helped me out through my hard time.

I would like to thank my family and Nilüfer İlhan for their continuous support and encouragement.

All my work is dedicated to my Grandmother, who grew me up and has had contributions to my improvement up to today.

Deniz TOPUZ

February 2008

TABLE OF CONTENTS

ABBREVIATIONS

LCST	: Lower critical solution temperature
UCST	: Upper critical solution temperature
TP gel	: Topological gel
NC gel	: Nanocomposite gel
DN gel	: Double network gel
PEG	: Poly(ethylene glycol)
CD	: Cyclodextrin
PNIPAAm	: Poly(N-isopropyl acrylamide)
OR	: Conventional Hydrogel
BC	: Bacterial cellulose
BIS	: *N*,*N*'- methylenebis(acrylamide)
MMT	: Montmorillonite
ADA	: 12-aminododecanoic acid
PNC	: Polymeric nanocomposite
SWNT	: Single-walled carbon nanotubes
MWNT	: Multi-walled carbon nanotubes
TEMED	: N,N,N′,N′-tetramethyl ethylenediamine
KPS	: $K_2S_2O_8$

LIST OF TABLES

LIST OF FIGURES

LIST OF SCHEMES

LIST OF SYMBOLS

χ	: Polymer–solvent interaction parameter
v	: Crosslinking density
M_c	: Inter-crosslinking molecular weight
D_{ic}	: Inter-crosslinking distance
C**clay**	: Clay content
τ	: Stress defined as the force per cross sectional area of the undeformed sample
G	: Shear modulus
λ	: Deformation ratio
ℓ	: Lengths of the deformed hydrogel sample
ℓ_0	: Lengths of undeformed hydrogel sample
E	: Young's modulus
ν_e	: The effective crosslinking density
R	: Gas constant
υ_{2r}	: Polymer volume fraction in the relaxed state
υ_{2s}	: Volume fraction of the polymer in the swollen hydrogel
C_0	: Initial monomer concentration
ρ_2	: Density of the dry polymer
$\overline{M_r}$	: Molecular weight of the repeating unit of hydrogel.
ρ_s	: Density of solvent
Q_d	: Equilibrium swelling ratio for a gel sample.
W_d	: Weights of the dried sample
W_s	: Weight of the fully swollen sample.
d	: Equilibrium diameters of the hydrogels
d_o	: Original diameters of the hydrogels
V_1	: Molar volume of swelling agent
CEC	: Cation exchange capacity

NETWORK PARAMETERS AND SWELLING PROPERTIES OF POLY(N-ISOPROPYLACRYLAMIDE)/MONTMORILLONITE NANOCOMPOSITE HYDROGELS

SUMMARY

N-alkyl substituted acrylamides, and in particular N-isopropyl acrylamide (NIPAAm) hydrogels are known as thermo-responsive crosslinked polymer networks and prepared by free radical polymerization using radical initiators. NIPAAm hydrogels exhibit a sharp phase transition from hydrophilic to hydrophobic structure that occurs at its lower critical solution temperature (LCST, T_c). This transition at around 32-34^{o}C takes place because the hydrogen bonding interactions that form stable hydration shells around the hydrophobic groups of PNIPAAm disappear and that the hydrophobic interactions among polymers chains increase above the LCST, which cause expulsion of water.

Pure NIPAAm hydrogels crosslinked by using hydrophilic tetrafunctional N,N'-methylene bisacrylamide (BIS) as crosslinker have low mechanical strength in the swollen state, i.e., below LCST. The combination of large swelling and high mechanical performance within the same gel structure is important for both industrial and biomechanical applications. Usually, an increase in the swelling is accompanied with a decrease in the mechanical properties. These properties can be modified by: (1) changing the hydrophilic monomer, (2) modifying the concentration and type of crosslinking agent, (3) varying the method of preparation or (4) by copolymerizing hydrophilic or hydrophobic monomers.

Haraguchi et al. have developed a new type of nanocomposite (NC) hydrogel composed of PNIPAAm and hectorite (synthetic clay) which shows improved mechanical and swelling/shrinking properties compare to chemically cross-linked PNIPAAm hydrogels. In this hydrogel, exfoliated and uniformly dispersed clay particles act as multifunctional cross-links.

Recently, polymer-clay nanocomposites have attracted strong research and commercial interest due to profound improvements in material properties (increased strength, modulus, heat resistance, and reduced gas permeability) using a clay, which consists of silicate planar layers 1 nm thick and attracted with van der Waals forces. The clay is any material (natural or synthesized) having a cation-exchange capacity of 50 to 200 milliequivalent/100g and a large surface area. Clay platelets are truly

nanoparticulate. In addition, platelets are not totally rigid, but have a degree of flexibility.

Many clays (natural or synthesized) are aluminosilicates, which have a sheet-like (layered) structure, and consist of silica SiO_4 tetrahedra bonded to alumina AlO_6 octahedra in a variety of ways. A 2:1 ratio of the tetrahedra to the octahedra results in smectite clays, the most common of which is montmorillonite (MMT).

MMT is a natural clay mineral which has a large layer space and has some excellent properties such as good water absorption, swelling, adsorbability, cation-exchange and drug delivery. In general, MMT, which is a hydrophilic, swollen natural clay, is treated by alkylammonium salts to improve hydrophobic compatibility with organic polymers.

An organophilic clay can be produced from a normally hydrophilic clay by ion exchange with an organic cation such as an alkylammonium ion. For example, in montmorillonite, the sodium ions in the clay can be exchanged for a quaternary ammonium salt

Na^+-MMT + R-$NH_3^+Cl^-$ → R-NH_3^+- MMT + NaCl

Tetramethylethylenediamine, commonly known as TEMED is the chemical compound with the formula **$(CH_3)_2NCH_2CH_2N(CH_3)_2$**. TEMED is used with ammonium persulfate (or potassium persulfate**,** **$K_2S_2O_8$**) to catalyze the polymerizations of acrylamide (AAm) and N-isopropylacrylamide **(NIPAAm)** in making PAAm and **PNIPAAm** hydrogels.

In this work, **TEMED and its quaternary salt (cationic surfactant), QTEMED** were used as accelerator. QTEMED were synthesized in our laboratories**.**

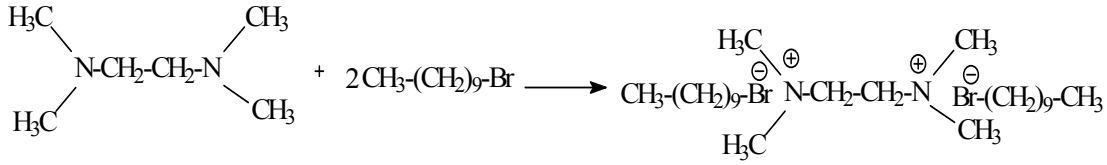

Scheme 1

Na^+-MMT (natural clay) was used as inorganic filler. The dispersed and activated MMT-TEMED and MMT-QTEMED particles (or layers) act as multifunctional cross-linkers.

Hydrogels were synthesized by free radical solution polymerizations of NIPAAm (0.7 mol/L) using KPS as initiator and, two different crosslinking agent, BIS (conventional crosslinker) and Na^+- MMT (multicrosslinker). Three type NIPAAm gels were prepared: (1) The networks made of neutral NIPAAm chains activated by TEMED and crosslinked with hydrophilic tetrafunctional constituent (BIS); (2) the neutral NIPAAm hydrogels containing layered silicate, MMT activated by TEMED; (3) the neutral NIPAAm hydrogels containing layered silicate, MMT activated by QTEMED.

After the reaction periods needed to complete gelation processes, each test tube was broken and the hydrogels were immersed in distilled water to remove linear polymer chains and unreacted constituents. Type (1) includes neutral NIPAAm hydrogels crosslinked with BIS (hydrophilic crosslinker) while Type (2) and (3) represent NIPAAm/MMT hydrogels.

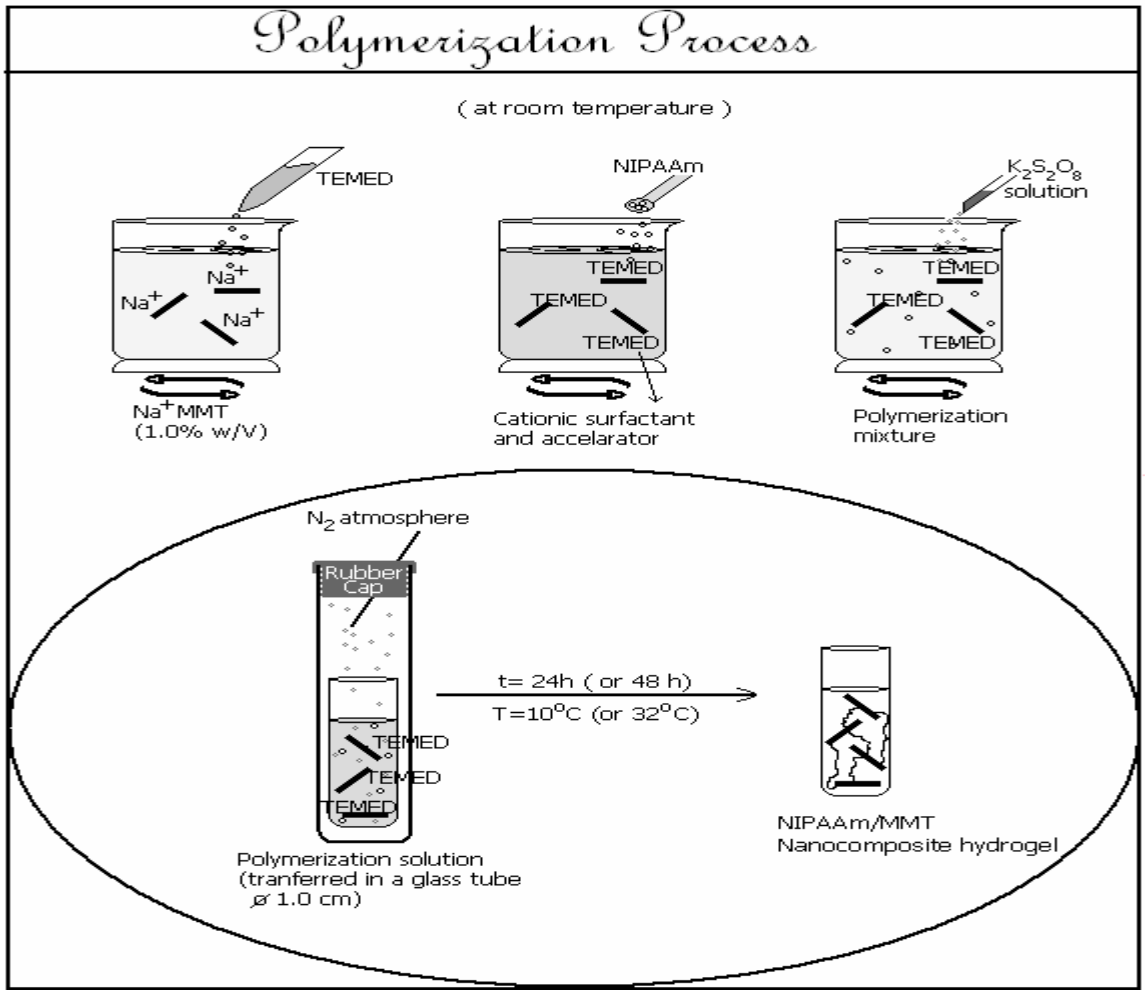

Figure 1: Polymerization process

Volumetric measurements were used to calculate the polymer volume fractions, υ_{2s} and υ_{2r}, i.e., volumetric compositions of the hydrogels. Assuming that the gels swell isotropically

$$V_s / V_r = \upsilon_{2r} / \upsilon_{2s} = (d / d_o)^3 \quad \textbf{(1)}$$

V_s = volume of the gel sample after equilibrium swelling

V_r = volume of the gel sample in the relaxed state

d = equilibrium diameter of the hydrogel.

d_o = initial diameter of the hydrogel, i.e., just after polymerization completed

υ_{2r} was obtained from

$$\upsilon_{2r} \approx V_{NIPAAm} /1000 \quad \textbf{(2)}$$

V_{NIPAAm} = volume of dry network

Elastic and shear moduli of NIPAAm hydrogels crosslinked with BIS, MMT/TEMED and MMT/QTEMED equilibrated in water in the range of 25-45^{o}C were determined by means of Hounsfield H5K-S model tensile testing machine, settled a crosshead speed of 1.0 cm/min and a load capacity of 5 N.

Hydrogel disks of known dimensions at equilibrium water uptake were put into a glass cell with double walled at constant temperature to maintain the equilibrium swelling, just before the compression measurements. It was not observed any loss of water and changing in temperature during the uniaxial compression measurements because of the compression period being less than 1 min.

Table 1: Effect of Accelerator Type, Temperature and Time on the Mechanical Properties ($T_{swelling}$ = 32^{o}C)

Sample	Composition	E Modulus (kPa)	Compression % (for total load, 5 N)	Stress (kPa) (for total load, 5 N)
*2	MMT + TEMED ($1.50x10^{-2}$ M)	1.3	66.3	32.6
*7	MMT + QTEMED ($1.50x10^{-2}$ M)	2.7	36.4	32.5
**4	MMT + TEMED ($1.50x10^{-2}$ M)	0.4	45.2	7.1
***5	MMT + TEMED ($1.50x10^{-2}$ M)	0.8	78.3	52.5
***6	MMT + TEMED ($3.00x10^{-2}$ M)	0.8	96.5	54.7
**8	MMT + QTEMED ($1.50x10^{-2}$ M)	1.1	91.8	75.0
***9	MMT + QTEMED ($4.50x10^{-2}$ M)	0.5	97.2	42.6

NIPAAm = 0.7 M; MMT = 1% (w/v, based on total monomer content)
* T = 10^{o}C; t = 24 h
** T = 32 ^{o}C; t = 24 h
*** T = 32 ^{o}C; t = 48 h

Young (or Elastic, E) and Shear (G) moduli were estimated in the linear deformation region according to

$$\tau = E (\lambda-1) \quad \textbf{(3)}$$

and

$$\tau = G\,(\lambda - \lambda^{-2}) \qquad \textbf{(4)}$$

Here τ is the compression stress and λ (= L/L_o) is the linear deformation ratio. The effective crosslinking density, ν_e was calculated from the value of G, i.e., slope of the linear portions of the τ vs $(\lambda-\lambda^{-2})$ plots using the equation

$$\nu_e = G / (RT\, \upsilon_{2s}^{1/3}\, \upsilon_{2r}^{2/3}) \qquad \textbf{(5)}$$

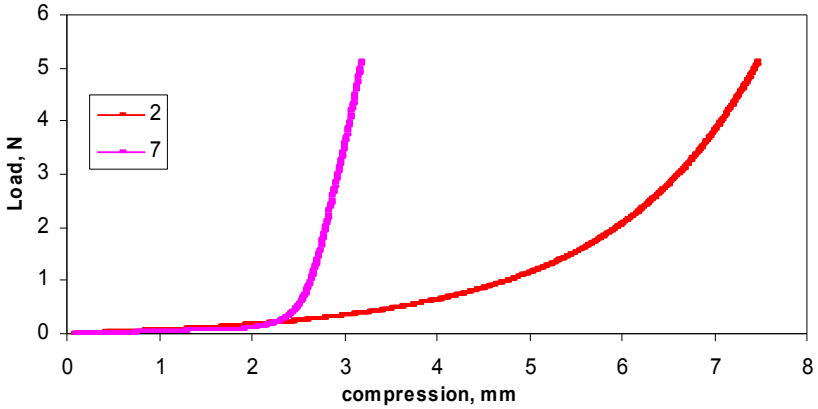

Figure 2: Load vs. compression curves for MMT/TEMED (1.50×10^{-2}M)/NIPAAm (0.7 M) (Sample 2) and MMT/QTEMED (1.50×10^{-2}M)/NIPAAm (0.7 M) (Sample 7)

Table 1 and **Figure 2** show that the mechanical strength of the sample containing cationic surfactant as accelerator is higher than that of the one synthesized using TEMED (reaction temperature = 10^oC).

From the values of ν_e, υ_{2r} and υ_{2s} the polymer-solvent interaction parameter, χ can be calculated from Flory-Rehner Equilibrium Swelling Equation

$$\chi = -\,[\ln(1-\upsilon_{2s}) + \upsilon_{2s} + \nu_e V_1 \upsilon_{2r} \{(\upsilon_{2s}/\upsilon_{2r})^{1/3} - (\upsilon_{2s}/\upsilon_{2r})(1/2)\}] / \upsilon_{2s}^2 \qquad \textbf{(6)}$$

V_1 = molar volume of the solvent,
ρ_2 = density of polrmer. The densities of all dried polymers prepared in this work were taken as $1.1\text{x}\ 10^3$ kg $/m^3$.

Table 2: Effect of Clay Content on the Mechanical Properties ($T_{swelling} = 25^oC$)

Sample	Composition	MMT %	E Modulus (kPa)	Compression % (for total load, 5 N)	Stress (kPa)
2	MMT + TEMED (1.50×10^{-2} M)	1	0.29	38.41	5.90
10	MMT + TEMED (1.50×10^{-2} M)	3	0.92	59.64	22.50
11	MMT + TEMED (1.50×10^{-2} M)	5	11.36	39.25	27.30

NIPAAm = 0.7 M; T = 10^oC (under N_2 atmosphere); t = 24 h

Table 3: Effect of Clay Content on the Network Parameters ($T_{swelling}$ = 25°C)

Sample	Composition	MMT %	G Modulus (kPa)	ν_e (mol/m^3)	χ
2	MMT + TEMED ($1.50x10^{-2}$ M)	1	0.05	0.45	0.504
10	MMT + TEMED ($1.50x10^{-2}$ M)	3	0.62	5.78	0.504
11	MMT + TEMED ($1.50x10^{-2}$ M)	5	3.58	30.49	0.504

NIPAAm = 0.7 M;T = 10°C(under N_2 atmosphere); t = 24 h

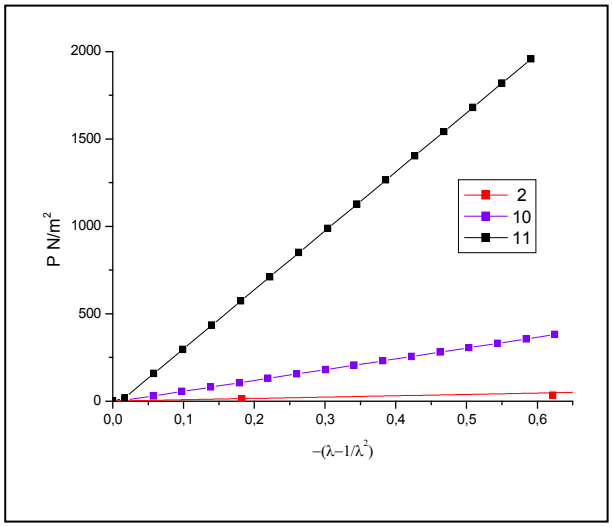

Figure 3: Compression stress-strain curves (Pressure (Pa) vs. $-(\lambda - \lambda^{-2})$) for Samples 2, 10, 11 given in **Table 3** (T = 25˚C)

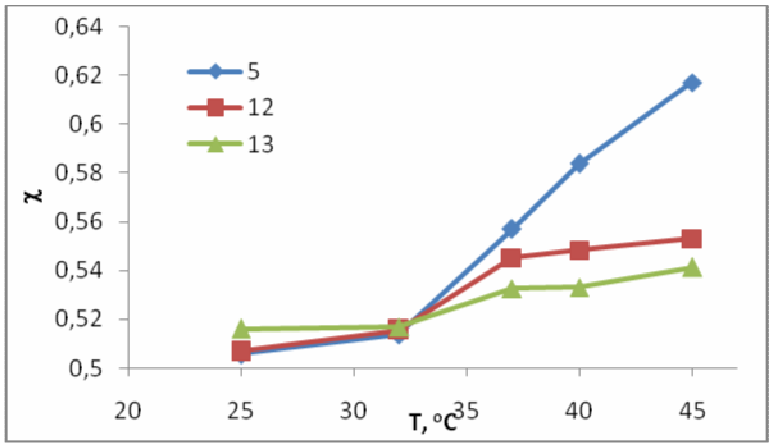

Figure 4: χ versus T curves for Samples 5 (1 % MMT), 12 (3 % MMT) and 13 (5 % MMT).

According to the mechanical properties and network parameters, which are given in **Table 2**, **Table 3**, and **Figure 3**, it is possible to conclude that mechanical strengths

and the crosslinking densities increase with increase in the concentration of Na^+-MMT.

Figure 4 indicates that the crosslinker concentration, i.e., MMT content is effected only on the swelling degrees of the NIPAAm/MMT hydrogels but not on their phase transition temperatures.

As a conclusion, it can be said that, in the case of the NIPAAm/MMT nanocomposite hydrogels, increase in the multicrosslinker content

(a)improve their mechanical properties, (b) increase the swelling degrees, and (c) does not change their LCST.

ÖZET

N-alkil sübstitüe akrilamidlerin ve özellikle N-izopropilakrilamidin (NIPAAm) hidrojelleri sıcaklığa duyarlı, çapraz bağlı polimer ağ yapılarıdır. Radikalik başlatıcı kullanılarak serbest radikal polimerizasyonu ile sentezlenirler. NIPAAm hidrojelleri alt kritik çözelti sıcaklığında hidrofilik yapıdan hidrofobik yapıya keskin bir geçiş gösterirler. Bu geçiş 32–34°C aralığında gerçekleşir. PNIPAAm'a ait hidrofobik grubun etrafında hidrojen bağlarının etkisiyle kararlı bir hidratasyon kabuğu oluşur ancak alt kritik çözelti sıcaklığı üzerine çıkıldığında hidrofobik etkileşimler polimer zinciri boyunca artış gösterir ve suyun itilmesine sebep olur. Hidrofilik, dört fonksiyonlu N-N'-metilen bisakrilamid çapraz bağlayıcısı kullanılarak oluşturulan saf NIPAAm hidrojelleri şişmiş durumda (alt kritik çözelti sıcaklığının altındaki değerlerde) düşük mekanik dayanım gösterirler. Yüksek şişme ve mekanik dayanımın aynı jel yapısı içinde bulunması hem sanayi hem de biyomekanik uygulamalar için önemlidir. Genellikle, şişmedeki artış mekanik özelliklerde bir düşüşle sonuçlanır. Bu özellikler 1) Hidrofilik yapıdaki monomeri değiştirerek 2) çapraz bağlayıcının tipini ve konsantrasyonunu değiştirerek 3) sentez yöntemini değiştirerek veya 4) hidrofilik veya hidrofobik monomerleri kopolimerizasyon ile yapıya katarak değiştirebilir.

Haraguchi ve arkadaşları PNIPAAm ve hektorit (sentetik kil) içeren yeni bir nanokompozit geliştirmişlerdir. Bu jel, kimyasal olarak çapraz bağlanmış PNIPAAm hidrojellerine göre daha iyi mekanik ve şişme-büzülme özellikleri göstermektedir. Bu hidrojelde rasgele dağılmış kil partikülleri çok fonksiyonlu çapraz bağlayıcı gibi davranırlar.

Son zamanlarda, 1nm kalınlığında ve van der Waals çekim kuvvetleriyle birbirine bağlı düzlemsel silikat tabakalarından oluşan killer kullanılarak oluşturulan polimer-kil nanokompozitlerinin mekanik özelliklerini (dayanım, modül, ısı, direnci artışı ve düşük gaz geçirgenliği) iyileştirmesi, ticari alandaki uygulamalara yönelik araştırılmaların yoğunlaştırılmasına sebep olmuştur. Kilin katyon değişim kapasitesi 50–200 meq / 100g'dır ve geniş yüzey alanı vardır. Kil tabakaları nano boyutta parçacıklardır. Buna ek olarak, tabakalar tümüyle sert değildir ama belli bir esnekliğe sahiptir.

Pek çok kil (doğal veya sentetik) tabakalı yapıdaki alüminyum silikatlardır. Tetrahedral yapıdaki silika $Si0_4$ ile oktahedral alümina AlO_6 tabakalarının oranı 2:1 olursa simektit killer oluşur ki bunların en yaygını MMT'dir.

MMT, tabakalar arasında geniş boşluklar içeren ve su absorplama, şişme, adsorplanma, katyon değişimi ve ilaç salınımı gibi üstün özellikler taşıyan doğal bir kildir. Genelde hidrofilik, şişmiş, doğal bir kil olan MMT, organik polimerlere hidrofobik uyumunu arttırmak amacı ile alkil ammonyum tuzları ile muamele edilir. Hidrofilik bir kilden, alkil ammonyum iyonu gibi bir organik katyon kullanarak iyon

değişimi ile organofilik kil oluşturulabilir. Örneğin, MMT de kilin içerdiği sodyum iyonları bir kuaterner ammonyum tuzu kullanılarak değiştirilebilir.

Na^+-MMT + R-$NH_3^+Cl^-$ → R-NH_3^+- MMT + NaCl

Tetrametiletilendiamin (TEMED) $(CH_3)_2NCH_2CH_2N(CH_3)_2$ formülüne sahip kimyasal bir maddedir. TEMED, PAAm ve PNIPAAm hidrojellerinin elde edilmesinde, Akrilamid (AAm) ve N-izopropilakrilamid (NIPAAm) polimerizasyonunu hızlandırmak için amonyumpersülfat (veya potasyumpersülfat, $K_2S_20_8$) ile birlikte kullanılır.

Bu çalışmada, TEMED ve onun kuaterner tuzu, QTEMED hızlandırıcı olarak kullanıldı. QTEMED laboratuvarlarımızda sentezlendi.

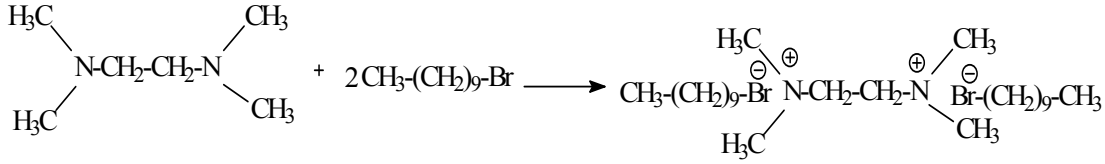

Şema 1

Na^+ -MMT anorganik bileşen olarak kullanılmaktadır. Dispers ve aktif hale getirilmiş MMT-TEMED ve MMT-QTEMED parçacıkları veya tabakaları çok fonksiyonlu çapraz bağlayıcı gibi davranırlar.

Hidrojeller, serbest radikal polimerizasyonu ile NIPAAm (0,7 mol/L) monomeri, KPS başlatıcısı ve iki farklı çapraz bağlayıcı; BIS (geleneksel çapraz bağlayıcı) ve Na^+ -MMT (çok fonksiyonlu çapraz bağlayıcı) kullanılarak sentezlendi. Üç farklı NIPAAm jeli; 1) TEMED ile aktif hale getirilmiş nötral NIPAAm zincirlerinin hidrofilik yapıdaki dört fonsiyonlu bileşen, BIS ile ağ yapıları oluşturuldu. 2) TEMED ile aktif hale getirilmiş tabakalı silikat MMT içeren nötral NIPAAm hidrojelleri 3) QTEMED ile aktif hale getirilmiş tabakalı silikat MMT içeren nötral NIPAAm hidrojelleri hazırlandı.

Jelleşme prosesi için gerekli reaksiyon süresi boyunca beklendikten sonra tüpler kırıldı ve oluşan hidrojeller, içerdiği lineer polimer zincirleri ve reaksiyona girmemiş bileşenlerinden arındırılması için, destile suda tutuldu. 1.jel çeşidi BIS ile çapraz bağlanmış nötral NIPAAm hidrojellerinin içeriklerini tanımlarken 2. ve 3. jel çeşitleri NIPAAm-MMT hidojellerini tanımlar.

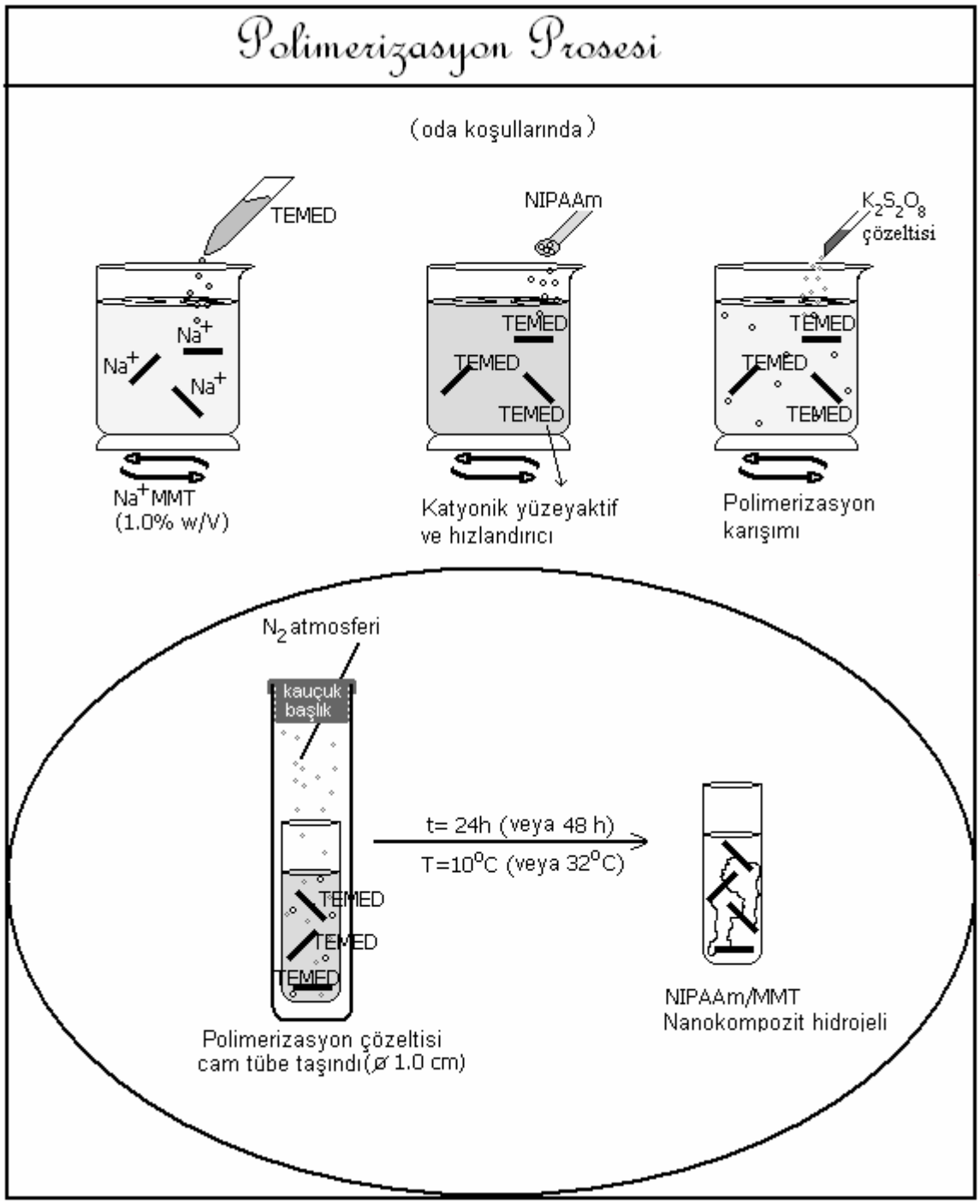

Şekil 1: Polimerizasyon prosesi

υ_{2s} ve υ_{2r} polimer hacim kesirlerinin, yani, hidrojellerin hacimsel bileşimlerinin hesaplanmasında volumetrik ölçümler kullanılmıştır. Jellerin izotropik olarak şiştikleri kabul edilirse

$$V_s / V_r = \upsilon_{2r} / \upsilon_{2s} = (d / d_o)^3 \quad \textbf{(1)}$$

V_s = dengedeki şişme sonrası jel hacmi,

V_r = relaks haldeki , yani sentezden hemen sonraki jel hacmi,

d = hidrojelin denge halindeki çapı,

d_0 = hidrojelin başlangıç çapı.

υ_{2r} aşağıdaki denklemden elde edilmiştir;

$$\upsilon_{2r} \approx V_{NIPAAm} /1000 \quad \textbf{(2)}$$

V_{NIPAAm} = Kuru ağ yapısının hacmi

BIS, MMT/TEMED ve MMT/QTEMED ile çapraz bağlanmış, 25-45^oC aralığında, suda dengeye gelen NIPAAm hidrojellerin Elastik ve Shear modülleri 5 N yük kapasiteli 1.0 cm/ dak hızla sıkıştırma yapmak üzere ayarlanmış H5K-S model gerilme ölçüm cihazı ile ölçüldü.

Dengedeki su tutma kapasitesine ulaşmış, boyutları bilinen hidrojel diskleri, ölçüm öncesi şişme dengesini korumak amcıyla, çift cidarlı ve sabit sıcaklıkta bir cam hücreye konmaktadır. Sıkışma süresi 1 dakikanın altında olması sebebiyle tek eksenli sıkıştırma ölçümlerinde herhangi bir su kaybı veya sıcaklık değişimi gözlemlenmemiştir.

Tablo 1: Hızlandırıcı Çeşidi, Sıcaklık ve Zamanın Mekanik Özellikler Üzerine Etkisi ($T_{şişme}$ = 32˚C)

Örnek	Bileşim	E Modülü (kPa)	Sıkışma % (toplam yük, 5 N)	Gerilim (kPa) (toplam yük, 5 N)
*2	MMT + TEMED ($1.50x10^{-2}$ M)	1.3	66.3	32.6
*7	MMT + QTEMED ($1.50x10^{-2}$ M)	2.7	36.4	32.5
**4	MMT + TEMED ($1.50x10^{-2}$ M)	0.4	45.2	7.1
***5	MMT + TEMED ($1.50x10^{-2}$ M)	0.8	78.3	52.5
***6	MMT + TEMED ($3.00x10^{-2}$ M)	0.8	96.5	54.7
**8	MMT + QTEMED ($1.50x10^{-2}$ M)	1.1	91.8	75.0
***9	MMT + QTEMED ($4.50x10^{-2}$ M)	0.5	97.2	42.6

NIPAAm = 0.7 M; MMT = 1% (w/v, toplam monomer içeriğine bağlı)
* T = 10˚C; t = 24 h
** T = 32˚C; t = 24 h
*** T = 32˚C; t = 48 h

Young (veya Elastik, E) ve Shear (G) modülleri doğrusal deformasyon bölgesinde, aşağıdaki denklemlerden hesaplanmıştır.

$$\tau = E\,(\lambda - 1) \qquad \textbf{(3)}$$

ve

$$\tau = G\,(\lambda - \lambda^{-2}) \qquad \textbf{(4)}$$

Burada τ, sıkıştırma gerilimidir ve λ (= L/L_0) deformasyon oranıdır. τ - (λ-λ^{-2}) grafiğinin doğrusal bölgedeki eğimi kullanılarak, G değeri hesaplandı. Etkin çapraz bağ yoğunluğu ν_e ise aşağıda verilen denklem ile hesaplandı.

$$\nu_e = G / (RT\, \upsilon_{2s}^{1/3}\, \upsilon_{2r}^{2/3}) \qquad \textbf{(5)}$$

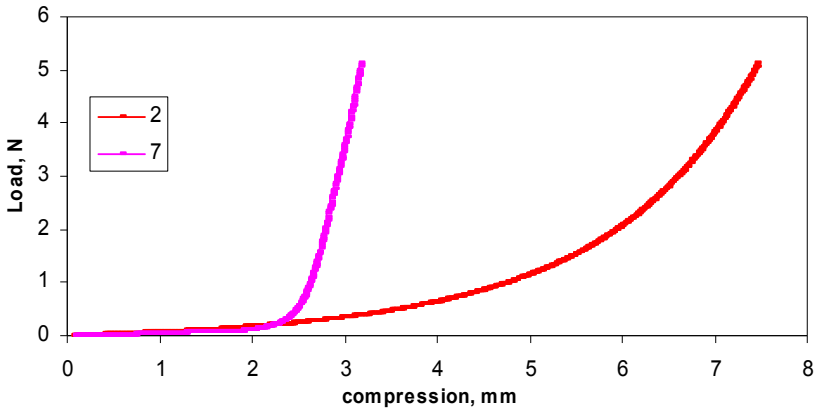

Şekil 2: Yük - sıkıştırma grafikleri MMT-TEMED ($1{,}5\text{x}10^{-2}$ M) / NIPAAm(0,7 M) (Örnek 2) ve MMT-QTEMED ($1{,}5\text{x}10^{-2}$ M) / NIPAAm(0,7 M) (Örnek 7)

Tablo 1 ve **Şekil 2**, katyonik yüzey aktif hızlandırıcı içeren örneğin mekanik dayanımının TEMED ile (reaksiyon sıcaklığı = 10˚C) sentezlenene göre daha fazla olduğunu göstermektedir.

ν_e , υ_{2r} ve υ_{2s} değerleri kullanılarak polimer - çözücü etkileşim parametresi χ, Flory Rehner denge şişme denklemi kullanılarak bulunur.

$$\chi = -\,[\ln(1-\upsilon_{2s}) + \upsilon_{2s} + \nu_e V_1\, \upsilon_{2r}\, \{(\upsilon_{2s}/\upsilon_{2r})^{1/3} - (\upsilon_{2s}/\upsilon_{2r})\,(1/2)\}] / \upsilon_{2s}^{2} \qquad \textbf{(6)}$$

V_1 = Çözücünün molar hacmi

ρ_2 = Polimer yoğunluğu.

Bu çalışmada kuru polimer örnekleri için yoğunluk, $1.1\text{x}10^3$ kg /m^3 olarak alınmıştır.

Tablo 2: Kil Bileşiminin Mekanik Özelliklere Etkisi ($T_{şişme}$ = 25˚C)

Örnek	Bileşim	MMT %	E Modülü (kPa)	Sıkışma % (Toplam yük, 5 N)	Gerilim (kPa)
2	MMT + TEMED ($1.50x10^{-2}$ M)	1	0.29	38.41	5.90
10	MMT + TEMED ($1.50x10^{-2}$ M)	3	0.92	59.64	22.50
11	MMT + TEMED ($1.50x10^{-2}$ M)	5	11.36	39.25	27.30

NIPAAm = 0.7 M; T = 10˚C (N_2 atmosferi altında); t = 24 h

Tablo 3:. Kil Bileşiminin Ağ Parametrelerine Etkisi ($T_{şişme}$ = 25˚C)

Örnek	Bileşim	MMT %	G Modülü (kPa)	ν_e (mol/m^3)	χ
2	MMT + TEMED ($1.50x10^{-2}$ M)	1	0.05	0.45	0.504
10	MMT + TEMED ($1.50x10^{-2}$ M)	3	0.62	5.78	0.504
11	MMT + TEMED ($1.50x10^{-2}$ M)	5	3.58	30.49	0.504

NIPAAm = 0.7 M;T = 10˚C (N_2 atmosferi altında); t = 24 h

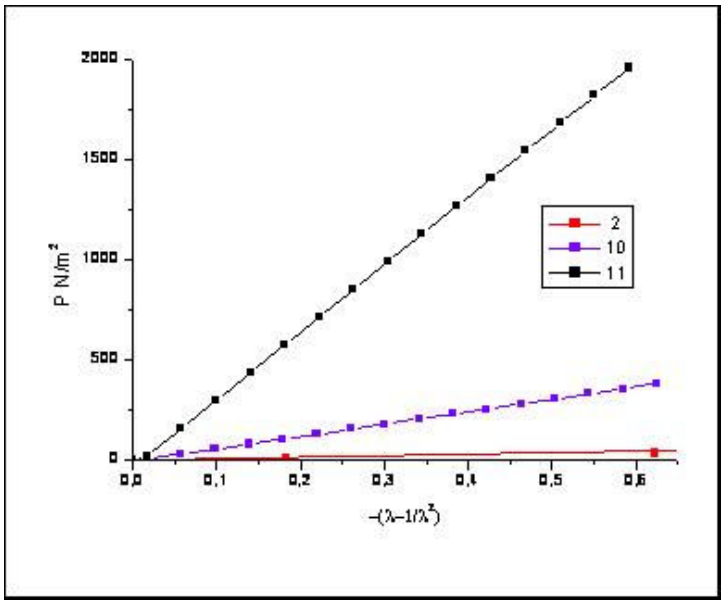

Şekil 3: Tablo 3'de verilen 2, 10, 11 no'lu örneklerin Basınç- biçim değiştirme eğrileri (Basınç (Pa) – $-(\lambda-1/\lambda^2)$)

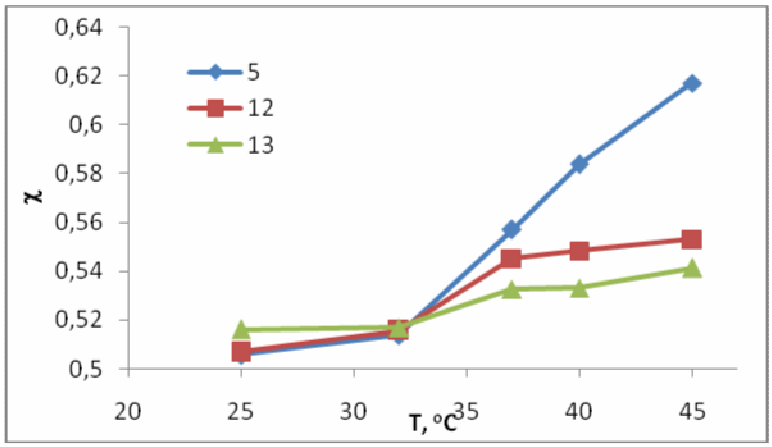

Şekil 4: Örnek 5 (% 1 MMT),12 (% 3 MMT) ve 13 (% 5 MMT) için χ−Ṭ grafiği.

Tablo 2, **Tablo 3** ve **Şekil 3**'de belirtilen mekanik özelliklere ve ağ parametrelerinden elde edilen verilere dayanılarak, Na^{+}-MMT konsanrasyonundaki artış ile mekanik dayanım ve çapraz bağ yoğunluğunun arttığı sonucuna varılmaktadır.

Şekil 4'den MMT içeriğinin NIPAAm/MMT hidrojellerinin şişme derecelerini etkilediğini ancak faz geçiş sıcaklığının çapraz bağ konsantrasyonu ile değişmediği gözlenmiştir.

Sonuç olarak, NIPAAm/MMT nanokompozitleri durumunda, çok fonksiyonlu çapraz bağlayıcı oranındaki artışın (a) mekanik özellikleri iyileştirdiği (b)şişme derecesini arttırdığı (c)LCST'yi değiştirmediği gözlenmiştir.

1 INTRODUCTION

1.1 Polymeric Gels

Polymeric gels are a class of macromolecular networks that contain a large fraction of solvent such as water within their structure. Polymeric gels are usually formed by the free radical polymerization of monomers in the presence of a difunctional crosslinking agent and a solvent. They can be made either in bulk or in nano-or micro particles. The bulk gels are easy to handle but usually have very slow swelling rate and amorphous structures arising from randomly crosslinked polymer chains, while the gel nanoparticles react quickly to an external stimulus in gels has attracted attentions. Such structures include gels with embedded self-assembled solid polymer spheres and the complex formation of polyelectrolyte gels with oppositely charge surfactants **[1]**.

As polymeric networks, both gels and hydrogels might be similar chemically, but they are physically distinct. Technically, gels are semi-solid systems comprising small amounts of solid, dispersed in relatively large amounts of liquid, yet possessing more solid-like than liquid-like character. Sometimes, hydrogels are also described as aqueous gels because of the prefix 'hydro'. Although the term 'hydrogel' implies a material already swollen in water, in a true sense hydrogels are cross-linked network of hydrophilic polymers. They possess the ability to absorb large amounts of water and swell, while maintaining their three-dimensional (3D) structure.

This definition differentiates hydrogels from gels, which are polymeric networks already swollen to equilibrium, and the further addition of fluids results only in dilution of the polymeric network (**Figure 1.1**). Although some of the gels are rigid enough to maintain their structure under a small stress, after exceeding the yield-value, gel fluidity is observed with loss of polymer structure. A hydrogel exhibits swelling in aqueous media for the same reasons that an analogous linear polymer

dissolves in water to form an ordinary polymer solution. Thus, the feature central to the functioning of a hydrogel is its inherent cross-linking. Conventional gels can also develop small levels of cross-links as a result of a gain in energy under the influence of shear forces, but this is reversible because of the involvement of weak physical forces. Because the basic framework of both gels and hydrogels is the polymer network, these polymers produce systems that span a range of rigidities, beginning with a sol and increasing to mucilage, jelly, gel and hydrogel. Thus, hydrogel, sometimes referred to as xerogel, is a more rigid form of gel. Although, these polymers exhibit swelling in an aqueous environment, at equilibrium their swelling contributes to a gain in solution viscosity, leading to aqueous gel formation **[2]**

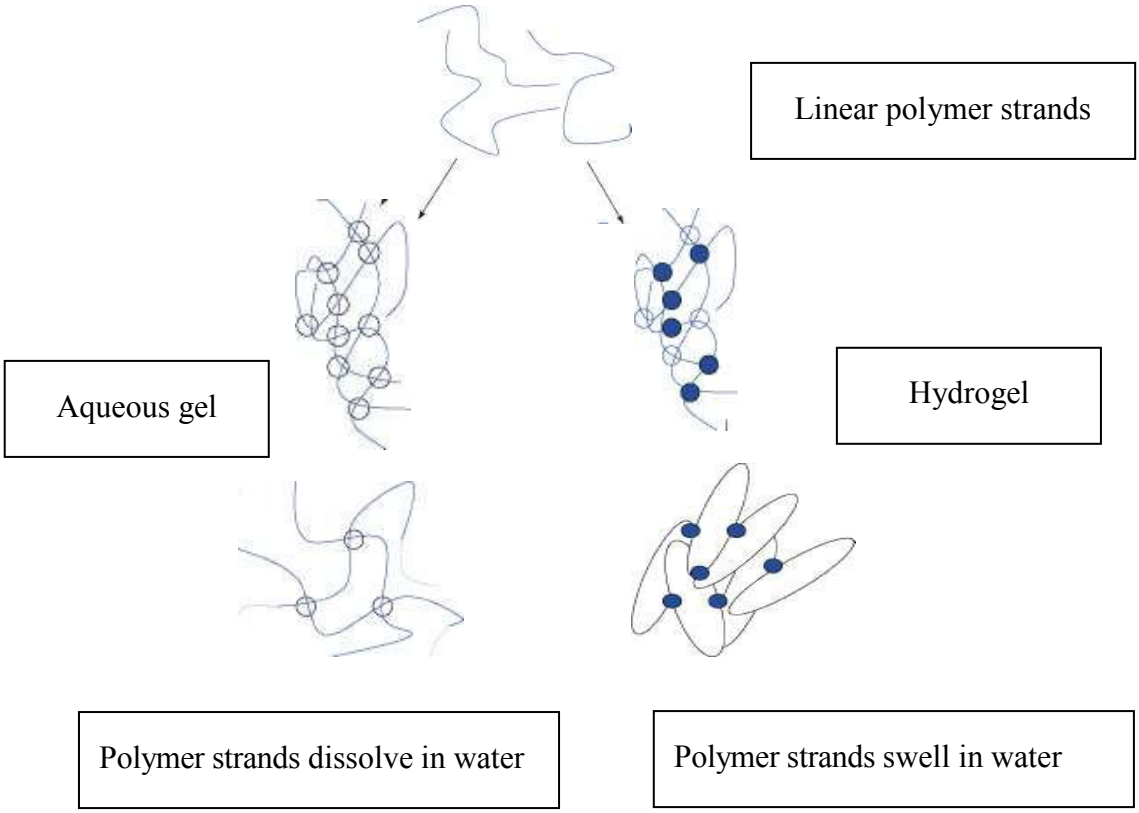

Figure 1.1: Polymer strands forming a gel and a hydrogel.

In **Figure 1.1**, polymer strands forming gel and hydrogel show different behaviour in an aqueous environment. Solid circles represent covalent cross-links and hollow circles represent virtual cross-links formed by entanglements.

1.2 Hydrogels

Hydrogels are water-swollen networks, which are crosslinked structures, composed of hydrophilic homopolymers or copolymers. They are rendered insoluble due to the presence of chemical covalent or ionic or physical crosslinks. The latter can be entanglements, crystallites, or hydrogen-bonded structures. The crosslinks provide the network structure and physical integrity **[3]**. Polymer hydrogels can be divided into two main classes, i.e., chemically cross-linked hydrogels, which are composed of polymer networks with covalent bonding, and physically cross-linked hydrogels, which are composed of physical networks with noncovalent interactions **[4]**. Hydrogels are crosslinked hydrophilic polymers with network structures consisting of acidic, basic, or neutral monomers, which are able to imbibe large amounts of water (**Table 1.1.1**). A variety of hydrogels have been employed for different biomedical applications. Because of their biocompatibility and biodegradability, they are used as bioabsorbable materials in surgeries and biotechnology and in other medical, agricultural, and pharmaceutical applications for delivery of medicines, among other possibilities. For the latter application they are unique carriers for controlled drug delivery **[5]**.

Due to their high water content, hydrogels possess excellent biocompatibility. The amount of water in the equilibrium swollen state is a balance between the thermodynamic force of mixing (hydration) and the retractive force of the three-dimensional network.

The mixing force depends mainly on the hydrophilicity of the polymer backbone (characterized by the polymer–solvent interaction parameter, χ), the retractive force on the number of crosslinks connecting polymer chains into a three-dimensional network. Consequently, there is a wide variety of design options for the preparation of hydrogels of different structures and properties.

Temperature-sensitive hydrogels are usually based on polymers exhibiting a lower critical solution temperature (LCST), i.e. the gels collapse as temperature increases (inverse temperature dependence). Apparently, below the LCST, water molecules form hydrogen bonds with polar groups on the polymer backbone and organize around hydrophobic groups as iceberg water. Above the LCST, bound water

molecules are released to the bulk with a large gain in entropy resulting in collapse of the polymer network **[6]**. Application of hydrogels as mechanical devices is fairly limited due to their lack of mechanical strength. Reported values of the fracture energy of typical hydrogels fall in the range10^{-1}–10^{0} J/m^2, much smaller than the fracture energy of usual rubbers. Many researchers may have thought that this feature of gels is unavoidable because of their solution-like nature, i.e. the low density of polymer chains and small friction between the chains. Furthermore, it is well known that in hydrogels synthesized from monomer solutions, inhomogeneity is formed during the gelation. This is also considered to be a factor decreasing the mechanical strength.

Table 1.1.1: Monomers for hydrogel synthesis

Monomers	Neutral	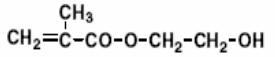	2-Hydroxyethyl methacrylate
		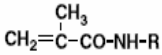	*N*-alkylmethacrylamides
		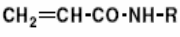	*N*-alkylacrylamides
		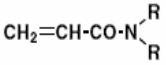	*N*,*N*-dialkylacrylamides
	Acidic	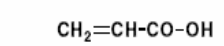	Acrylic acid
		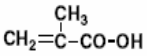	Methacrylic acid
		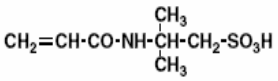	2-Acrylamido-2-methyl propane sulfonic acid
	Basic	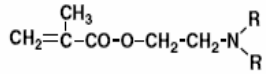	*N*,*N*-dialkylaminoethyl methacrylate
		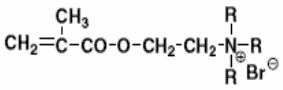	Methacryloyloxyethyltrialkylammonium bromide
Crosslinking agents		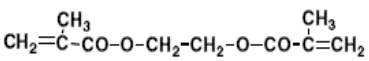	Ethylene dimethacrylate
		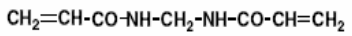	Methylenebisacrylamide

Recently, three new hydrogels with good mechanical performance have been developed: a ‘topological (TP) gel, ’a ‘nanocomposite (NC) gel’, and a ‘double network (DN) gel’. The TP gels have figure-of-eight cross-linkers that can slide along the polymer chains. Reflecting this flexible cross-linker, TP gels absorb large amounts of water, and can be highly stretched without fracture. In NC gels, polymer chains are cross-linked by inorganic clay slabs on the scale of a several tens of

nanometers, instead of organic crosslinking agents. The NC gels are also highly stretchable, and possess other favorable physical properties such as excellent optical transparency.

Finally, DN gels consist of two interpenetrating polymer networks: one is made of highly cross-linked rigid polymers and the other is made of loosely cross-linked flexible polymers. Such DN gels, containing about 90 wt. % water, possess both hardness (elastic modulus of 0.3 MPa) and toughness (fracture stress of w10 MPa). The invention of these three kinds of novel gels not only has made a breakthrough in finding wide applications of gels in industry and biomedical field, but also proposes fundamental problems in gel science.

1.2.1 Topological Gel

As shown schematically in **Figure 1.2a**, TP gels have figure-of-eight cross-linkers that can slide along polymer chains. A typical example is the polyrotaxane gel synthesized by a technique of supramolecular chemistry by Okumura and Ito; a polyrotaxane molecule consists of a poly(ethylene glycol) (PEG) chain, a-cyclodextrin (CD) circles threaded on the PEG chain and large end groups trapping the a-CD cycles (**Figure 1.2b**). Chemically cross-linking, the a-CD (**Figure 1.2c**) in an aqueous solution of polyrotaxane results in the polyrotaxane gel.

The TP gels are highly water absorbent and stretchable. **Figure 1.3** shows a comparison of a polyrotaxane gel in as-prepared, dried, and fully swollen (equilibrium) states. The gel swells to about 500 times of its original (as-prepared) weight. A TP gel (in the as-prepared state) can be stretched to about 20 times its original length. Another unique nature of the TP gels appears in macroscopic and equilibrium mechanical behavior when the cross-linking density is low: stress–strain (S–S) curve of the TP gels under uniaxial elongation exhibit low convexity in all ranges of strain. This is quite different from the usual chemical gels, for which the S–S curve exhibits upper convexity in the small strain regime.

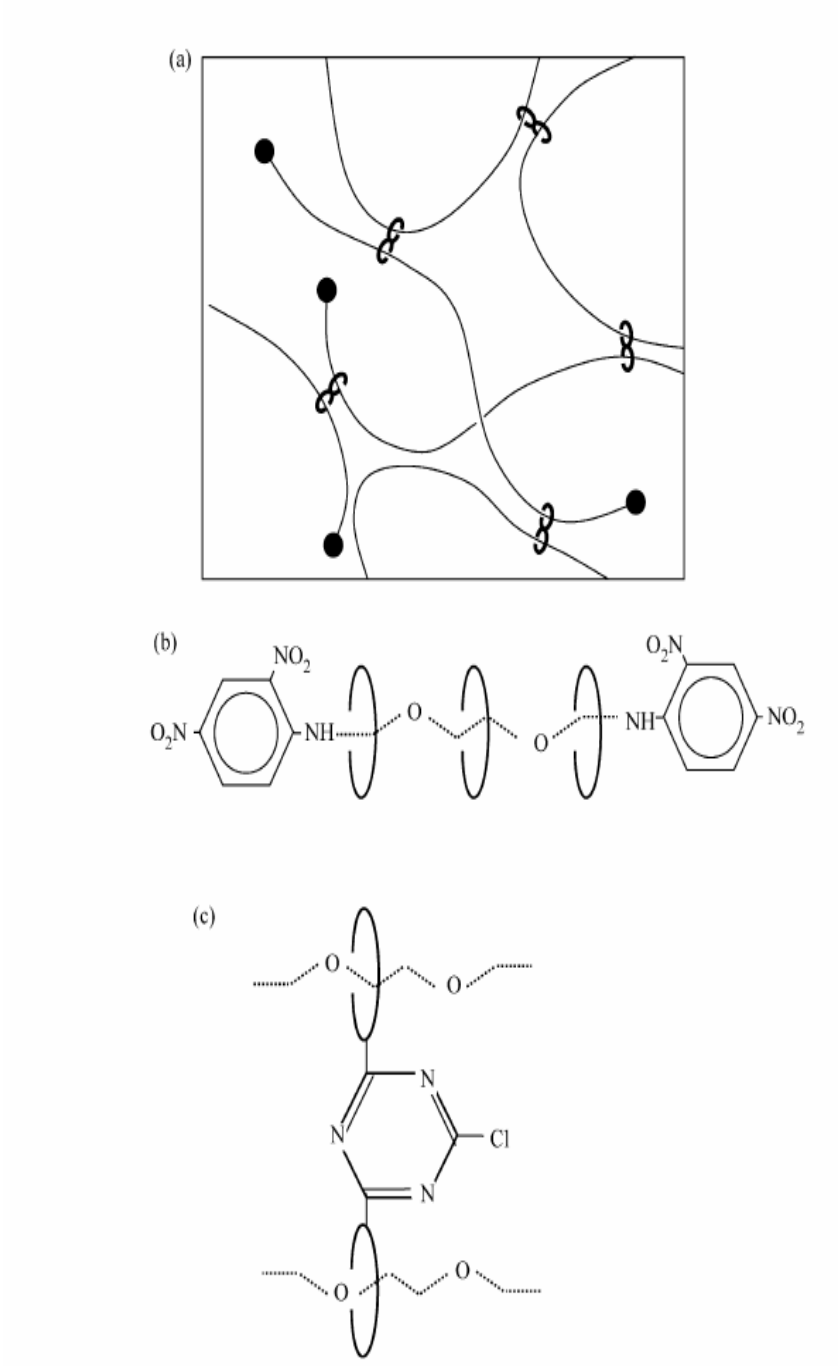

Figure 1.2: Topological gel

(a) Schematic of the topological gel. The figure-of-eight structures are the cross-linkers that can slide along the polymer chain. **(b)** A polyrotaxane chain used in synthesizing the polyrotaxane gel. **(c)** The chemical cross-linking in the polyrotaxane gel.

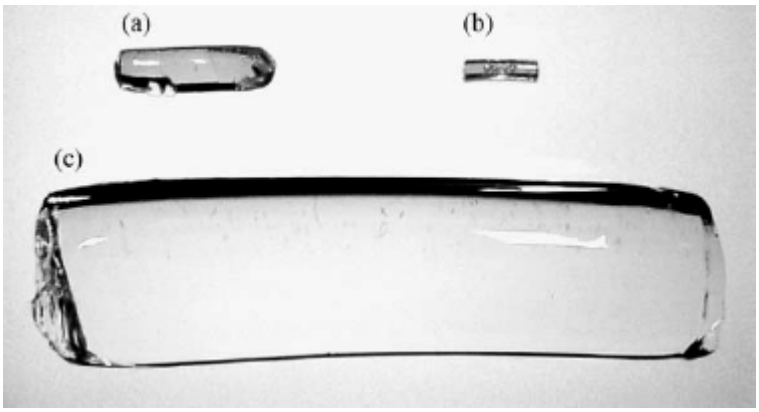

Figure 1.3: Comparison of volumes of a TP gel (polyrotaxane gel) in as-prepared (a), dried (b), and swelling equilibrium (c) states.

The sliding motion of the figure-of-eight crosslinkers accounts for the special feature of the TP gels that distinguish the gels from the usual chemical and physical gels. **Figure 1.4** shows conceptual models for elongation of the topological gel (**Figure 1.4a**) and that of the usual chemical gel (**Figure 1.4b**). In the chemical gel, the tension is distributed unevenly among the polymer chains; scission of the polymer chains gradually occurs. On the other hand, in a topological gel, the relative sliding of the polymer chains by figure-of-eight cross-linkers occurs to equalize the tension among the polymer chains.

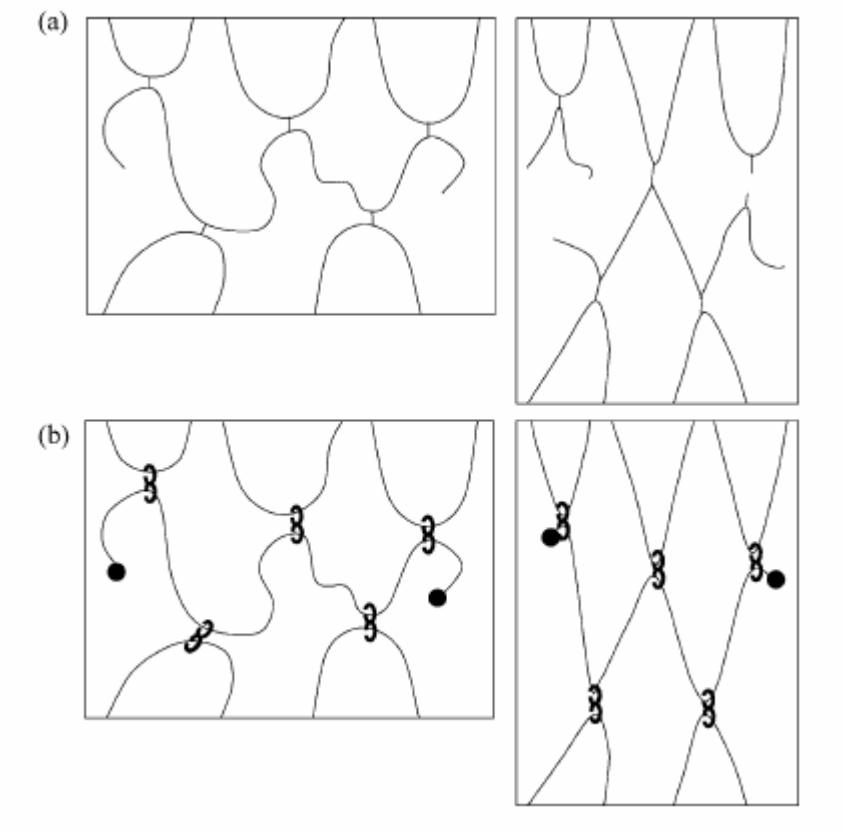

Figure 1.4: Comparison of conceptual models between the chemical gel and the TP gel under elongation.

(a) In the chemical gel, tension of chains is unequal, and short chains are cut first. **(b)** In the TP gel, the chains and the figure-of-eight cross-linkers can slide each other. Due to this motion, the tension can be regulated.

1.2.2 Nanocomposite Gel

As shown schematically in **Figure 1.5**, the clay slabs work as multifunctional crosslinkers in the NC gels **[7]**. In the last two decades, polymeric hydrogels, such as poly(N-isopropyl acrylamide) (PNIPAAm) gel, that display a sensitivity to external stimuli (e.g., temperature, solvent composition, pH, light, pressure, magnetic, and electric fields) have attracted much scientific interest and have been used in many applications.However, they have several significant limitations due to their chemically crosslinked network structures. A major goal has been to control the crosslinking density v (= number of crosslinked chains per unit volume) and the inter-crosslink-ing molecular weight Mc (i.e., the chain lengths between cross-linking points) independently. However, in conventional syntheses, independent control of these parameters was a contradiction because an increase in v was always

accompanied by a decrease in Mc ($v <= Mc^{-1}$). Also, since the crosslinking reaction (using crosslinking agents) could not occur at regularly separated positions, the chain lengths between crosslinking points always had a broad distribution, as shown in **Figure 1.6**. Furthermore, structural inhomogeneity (i.e., the heterogeneous aggregation of crosslinking points) always occurred when the concentration of crosslinker was high. Therefore, hydrogels composed of chemically crosslinked polymer networks have severe limitations such as morphological homogeneity (optical transparency) and mechanical properties. That is, conventional organic, crosslinked, polymeric hydrogels (conventional hydrogel) always exhibit mechanically weak and brittle properties irrespective of v and are often cloudy. Furthermore, since the polymer chains are molecularly restricted by a large number of crosslinks, they do not behave like flexible linear polymer chains in terms of their own characteristics such as sensitivity to external stimuli. Thus, many potential applications of conventional conventional hydrogelgels have been restricted or abandoned because of these limitations.

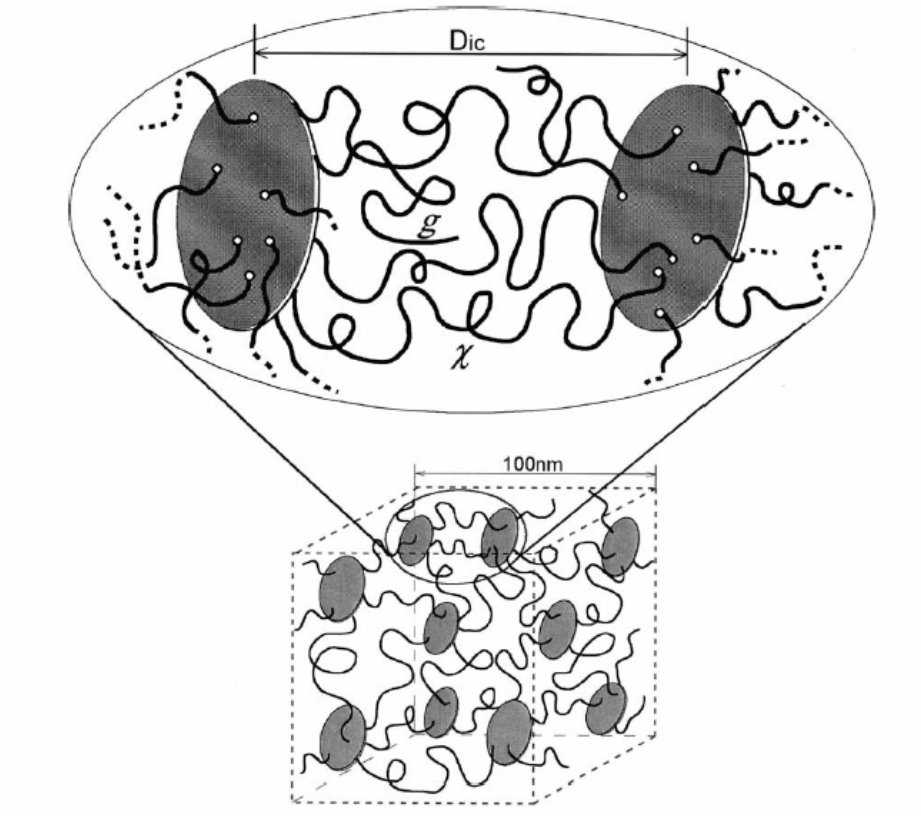

Figure 1.5: Schematic representation of a 100 nm cube of an NC3 gel

In **Figure 1.5**, an NC3 gel consisting of uniformly dispersed (exfoliated) inorganic clay and two primary types of flexible polymer chains, *%* and *g,* grafted onto two neighboring clay sheets and one clay sheet, respectively. In the model, only a small number of polymer chains are depicted for simplicity **[8]**.

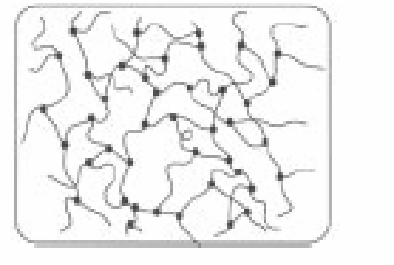

Figure 1.6: Conventional conventional hydrogel network structure model.

New type of polymeric hydrogel solves these problems. The proposed hydrogel is a nanocomposite hydrogel (NC gel) composed of specific polymers and water-swellable inorganic clay. The schematic illustration of the structural model for the NC gel is shown in **Figure 1.5**. In the NC gel, inorganic clays are exfoliated and uniformly dispersed in an aqueous media. Then, neighboring clay sheets are connected by polymer chains %, in other words, clay sheets act as multifunctional crosslinking agents for the polymer. Here, the inter-crosslinking distance (Dic) is equivalent to the neighboring clay-clay interparticle distance. Then, Dic can be determined by the clay concentration provided the exfoliated clay platelets and clay sheets are fixed in uniformly dispersed positions. Taking the polymer chain conformations into account, Dic can be converted to Mc. On the other hand, v, which is equivalent to the number of polymer chains % per unit volume, is mainly determined by the polymer and the initiator concentrations at a fixed clay content **[8]**.

1.2.3 Double Network Gel

A DN gel is synthesized via a two-step network formation: the first step forms a highly cross-linked rigid gel, and the second forms a loosely crosslinked network in the first gel.

Randomness or inhomogeneity in structure exists in all kinds of gels. The TP, NC and DN gels approach the problem with different ways: TP gels have adjustable cross-linking structures; NC gels utilize a cross-linking method effectively reducing

the inhomogeneity; and DN gels reveal that the inhomogeneity may serve to improve the mechanical strength.

The discovery of hydrogels with a good mechanical performance should enable hydrogels to find wide application in industry, including for fuel cell membranes, load-bareing water absorbents, and separation membranes, in the printing industry, optical devices, low friction gel machines, and in mechanical fields, such as artificial cartilages, tendons, blood vessels, and other bio-tissues. To realize the biomedical applications, it is important to apply the concept of the high performance gels to biocompatible polymers. Some progresses have been made recently by combining bacterial cellulose (BC) and gelatin **[7]**.

1.3 Temperature-Responsive Permanently Crosslinked Gels

Covalently crosslinked temperature-sensitive gels are perhaps the most extensively studied class of environmentally-sensitive polymer systems in drug delivery. At least one component of the polymer system should possess temperature-dependent solubility in a solvent (i.e. water, with a few exceptions). In order to obtain a hydrogel that dramatically changes its swelling degree in water, the gel constituents must be insoluble above or below a certain temperature, called the lower or upper critical solution temperature (LCST or UCST, respectively). For drug release applications, mainly LCST systems are relevant. The phenomenon of polymer aggregation at LCST is thermodynamically similar to that causing temperature-induced protein folding. Namely, the driving force for the aggregation is the entropy (S) of the two-phase polymer and water system, which is greater than in polymer solution. Positive ΔS renders the temperature increase to contribute to the trend of the system to aggregate, as the positive enthalpy term ΔH is smaller than the entropy term and does not influence the spontaneous association to a great extent. Under these circumstances the free energy of association ($\Delta G = \Delta H - T\Delta S$) is negative, and thus association is favorable. A schematic diagram of the hydrophobic association is given in **Figure 1.7**.

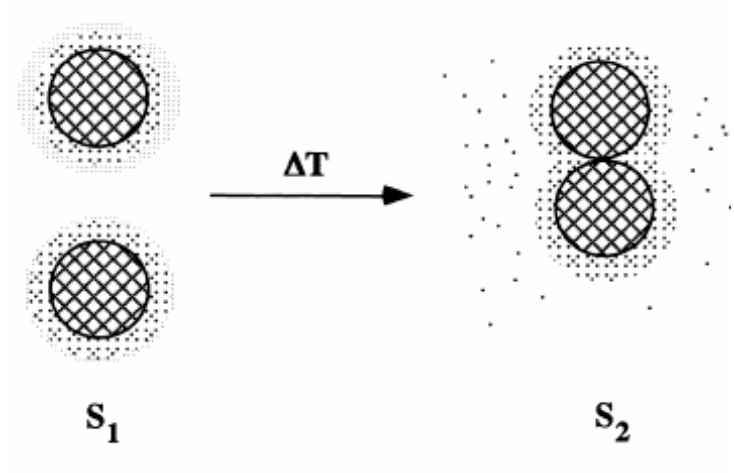

Figure 1.7: Schematic representation of the hydrophobic interaction.

In **Figure 1.7**, State 1 corresponds to two non-associated molecules with the layers of structured water; state 2 represents aggregation when some water molecules leave structured layers for less structured bulk. $S_2 > S_1$ Adopted, with changes.

When a hydrophilic drug is incorporated into a swollen gel, it can show a Fickian release below the LCST (**Figure 1.8A**). Conversely, a more hydrophobic drug can show Fickian diffusion from the collapsed gel above. (**Figure 1.8B**) If a drug is loaded below the LCST, it can be squeezed out above the LCST due to the pressure generated during gel collapse. A similar idea was realized with gels immobilized within porous membranes (**Figure 1.8C**). Alternatively, if a gel is essentially heterogeneous, it may form a dense 'skin' layer of the collapsed component while the core remains swollen (**Figure 1.8D**).

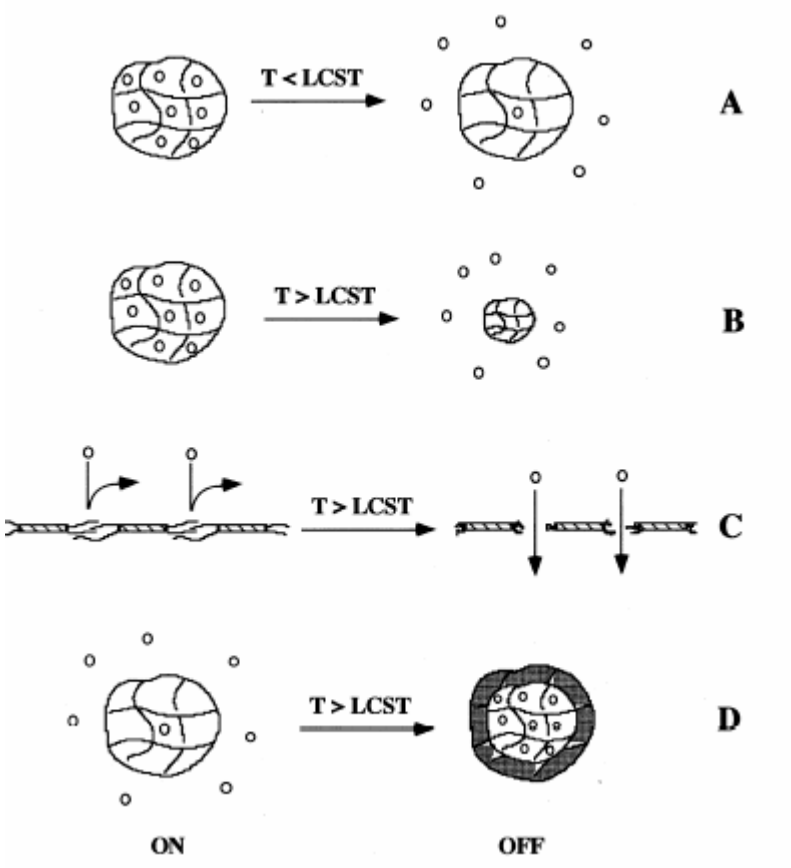

Figure 1.8: Modes of drug delivery from temperature-sensitive hydrogels.

1.3.1 Poly(N-isopropylacrylamide)

Chemically, the area of temperature-responsive gels has been dominated by *N*-alkylacrylamides with *N*-isopropylacrylamide (NIPAAm) being the most prominent example **[9]**. Hydrogels are crosslinked, three-dimensional hydrophilic polymeric networks that swell but do not dissolve when brought into contact with water **[12]**. PNIPAAm is one of the most attractive environmentally sensitive polymers and has been studied extensively from both basic and application points of view. Linear PNIPAAm chains undergo a fast and reversible coil-to-globule transition around its lower critical solution temperature (LCST) in aqueous media. At temperatures below the LCST, PNIPAAm chains are hydrated and adopt flexible and expanded random-coil conformations in water. Above the LCST, PNIPAAm chains become dehydrated and collapse into a tightly packed globular conformation. Currently, PNIPAAm is widely utilized in functional hydrogels. PNIPAAm hydrogels exhibit a clear volume phase transition in response to external stimuli such as temperature, pH, solvent composition, salt concentration, light, mechanical stress, and magnetic field. Many

potential applications such as biotechnological devices, tissue engineering, immobilization of enzymes, and drug-delivery systems stem from the stimuli-responsive properties of PNIPAAm described above. PNIPAAm hydrogels are commonly prepared by chemical cross-linking using an organic cross-linker such as *N*,*N*'- methylenebis(acrylamide). In conventional PNIPAAm hydrogels, many properties such as volume (swelling ratio) along with optical transparency, mechanical modulus, surface properties, and electrophoretic mobility change significantly as a consequence of the hydrophilic/hydrophobic transition at the LCST **[10]**. PNIPAAm show a very well defined LCST at about 32˚C [**9**]. However, it is also true that conventional hydrogels have several important limitations. For example, conventional hydrogels often become turbid when the polymerization conditions, such as cross-linker content, polymerization temperature, and pressure, are changed. Typically, conventional hydrogels prepared with high cross-linker concentrations become opaque even at temperatures below LCST. This is attributed to the development of permanent structural inhomogeneities on an optical-wavelength scale created by a high cross-link density. Regarding swelling in water, conventional hydrogels exhibit a quite low equilibrium swelling ratio in the range of cross-linker concentrations commonly used. Also, conventional hydrogels generally exhibit very slow deswelling behavior, often taking more than a month to approach equilibrium, although higher deswelling rates are required for many potential applications. Furthermore, conventional hydrogels always exhibit very weak mechanical properties and are easily broken by applying external stresses. Therefore, conventional hydrogels can not be used where they are extended or bent. Since all these disadvantages of conventional hydrogels arose from the inherent problems of chemically cross-linked polymer networks, they are considered inevitable. That is, these limitations are observed in any conventional hydrogels having a broad distribution of polymer chain lengths between crosslinking points.

Among these disadvantages, slow rates of deswelling have been studied most extensively. As a result, fast deswelling has been achieved by introducing porosities, structural inhomogeneities, or a tailored graft structure into conventional hydrogels. The modified conventional hydrogels were prepared, for example, by polymerization using selected conditions such as high and low polymerization temperatures or high cross-linker concentration, and also by polymerization in the presence of other

components having a siloxane linkage, a carboxylate group, However, in most cases, other properties such as mechanical properties, swelling ratio, and optical transparency were not improved and were often made worse. Therefore, it was a dream to develop a new material that could overcome all these disadvantages simultaneously. In an ideal PNIPAAm hydrogel, desirable properties in structural homogeneity (i.e., high transparency), mechanical properties (high strength and toughness), and swelling/deswelling behaviors (high swelling ratio and fast deswelling rate) should be achieved simultaneously.

Recently,it is succeeded in synthesizing a new type of PNIPAAm hydrogel with almost ideal properties. The novel hydrogel was a nanocomposite type hydrogel. The NC gel is composed of PNIPAAm, inorganic clay, and water, in which the exfoliated inorganic clay acts as an effective multifunctional cross-linker. The model is based on a uniform dispersion of exfoliated inorganic clay in an aqueous medium and PNIPAAm chains grafted on the clay surface at one or both ends. NC gels mainly consist of polymer chains connecting neighboring clay sheets. In other words, polymer chains are effectively cross-linked by clay sheets. Also, because of the large distance between the clay sheets, all polymer chains in NC gels are long and flexible, adopting random conformations. Thus, the chain lengths between clay sheets may be proportional to the clay-clay interparticle distance (*D*ic) and with a fairly narrow distribution of chain lengths.

In contrast, PNIPAAm chains in conventional hydrogels are randomly cross-linked by a large number of organic cross-linking units and the chain lengths between cross-linking points are short on average and have a wide distribution of chain lengths between random cross-linking points.

Nanocomposite gels could be prepared by in situ free-radical polymerization of *N*-isopropylacrylamide (NIPAAm) in the presence of a water-swollen inorganic clay and without using any organic crosslinker. It is found that because of their unique organic (polymer)/inorganic (clay) network structure, nanocomposite gels exhibit extraordinary mechanical, optical, and swelling/deswelling properties. In this thesis, it is presented the characteristics of nanocomposite gels in more detail, focusing on the effect of crosslinker content, i.e., clay content (C_{clay}). It is shown that all

characteristics of nanocomposite gels exhibit strong dependencies on *C*clay and that the effects of crosslinker content on the properties of nanocomposite gels **[10]**.

The properties of PNIPAAm hydrogels can be modified in several ways. For instance, the degree of swelling and the LCST values can be altered by cross-linking NIPAAm in the presence of comonomers of various degrees of hydrophilicity or by changing the medium properties through the addition of cosolvents, salts, or surfactants. The response rate can be enhanced by preparing hydrogels with a porous structure, containing dangling chains, or, finally, by copolymerizing NIPAAm with suitable monomers. Recently, thermoresponsive composite materials were synthesized by incorporating montmorillonite into PNIPAAm gels in the presence of a chemical crosslinker **[11]**.

1.3.2 Montmorillonite as a Crosslinker

Montmorillonite (MMT) is a natural clay mineral which has a large layer space and has some excellent properties such as good water absorption, swelling, adsorbability, cation exchange, and drug-carrying ability. Montmorillonite (MMT) is a kind of loose-layer silicate. When MMT/polymer is synthesized, the polymer chains entering the space between the layers by diffusion or shear stress effect intercalation polymerization. MMT, which is a hydrophilic, swollen natural clay, lacks affinity with the hydrophobic organic polymer. In general, natural clay has been treated by long alkylchain ammonium salt to replace Na^{+} and Ca^{+2} ions in the clay and render it hydrophobic as an organoclay. It is well known that a number of organic/ inorganic nanocomposites can be prepared by intercalation polymerization from organic polymer and MMT, such as epoxies/MMT, polystyrene/MMT, and polyimide /MMT **[12, 13]**.

It should be uniformly dispersed in an aqueous medium. However, large interactions on the surface of MMT make it easy to agglomerate. But, using the anionic surfactant, SLS, can make MMT uniformly disperse in aqueous medium **[13]**.

In comparison with unfilled polymers, these materials exhibit an unusual improvement in the mechanical properties for filler contents. Therefore, the

incorporation of montmorillonite into hydrogels might improve their mechanical properties, which represent a weak point of these materials **[11]**.

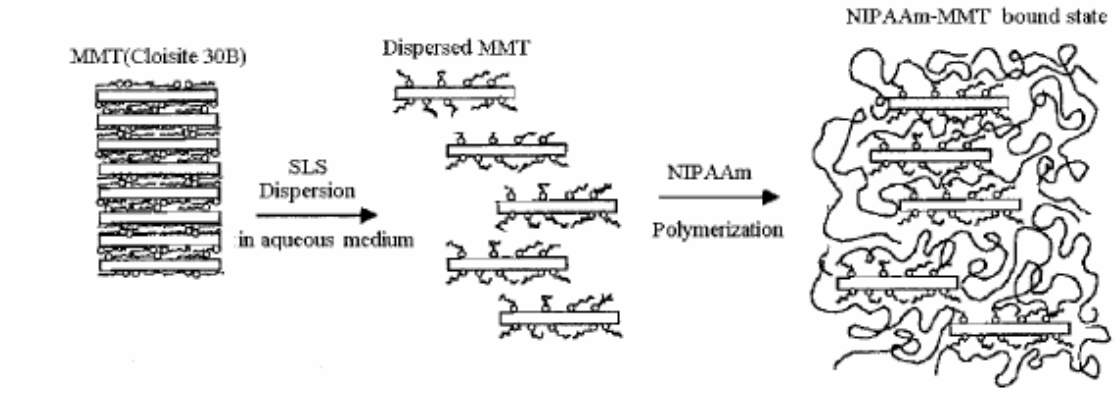

Figure 1.9: Schematic illustration of the formation of NIPAAm / MMT nanocomposite gels.

1.3.2.1 Clays and Clay Modifications

Common clays are naturally occurring minerals and are thus subject to natural variability in their constitution. The purity of the clay can affect final nanocomposite properties. Many clays are aluminosilicates, which have a sheet-like (layered) structure, and consist of silica SiO_4 tetrahedra bonded to alumina AlO_6 octahedra in a variety of ways. A 2:1 ratio of the tetrahedra to the octahedra results in smectite clays, the most common of which is montmorillonite. Other metals such as magnesium may replace the aluminium in the crystal structure. Depending on the precise chemical composition of the clay, the sheets bear a charge on the surface and edges, this charge being balanced by counter-ions, which reside in part in the inter-layer spacing of the clay. The thickness of the layers (platelets) is of the order of 1 nm and aspect ratios are high, typically 100–1500. The clay platelets are truly nanoparticulate. In the context of nanocomposites, it is important to note that the molecular weight of the platelets *(*ca. $1.3x10^8$) is considerably greater than that of typical commercial polymers, a feature which is often misrepresented in schematic diagrams of clay-based nanocomposites. In addition, platelets are not totally rigid, but have a degree of flexibility. The clays often have very high surface areas, up to hundreds of m^2 per gram. The clays are also characterised by their ion (e.g. cation)

exchange capacities, which can vary widely. One important consequence of the charged nature of the clays is that they are generally highly hydrophilic species and therefore naturally incompatible with a wide range of polymer types. A necessary prerequisite for successful formation of polymer-clay nanocomposites is therefore alteration of the clay polarity to make the clay 'organophilic'. An organophilic clay can be produced from a normally hydrophilic clay by ion exchange with an organic cation such as an alkylammonium ion. For example, in montmorillonite, the sodium ions in the clay can be exchanged for an amino acid such as 12-aminododecanoic acid (ADA):

Na^+-CLAY + HO_2C-R-$NH_3^+Cl^-$ → HO_2C-R-NH_3^+-CLAY + NaCl

The way in which this is done has a major effect on the formation of particular nanocomposite product forms and this is discussed further below. Although the organic pre-treatment adds to the cost of the clay, the clays are nonetheless relatively cheap feedstocks with minimal limitation on supply. Montmorillonite is the most common type of clay used for nanocomposite formation; however, other types of clay can also be used depending on the precise properties required from the product. These clays include hectorites (magnesiosilicates), which contain very small platelets, and synthetic clays (e.g. hydrotalcite), which can be produced in a very pure form and can carry a positive charge on the platelets, in contrast to the negative charge found in montmorillonites.

1.3.2.2 Synthetic Processing of Clay-Based Nanocomposites

The synthetic route of choice for making a nanocomposite depends on whether the final material is required in the form of an intercalated or exfoliated hybrid (**Figure 1.10**). In the case of an intercalate, the organic component is inserted between the layers of the clay such that the inter-layer spacing is expanded, but the layers still bear a well-defined spatial relationship to each other. In an exfoliated structure, the layers of the clay have been completely separated and the individual layers are distributed throughout the organic matrix. A third alternative is dispersion of complete clay particles (tactoids) within the polymer matrix, but this simply represents use of the clay as a conventional filler **[14]**.

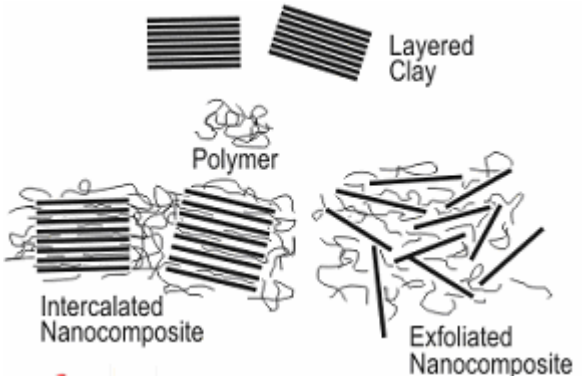

Figure 1.10: Formation of intercalated and exfoliated nanocomposites from layered silicates and polymers.

1.4 Nanocomposites

Polymer materials have been filled with several inorganic synthetic and/or natural compounds in order to increase several properties like heat resistance, mechanical strength and impact resistance or to decrease other properties like electrical conductivity or permeability for gases like oxygen or water vapour. The resulting materials must be seen, however, as filled polymers since there is no or only little interaction between the two mixed components. These filled materials mostly lack from an intense interaction at the interface between the two partners. In general, macroscopic reinforcing elements contain always imperfections. Structural perfection is however more and more reached, if the reinforcing elements become smaller and smaller. The ultimate properties of reinforcing composite elements may be expected, if their dimensions reach atomic or molecular levels. Carbon nanotubes display the so far highest values of elastic modulus (~1.7 TPa). Similar to that, individual clay sheets, being only 1 nm thick (constructed from three metal oxide layers only), display a perfect crystalline structure. However, the smaller the reinforcing composite elements are, the larger is their internal surface and hence their tendency to agglomerate rather than to disperse homogeneously in a matrix. Also, the contact surface in such a dispersion between the elements and the matrix material grows dramatically and consequently the problems in creating an intense interaction at this interface. Anyway, several procedures are known so far to incorporate layered silicate materials in a fine-dispersed manner into polymer matrix materials using

firstly a step of swelling of the layers via an exchange process of the cations located between the crystalline layers against organic onium type cations (**Figure 1.11**).

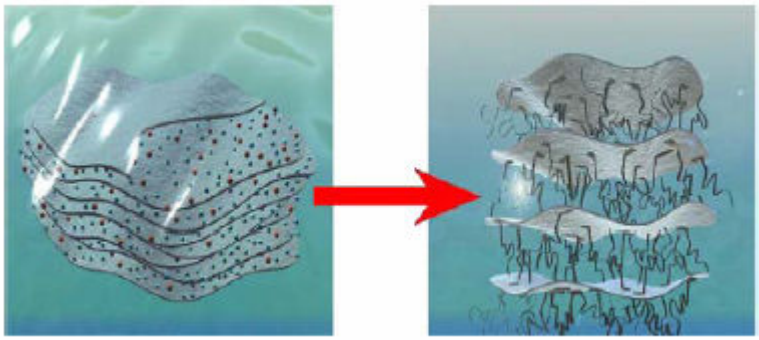

Figure 1.11: Schematic picture of an ion-exchange reaction.

In **Figure 1.11**, the inorganic, relatively small (sodium) ions are exchanged against more voluminous organic onium cations. This ion-exchange reaction has two consequences: firstly, the gap between the single sheets is widened, enabling polymer chains to move in between them and secondly, the surface properties of each single sheet are changed from being hydrophilic to hydrophobic **[15]**.

Those cations are required to have another functional group in order to react with monomers, oligomers or polymers in a subsequent step to separate the platelets completely from each other and / or to form finally the matrix material with homogeneously dispersed platelets (molecular composites) (**Figure 1.12**).

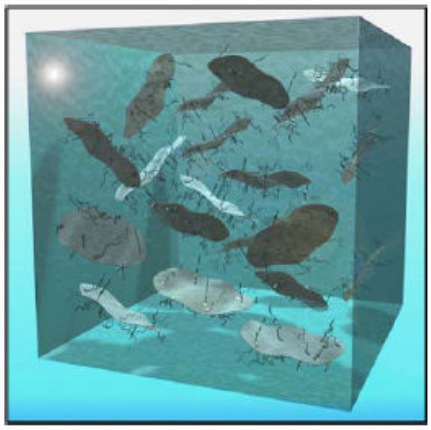

Figure 1.12: Schematic picture of a polymer-clay nanocomposite material with completely exfoliated (molecular dispersed) clay sheets within the polymer matrix material.

In these cases, the growing chains are closely attached (grafted) onto the nano-particles and act as compatibiliser and matrix material at the same time. This scheme can not be applied to all material combinations. Attempts to incorporate nano-particles in a matrix polymer simply by a surface modification of the particles using the ionic interaction with surfactant molecules gained only a moderate success or failed completely. In most of the cases, the natural agglomeration tendency of the nano-particles has either been difficult to overcome or led to thermodynamically instable mixtures. In such systems, three components have to be considered: the particle (surface), the interfacial component (surfactant) and the matrix polymer chains.

Early theoretical work has stated that the entropy loss of the gap, between particles (sheets), penetrating polymer coils will be approximately compensated by the entropy gain of the surfactant molecules in the status of interaction with polymer chains (**Figure 1.13**)

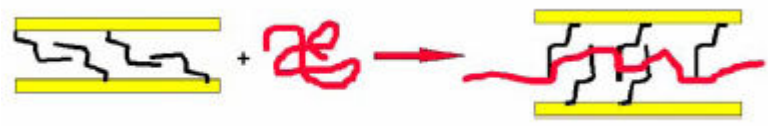

Figure 1.13: Schematic picture of the situation when a polymer chain is entering the gap between two clay sheets (first stage of dispersion).

In **Figure 1.13**, the entropy loss of the polymer (3-D coil will be transferred in 2-D structure) is approximately compensated by the entropy gain of surfactant chains attached on the sheet surface.

The nanoscale, and the associated excitement surrounding nanoscience and technology, affords unique opportunities to create these revolutionary material combinations. These new materials promise to enable the circumvention of classic material performance trade-offs by accessing new properties and exploiting unique synergisms between constituents that only occur when the length scale of the morphology and the critical length associated with the fundamental physics of a given property coincide. From a materials perspective, morphologies that exhibit nanoscopic features are necessary but far from sufficient - the key opportunities are afforded either when (i) the physical size of the material's constituents is engineered

to coincide with the onset of nonbulk-like behavior, such as observed for the size-dependent light emission of quantum dots (QDs), or (ii) when a structure-property relationship approaches a singularity or depends nonlinearly on aspects of the morphology, such as the internal interfacial area.

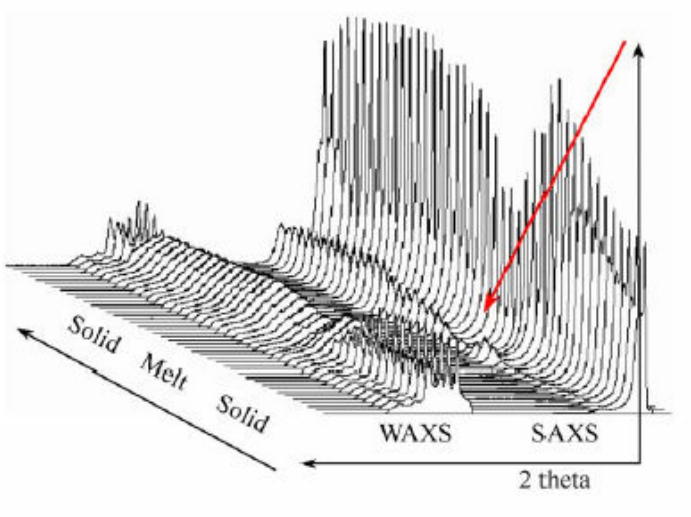

Figure 1.14: In situ experiment of the melting/crystallisation of a clay nanocomposite material.

Figure 1.14, the interaction enthalpy between the surfactant molecules and the polymer chain may be the deciding value for a thermodyamically stable, homogenous incorporation of nano-particles into a matrix material **[15]**.

Polymeric nanocomposites (PNCs) have been an area of intense industrial and academic research for the past 20 years. No matter the measure - articles, patents, or R&D funding - efforts in PNCs have been exponentially growing worldwide over the last ten years. PNCs represent a radical alternative to conventional filled polymers or polymer blends - a staple of the modern plastics industry. In contrast to conventional composites, where the reinforcement is on the order of microns, PNCs are exemplified by discrete constituents on the order of a few nanometers, ~10 000 times finer than a human hair. The value of PNC technology is not solely based on the mechanical enhancement of the neat resin nor the direct replacement of current filler or blend technology. Rather, its importance comes from providing value-added properties not present in the neat resin, without sacrificing the resin's inherent processibility and mechanical properties, or by adding excessive weight. Traditionally, blend or composite attempts at 'multifunctional' materials impose a

trade-off between desired performance, mechanical properties, cost, and processibility. However, over and over again, property suites comparable to, or improved beyond, those common for traditional fillers are reported for PNCs containing substantially less filler (1–5 vol%) and thus enabling greater retention of the inherent processibility and toughness of the neat resin.

Considering the plurality of potential nanoparticles, polymeric resins, and applications, the field of PNCs is immense. For example, **Figure 1.15** presents a hierarchy of nanoparticles based on increasing functionality and thus, the potential to increase the functionality of the polymer matrix.

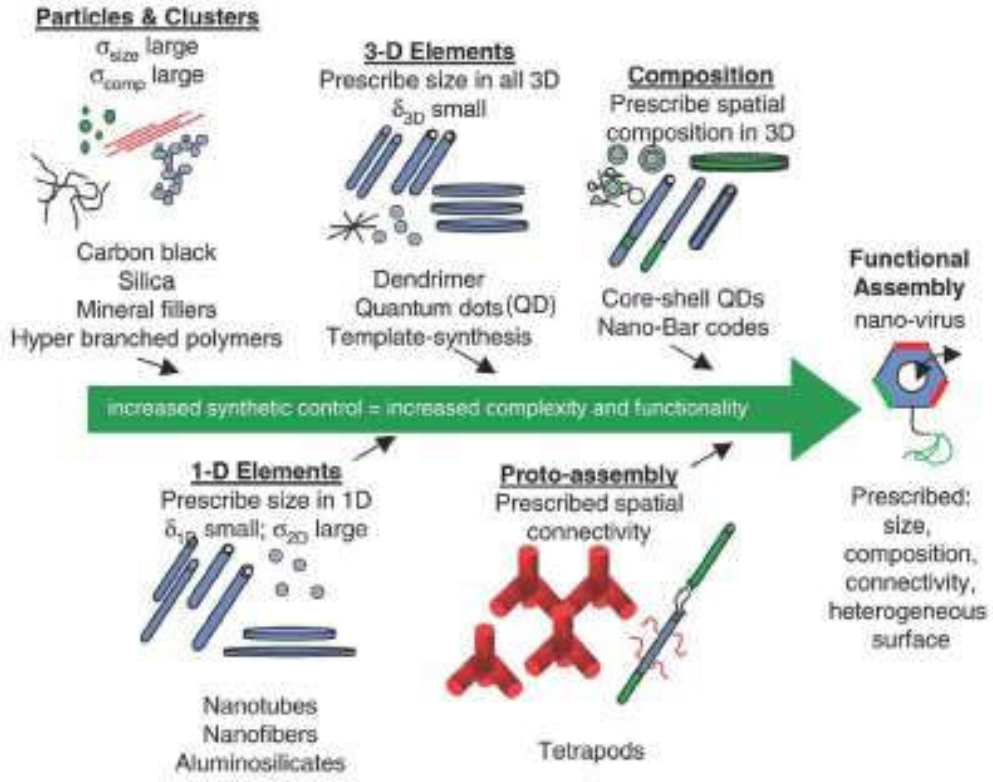

Figure 1.15: Categorization of nanoparticles based on increasing functionality.

In **Figure 1.15**, categorization of nanoparticles based on increasing functionality and thus, potential to increase functionality of the polymer matrix, which in turn is based on increasing spatial and compositional precision in nanoparticle fabrication. Increased complexity and function require increased synthetic control. Nanoscale particles and clusters are polydisperse in size (σ_{size}) and composition (σ_{comp}). One-dimensional elements are compositionally uniform, with narrow size dispersion in

one dimension ($\delta 1_D$), but polydisperse in the other two (σ_{2D}). Three-dimensional elements exhibit narrow size dispersion in all dimensions (δ_{3D}). Rather than compositional uniformity, prescribed composition variation in three dimensions results in tailored functionality, where proto-assembly of any of the aforementioned elements enables the creation of an infinite variety of tailored nanoparticles. Finally, the ultimate active and functional nano-unit would embody the characteristics of a virus - prescribed size, composition, site-specific surface functionality, and dynamic responsivity leading to alteration of the particle's properties, composition, or size **[16]**.

The initial question when beginning to examine polymer nanocomposites is: how are these materials different from classic filled polymers or traditional composites? As anticipated, there is no simple answer; rather 'they are related, but bring new opportunities, perspectives, and issues. Whether tubes (e.g. single- and multi-walled carbon nanotubes, SWNT and MWNTs, respectively) or plates (e.g. exfoliated graphite, layered silicates), the nanoscopic dimensions and extreme aspect ratios inherent in these nanofillers result in six interrelated characteristics distinguishing the resultant PNCs from classic filled systems:

- Low percolation threshold (~ 0.1–2 vol %);
- Particle-particle correlation (orientation and position) arising at low volume fractions ($\varphi_C < 0.001$);
- Large number density of particles per particle volume (10^6–10^8 particles/μm^3);
- Extensive interfacial area per volume of particles (10^3–$10^4 m^2$/ml);
- Short distances between particles (10–50 nm at φ ~ 1–8 vol %);
- Comparable size scales among the rigid nanoparticle inclusion, distance between particles, and the relaxation volume of polymer chains

For spherical nanoparticles, the first two characteristics are not commonly observed because of the small aspect ratio of the particle. Nevertheless, PNCs containing low-aspect ratio nanoparticles are a critical bridge between conventional micron-scale fillers and high-aspect ratio nanoparticles where, from the nanoparticle perspective,

size is reduced and number density is increased prior to the additional complexity of orientational correlations introduced by an extreme aspect ratio. Note that the first two characteristics can manifest in spherical nanoparticles systems also, vis-à-vis innovative processing or proto-assembly of these nanoparticles. Overall, the key concept to answer what a PNC is not specifically embodied within the shape of the particle. To convey the origin and interrelation of these distinguishing characteristics, **Figure 1.16** compares the dominant morphological scale of a classic filled polymer containing 1 pm x 25 pm fibers in an amorphous matrix to that of a nano-filled system at the same volume fraction of filler, but containing 1 nm x 25 nm fibers. There are three main material constituents in any composite: the matrix, the reinforcement (fiber), and the so-called interfacial region. The interfacial region is responsible for 'communication' between the matrix and filler and is conventionally ascribed properties different from the bulk matrix because of its proximity to the surface of the filler.

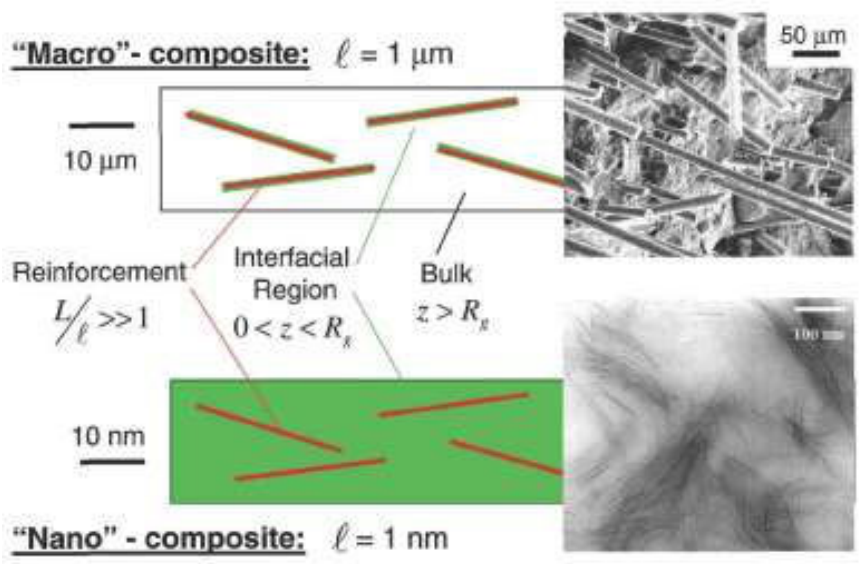

Figure 1.16: Schematic comparison of a 'macro'-composite containing 1 μm x 25 μm (ℓ x L) fibers in an amorphous matrix to that of a 'nano'-composite at the same volume fraction of filler.

In **Figure 1.16**, there are three main material constituents in any composite: the matrix (white), the reinforcement (fiber, red), and the so-called interfacial region (green), which extends (z) into the matrix on the order of R_g, the radius of gyration of the polymer. Scanning electron micrograph shows E-glass reinforced polyolefin (15

μm fiber) and transmission electron micrograph shows montmorillonite-epoxy nanocomposite (1 nm thick layers) **[16]**.

1.5 Characterization of Network Structure

According to the theory of rubber elasticity, the stress–deformation function relationship that applies to swollen gels is the simplified Mooney–Rivlin equation;

$$\tau = G\,(\lambda - \lambda^{-2}) \qquad \textbf{(1)}$$

in which τ is the stress defined as the force per cross sectional area of the undeformed sample, G is the shear modulus and λ is the deformation ratio equal to ℓ / ℓ_0, where ℓ and ℓ_0 are the lengths of the deformed and undeformed hydrogel sample, respectively **[17]**.

In a plot of stress vs. $(\lambda - \lambda^{-2})$, the slope of the curve at small strains is equal to the shear modulus G. Therefore, the initial linear part of the curves is used to fit straight lines and the slope of these lines is used to calculate G.

The strain (positive in extension and negative in compression) is $\Delta\ell/\ell_0$, where $\Delta\ell = \ell - \ell_0$. Also $\Delta\ell/\ell_0 = \lambda - 1$. Hence in the initial linear region of a plot of stress vs. strain, Young's modulus (E) is given as the slope;

$$E = d\tau / d(\Delta\ell/\ell_0) = d\tau / d\lambda \qquad \textbf{(2)}$$

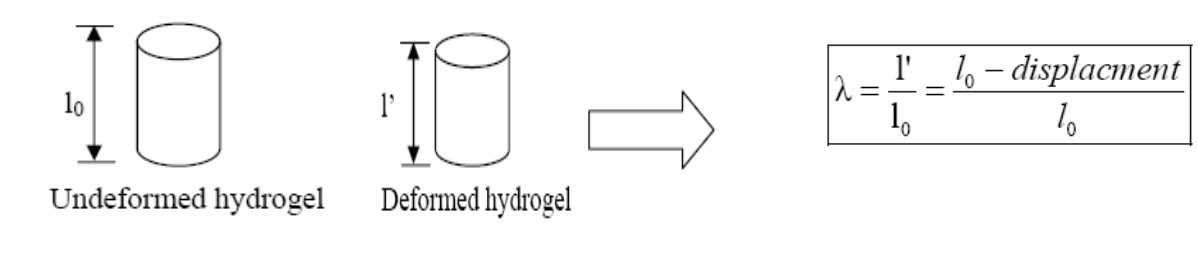

Figure 1.17: Determining of the extension ratio, λ.

As a result of this; Young (or Elastic**,** E) and Shear (G) moduli are estimated in the linear deformation region according to

$$\tau = E(\lambda - 1) \quad \textbf{(3)}$$

and

$$\tau = G(\lambda - \lambda^{-2}) \quad \textbf{(1)}$$

1.5.1 Measurement of Polymer Volume Fractions and Compression Moduli

The effective crosslinking density ν_e is obtained from the results of compression measurements using Mooney–Rivlin equation;

$$\nu_e = G / (RT\, \upsilon_{2s}^{1/3}\, \upsilon_{2r}^{2/3}) \quad \textbf{(4)}$$

in which R is the gas constant, T is absolute temperature, υ_{2r} is the polymer volume fraction in the relaxed state (after preparation) and υ_{2s} is the volume fraction of the polymer in the swollen hydrogel.

$$\upsilon_{2r} = C_0 \overline{M_r} / \rho_2 \quad \textbf{(5)}$$

C_0 is the initial monomer concentration, ρ_2 is the density of the dry polymer and $\overline{M_r}$ is the molecular weight of the repeating unit of hydrogel.

$$\upsilon_{2s} = [1 + Q_d \,.\, \rho_2 / \rho_s] \quad \textbf{(6)}$$

ρ_s is the density of solvent and Q_d is the equilibrium swelling ratio for a gel sample.

$$Q_d = W_s - W_d / W_d \quad \textbf{(7)}$$

where W_d and W_s are weights of the dried sample and weight of the fully swollen sample, respectively.

$$M_c = \rho_2 / \nu_e \quad \textbf{(8)}$$

M_c is the effective molecular weight between crosslinks **[18]**.

$$V_s / V_r = \upsilon_{2r} / \upsilon_{2s} = (d / d_o)^3 \quad \textbf{(9)}$$

V_s and V_r are the gel sample volumes after and before equilibrium swelling, respectively. d and d_o indicate the equilibrium and original diameters of the hydrogels **[19]**.

1.5.2 Flory-Rehner Equilibrium Swelling Equation

The extent of swelling a network undergoes when placed in a good solvent is predicted by various models. The classical Flory-Rehner expression for the swelling of a polymer network, which is based on the assumption of addivitity of the free energy of mixing and free energy of elasticity, can be used to relate the elastic modulus of a network to its swelling behaviour.

For a phantom network at equilibrium;

$$\ln (1- \upsilon_{2s}) + \upsilon_{2s} + \chi (\upsilon_{2s})^2 + (1- 2/\varphi)[V_1 /\nu_e](\upsilon_{2s} / \upsilon_{2r})^{1/3} = 0 \quad \textbf{(10)}$$

According to this model, the polymer–solvent interaction parameter, χ, can be calculated from the following equation;

$$\chi = - [\ln (1- \upsilon_{2s}) + \upsilon_{2s} + \nu_e V_1 \upsilon_{2r} \{(\upsilon_{2s}/ \upsilon_{2r})^{1/3} – (\upsilon_{2s}/ \upsilon_{2r}) (1/2)\}] / \upsilon_{2s}^2 \quad \textbf{(11)}$$

in which V_1 is the molar volume of swelling agent. This equation describes the total interaction (mixing and ionic) of the gel with water. Therefore, temperature, pH and hydrogel chemical composition all significantly affect the value of the interaction parameter **[19, 20].**

2 EXPERIMENTAL SECTION

This study includes the results of the mechanical properties of the NIPAAm hydrogels synthesized by multicrosslinker MMT and activator TEMED.

Starting materials, synthesis procedure and characterization methods are described in the following sections.

2.1 Materials

2.1.1 Activator Agents

2.1.1.1 N,N,N′,N′-tetramethyl ethylenediamine (TEMED)

TEMED was supplied from Sigma-Aldrich GmbH, at ReagentPlus®, 99 % grade. MW: 116.20 g mol^{-1}.

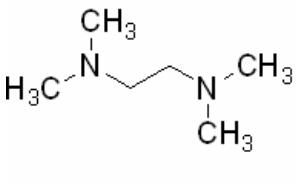

Scheme 2.1: TEMED

2.1.1.2 Quaternized TEMED (QTEMED)

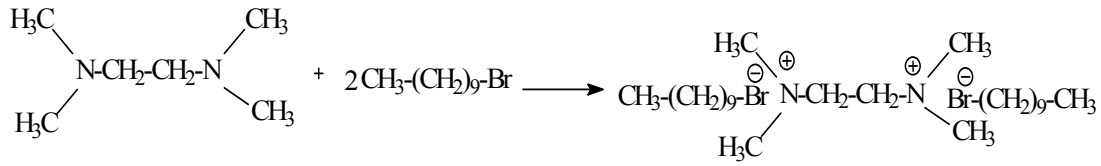

TEMED decil bromide QTEMED

Scheme 2.2: QTEMED

In this work, TEMED and its quaternary salt (cationic surfactant), QTEMED were used as accelerator. QTEMED was synthesized by Senkal group for the project **[21]**.

Characterization of the accelerators, i.e., TEMED and its quaternary ammonium salt QTEMED was achieved by FTIR spectroscopy. The most intense and/or the characteristic bands for alkyl chains were appeared around 2850–2950 cm^{-1} (C-H from CH_2 and CH_3 stretch). Further, new band was observed at 2995 cm^{-1} because of quaternization.

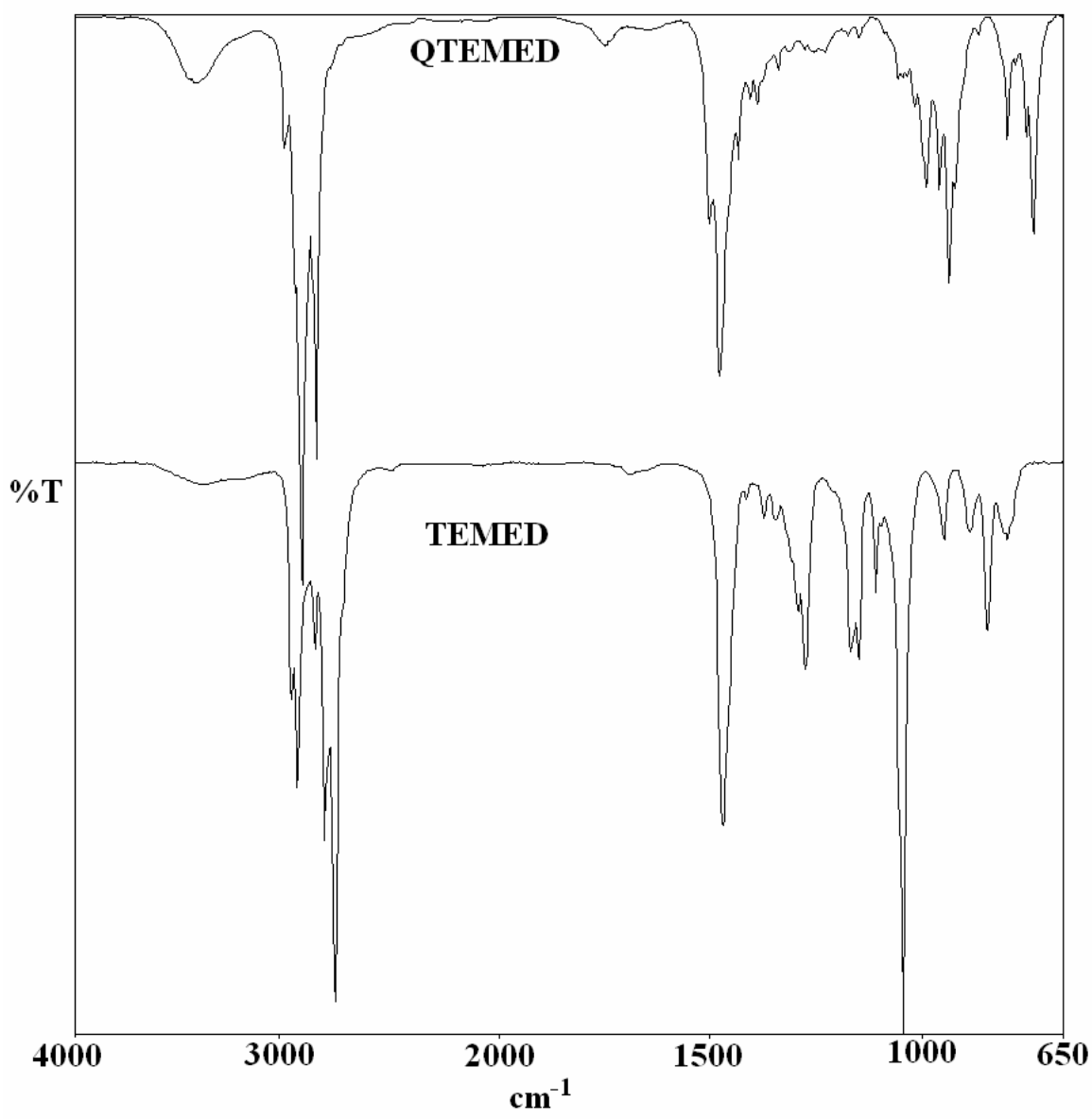

Figure 2.1: FTIR Spectra of QTEMED and TEMED

2.1.2 Monomer, Initiator, Conventional Crosslinker and Multicrosslinker

2.1.2.1 N-isopropylacrylamide (NIPAAm)

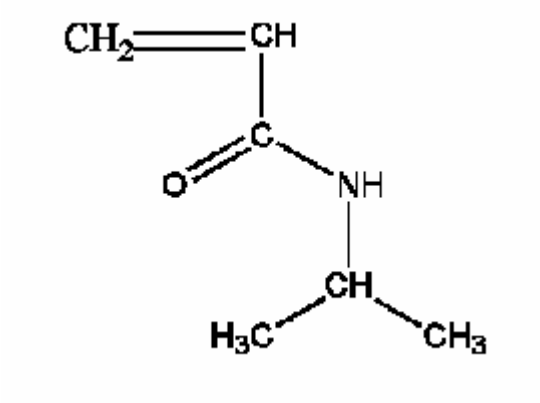

Scheme 2.3: NIPAAm

The product was purchased from Sigma-Aldrich GmbH. MW: 131.16 g mol^{-1}, bp: 120˚C, mp: -55˚C, density: 0.775 g /mL (at 20˚C). The product was used without any further purification.

2.1.2.2 Potassium persulphate (KPS, $K_2S_2O_8$)

The product was purchased from Merck. The reagent (99 %) was used as initiator.

2.1.2.3 Conventional Crosslinker BIS (Methylenebis(acrylamide))

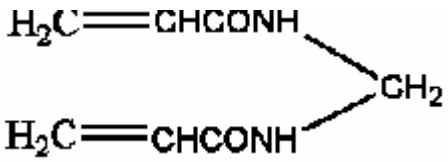

Scheme 2.4: BIS

2.1.2.4 Sodium Montmorillonite (Na^+- MMT)

Synthesised from natural bentonite stepwise purification to sodium montmorillonite by Süd-Chemie with trademark Nanofil 757. The cation exchange capacity (CEC) 80 meq./100 g. Powder has particle size <10 μm and 2,6g cm^{-3} density. The product was used without any further purification.

2.1.2.5 Distilled Water

Distilled water was used as solvent for polymerization synthesis and swelling experiments.

2.1.2.6 Nitrogen (N_2)

Nitrogen gas that is used to avoid O_2 inhibition during the polymerization reactions was purchased from Habaş A.Ş. (99.9 %).

2.2 Swelling and Compression Measurements

The cylindrical NIPAAm hydrogels were cut into pieces of 0.5 cm height. The diameters of the gels were measured by a digital compass. Before the compression measurements, both the conventional and the nanocomposite hydrogel samples were maintained in distilled water at constant temperature to achieve swelling equilibria. Temperatures of the samples (in the range of 25–45˚C) were controlled by using an air oven (BINDER) and by circulating water from an external thermostated water bath (EDMUND BÜHLER) through the double-walls of measuring cell during the swelling equilibria and uniaxial compression measurements, respectively. Elastic and shear moduli of NIPAAm hydrogels crosslinked with BIS, MMT/TEMED and MMT/QTEMED equilibrated in water from 25˚C to 45˚C were determined by means of Hounsfield H5K-S model tensile testing machine, settled a crosshead speed of 1.0 cm/min and a load capacity of 5 N (**Figure 2.2**).

Figure 2.2: Hounsfield H5K-S model tensile testing machine

2.3 Hydrogel Synthesis

Hydrogels were synthesized by free radical solution polymerizations of NIPAAm (0.7 mol/L) using KPS as initiator and, two different crosslinking agent, BIS (conventional crosslinker) and Na^{+}- MMT (multicrosslinker). Three type NIPAAm gels were prepared: (1) The networks made of neutral NIPAAm chains activated by TEMED and crosslinked with hydrophilic tetrafunctional constituent (BIS); (2) the neutral NIPAAm hydrogels containing layered silicate, MMT activated by TEMED; (3) the neutral NIPAAm hydrogels containing layered silicate, MMT activated by QTEMED.

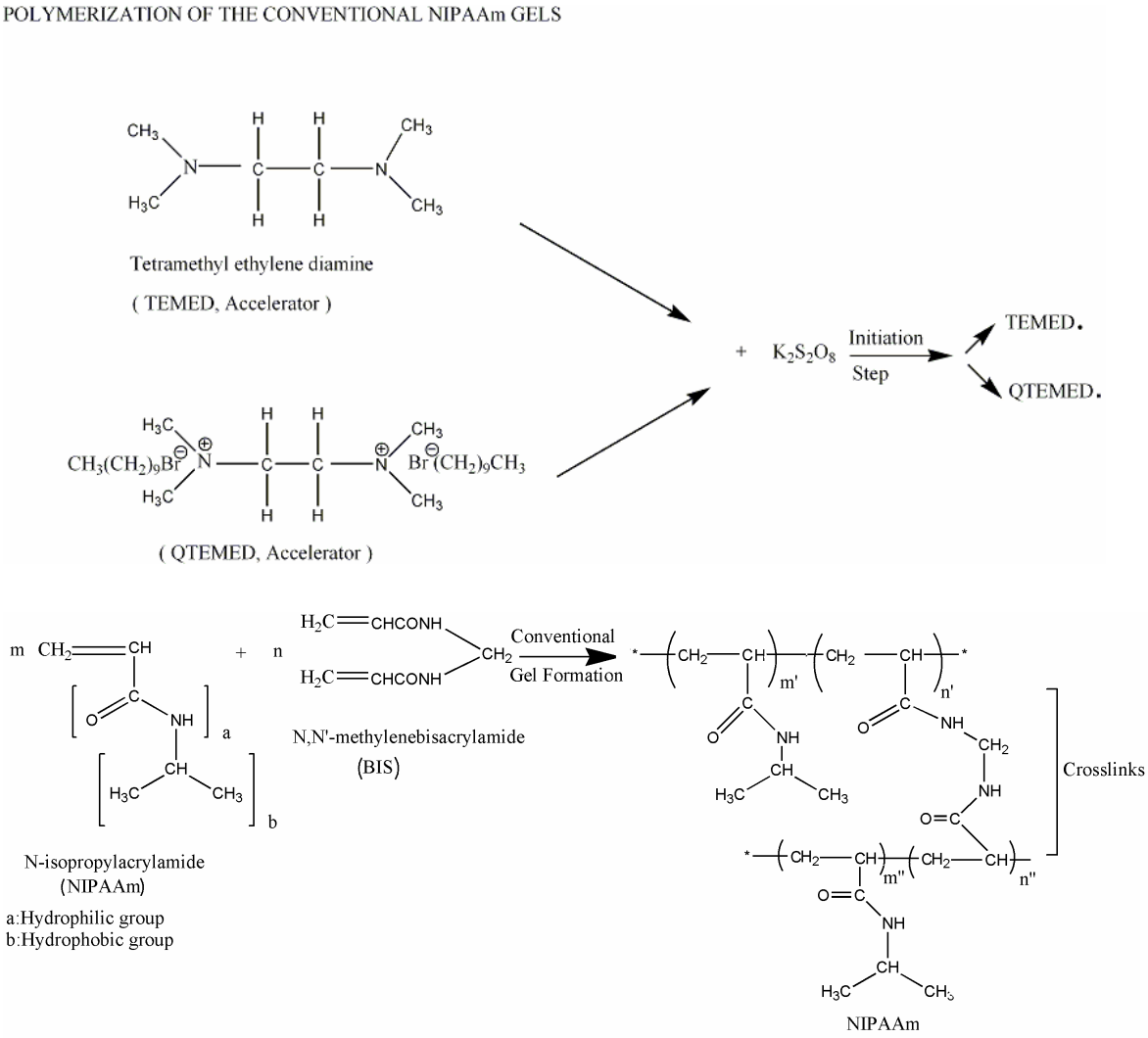

Scheme 2.5 a: Polymerization of conventional NIPAAm Gels

(1) The gelation solutions containing NIPAAm (0.7 mol/L), BIS ($1.25x10^{-2}$ mol/L) and KPS / TEMED ($1.50x10^{-2}$ mol/L, for each constituent of redox initiator pair) were prepared using distilled water as polymerization solvent. The pregel solutions introduced into glass tubes of ~10 mm inner diameter were placed vertically in a large glass tube that was closed tightly with a rubber cap, then filled oxygen-free nitrogen by using a syringe, and placed in a cryostat (JULABO) at 10˚C for 24 hours **(Scheme 2.5 a)**.

(2) The gels were prepared by free radical crosslinking polymerizations at 10˚C and 32˚C under nitrogen atmosphere or air for 1 or 2 days, depending on the MMT/TEMED concentrations. The polymerization mixtures loaded in test tubes with ~10 mm diameter were inserted into large glass tubes equipped with a rubber cap and a syringe. In the case of the gelation solutions containing MMT higher than

1% of total monomer content, polymerizations were carried out into the small beakers and under atmospheric oxygen because of the high reaction rate of the indicated samples **(Scheme 2.5 b** and **Figure 2.3)**.

(3) MMT (1.0 w/v % of total NIPAAm concentration) and QTEMED ($1.50x10^{-2}$ mol/L) were used as multicrosslinker and activator, having cationic surfactant structure. The polymerization solutions were gelated in the same manner used for (1) and (2).

After the reaction periods needed to complete gelation processes, each test tube was broken and the hydrogels were immersed in distilled water to remove linear polymer chains and unreacted constituents. Type (1) includes neutral NIPAAm hydrogels crosslinked with BIS (hydrophilic crosslinker) while Type (2) and (3) represent NIPAAm/MMT hydrogels.

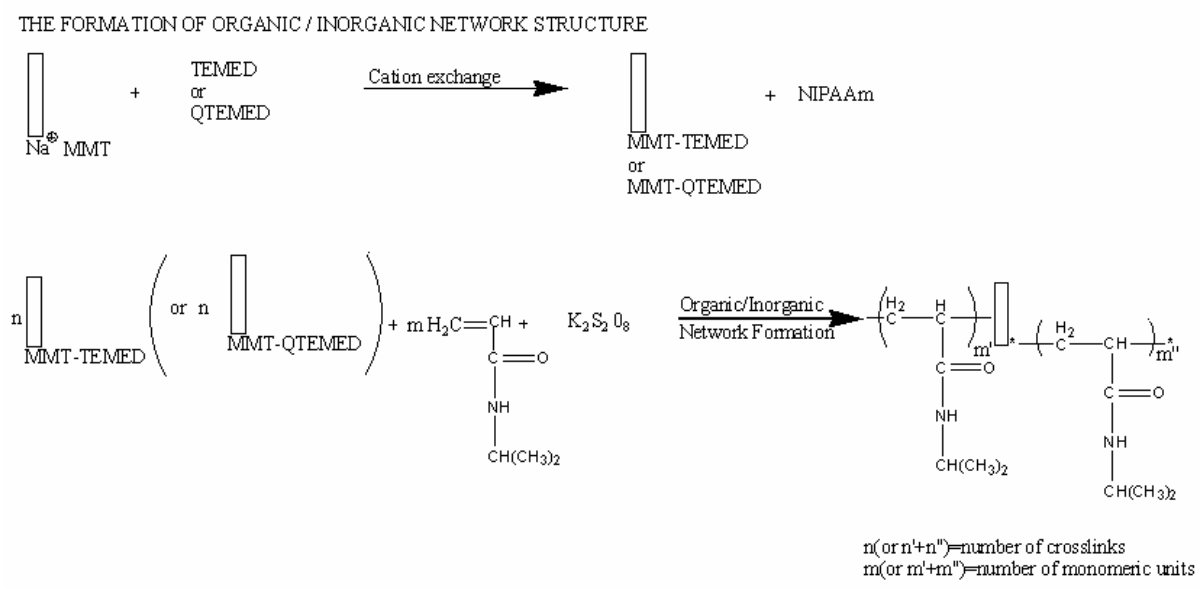

Scheme 2.5 b: Formation of organic/inorganic network structure

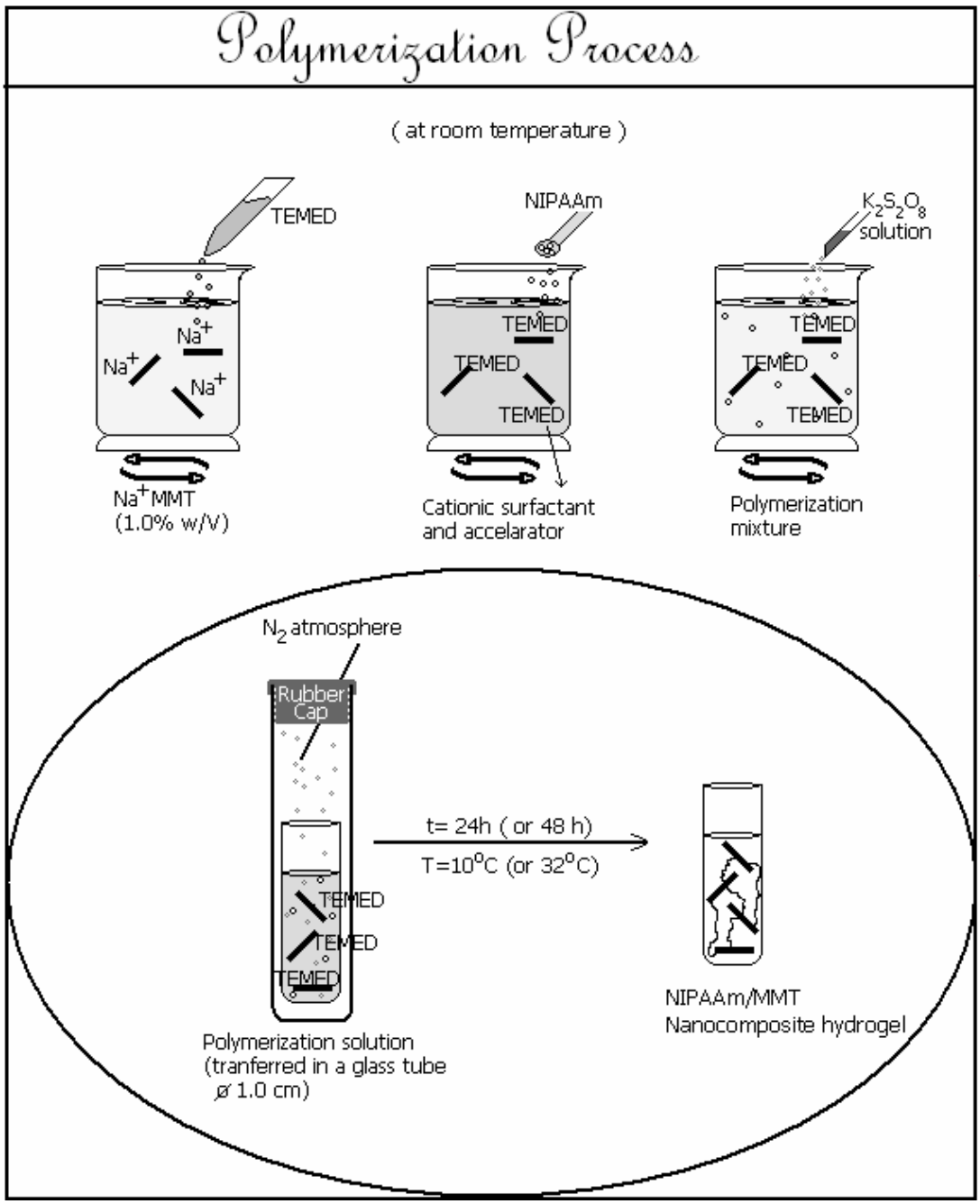

Figure 2.3: Polymerization process

3 RESULTS AND DISCUSSION

NIPAAm/MMT nanocomposite hydrogels were synthesized by free radical polymerization in aqueous solutions containing different amounts of clay. After the polymerization process, the hydrogels put into a large excess of water swelled while retaining their shapes but not dissolved. This result shows that NIPAAm, TEMED and Na^+ - MMT formed network structures without any conventional crosslinker.

The synthesis conditions, compression moduli obtained from the original Load (N) vs. compression (mm) curves, compression % and stress (kPa) for total load 5 N are given in **Table 3.1**, **Table 3.2** and.**Table 3.3**.

Table 3.1: Effect of Composition on the Mechanical Properties ($T_{swelling}$ = 32˚C)

Sample	Composition	E Modulus (kPa)	Compression % (for total load, 5 N)	Stress (kPa) (for total load, 5 N)
1	BIS + TEMED ($1.50x10^{-2}$ M)	1.7	48.8	57.2
2	MMT + TEMED ($1.50x10^{-2}$ M)	1.3	66.3	32.6
3	BIS + TEMED + MMT ($1.50x10^{-2}$ M)	3.2	74.8	27.5

BIS = $1.25x10^{-2}$M; NIPAAm = 0.7 M; MMT = 1 % (w/v, based on total monomer content); T = 10˚C; t = 24h

The increase in compression % and decreasing stress (kPa, total force) indicate the presence of MMT layers increased the compressibility of NIPAAm hydrogels.

Table 3.2 Effect of Temperature and Time on the Mechanical Properties ($T_{swelling}$ = 32˚C)

Sample	Composition	E Modulus (kPa)	Compression % (for total load, 5 N)	Stress (kPa) (for total load, 5 N)
*4	MMT + TEMED ($1.50x10^{-2}$ M)	0.4	45.2	7.1
5	MMT + TEMED ($1.50x10^{-2}$ M)	0.8	78.3	52.5
6	MMT + TEMED ($3.00x10^{-2}$ M)	0.8	96.5	54.7

NIPAAm = 0.7 M; MMT = 1 % (w/v, based on total monomer content)
T = 32˚C; t = 48 h (except Sample 4) ;* t = 24 h

Table 3.3: Effect of Accelerator Type, Temperature and Time on the Mechanical Properties ($T_{swelling}$ = 32˚C)

Sample	Composition	E Modulus (kPa)	Compression % (for total load, 5 N)	Stress (kPa) (for total load, 5 N)
*2	MMT + TEMED ($1.50x10^{-2}$ M)	1.3	66.3	32.6
*7	MMT + QTEMED ($1.50x10^{-2}$ M)	2.7	36.4	32.5
**4	MMT + TEMED ($1.50x10^{-2}$ M)	0.4	45.2	7.1
**8	MMT + QTEMED ($1.50x10^{-2}$ M)	1.1	91.8	75.0
***9	MMT + QTEMED ($4.50x10^{-2}$ M)	0.5	97.2	42.6

NIPAAm = 0.7 M; MMT = 1 % (w/v, based on total monomer content)
* T = 10^{o}C; t = 24 h
** T =32 ^{o}C; t = 24 h
*** T =32 ^{o}C; t = 48 h

From the comparison of Samples 2 and 9 in Table 3.3.4, it can be seen that the higher polymerization temperature and reaction time (T = 32˚C; t = 48 h) (for the sample containing) increasing amount of QTEMED (hydrophobically modified accelerator) in the structure of MMT (inorganic filler) / NIPAAm (organic constituent) hydrogels improve their elasticities for approximately same stress.

In the nanocomposite PNIPAAm hydrogels synthesized in this thesis, Na^{+}- MMT acts as multicrosslinker in place of organic crosslinker (BIS) as used in conventional PNIPAAm gels. Compression moduli of NIPAAm/MMT hydrogels crosslinked with Na^{+}-MMT equilibrated in water at 25˚C were determined by means of Hounsfield

H5K-S model tensile testing machine. It was not observed any loss of water and changing in temperature during the measurements because of the compression period being less than 1 min., **Figure 2, Figure 3, Figure 3.1 - Figure 3.5, Table 2**, **Table 3** and all figures and tables given in appendix part show a comparison of the mechanical behaviours and network parameters of neutral NIPAAm/MMT nanocomposite hydrogels crosslinked with three different clay content (1, 3 and 5 % clay of total monomer concentration), under uniaxial compression. **Figure A. 1**, **Figure A. 3**, **Figure A. 6**, **Figure A. 9**, **Figure A. 12**, **Figure A. 15**, **Figure A. 18**, **Figure A. 21**, **Figure A. 24**, **Figure A. 27**, **Figure A. 30**, **Figure A. 33**, **Figure A. 36**, **Figure A. 39** and **Figure A. 42** show the measured force (F) for compressing samples (2, 10, 11), (5, 12, 13), (6, 14, 15) at 25, 32, 37, 40 and 45˚C, respectively. Forces (F) or loads (N) corresponding to compressions (mm) were obtained from the original curves of uniaxial compression experiments. Pressure (Pa)- strain, -(λ-1) and Pressure (Pa) – linear deformation factor , -($\lambda - \lambda^{-2}$) plots of all samples were drawn by using the data obtained from the linear portions of Load (N) versus compression (mm) curves (**Figure A. 2**, **Figure A. 4**, **Figure A. 5**, **Figure A. 7**, **Figure A. 8**, **Figure A. 10**, **Figure A. 11**, **Figure A. 13**, **Figure A. 14**, **Figure A. 16**, **Figure A. 17**, **Figure A. 19**, **Figure A. 20**, **Figure A. 22**, **Figure A. 23**, **Figure A. 25**, **Figure A. 26**, **Figure A. 28**, **Figure A. 29**, **Figure A. 31**, **Figure A. 32**, **Figure A. 34**, **Figure A. 35**, **Figure A. 37**, **Figure A. 38**, **Figure A. 40**, **Figure A. 41**, **Figure A. 43**, **Figure A. 44**, **Figure 2**). The slopes of these straight lines, i.e. compression moduli E and shear moduli G were calculated from the equations **(3)** and **(1)** respectively. Shear moduli G, polymer volume fractions at equilibrium and relaxed states and equation **(4)** were used to compute the effective network concentration, ν_e.

To understand the effect of reaction Temperature (10˚C and 32˚C), clay content 1.0, 3.0 and 5.0 % of MMT (weight percentage based on total monomer content), accelerator type (TEMED and QTEMED) and MMT/TEMED ratio on the mechanical performance and swelling properties of neutral NIPAAm/MMT nanocomposite hydrogels, the parameters υ_{2r}, υ_{2s}, ν_e and χ, which were used to describe the polymer-solvent systems, were calculated from the equations **(4)**–**(6)**, **(11)**.

Table 3.1, Table 3.2 and **Table 3.3** summarize the synthesis conditions and the mechanical properties of neutral NIPAAm/MMT hydrogels crosslinked with conventional crosslinker BIS and multicrosslinker Na^+-MMT. Because reaction time, polymerization temperature and accelerator concentration, i.e., all these reaction parameters modified the mechanical strengths of hydrogels containing 1.0 % of MMT (weight percentage), Samples 2, 5 and 6 containing 1.0 % of Na^+-MMT were chosen to investigate the effect of clay content on the network parameters for three different reaction conditions: $T_{reaction} < T_{room}$; $T_{reaction} > T_{room}$ and higher activator concentration.

It is known that the values of elastic modulus of neutral and/or hydrophobically modified NIPAAm hydrogels increase as the temperature is increased. This mechanical behaviour may be understood by taking into account the negative temperature-dependence of swelling degrees for PNIPAAm hydrogels.

Hydrogen bonding occurs between water molecules and the amide groups of NIPAAm when the temperature is lower than LCST. It means that the absorbed water molecules within the network structure interact with the amide groups on the side chains before the beginning of gel shrinking, ie., hydrophobic hydration. If the solution temperature is increased, absorbed water molecules are released. The entropic contribution of the polymer-water interaction parameter becomes dominant during this period and solubility of polymer chains decrease while χ increase with increasing temperature. This means that the water molecules formed random structure when expelled from the collapsed polymer network and the total entropy of the NIPAAm gel-water system increases. Therefore, the shrinking process above their LCSTs is a spontaneous process for NIPAAm hydrogels.

In this work, the multifunctional component, i.e., Na^+-MMT platelets were incorporated covalently into the gel structures by free radical solution copolymerization method. The effect of increasing reaction temperature, swelling temperature, accelerator and clay content in reducing the polymer-solvent interaction parameter χ and in increasing the compression modulus (E or G) for Samples 5, 12, 13 and Samples 6, 14, 15 was similar to those of the conventional crosslinking agents, i.e. BIS-crosslinked gels. In hyrdogels crosslinked with an organic crosslinker such as BIS, transparency decrease with increase in crosslinker

concentration. This is ascribed to inhomogenity, introduced locally concentrated crosslinking-points. It was observed that in the case of the Samples 5, 12, 13 and Samples 6, 14, 15, increase in both reaction temperature and activator concentration decreased the homogenity of crosslinking. The possible effect of a random crosslinking on the elastic moduli and NIPAAm-water interaction parameters of these networks were estimated by mechanical and swelling measurements. χ parameters (and shrinking degrees) of these samples increased with increase in temperature. Further, the χ parameters were decreased as clay content increased in a manner similar to that in a conventional crosslinking process. This means that for the fixed monomer concentration, increasing clay content, synthesis temperature and accelerator concentration result in an increase in the number of uncrosslinked and/or short chains, being not effected on the elastic moduli of the hydrogels.

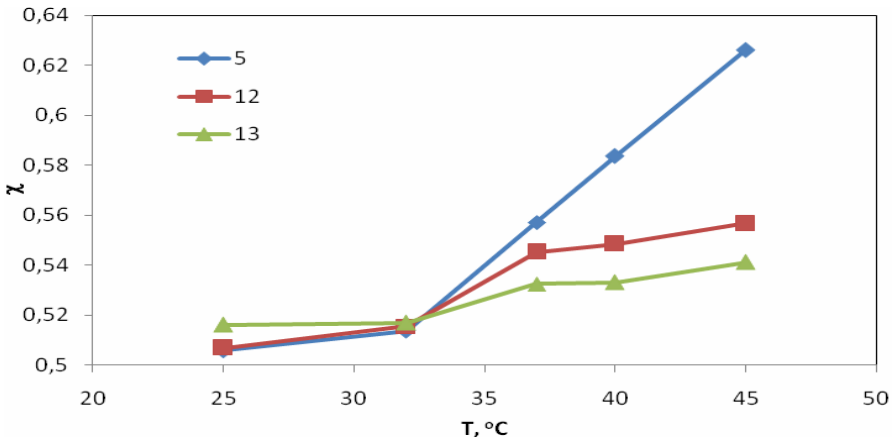

Figure 3.1: χ versus T curves for Samples 5 (1 % MMT), 12 (3 % MMT) and 13 (5 % MMT).

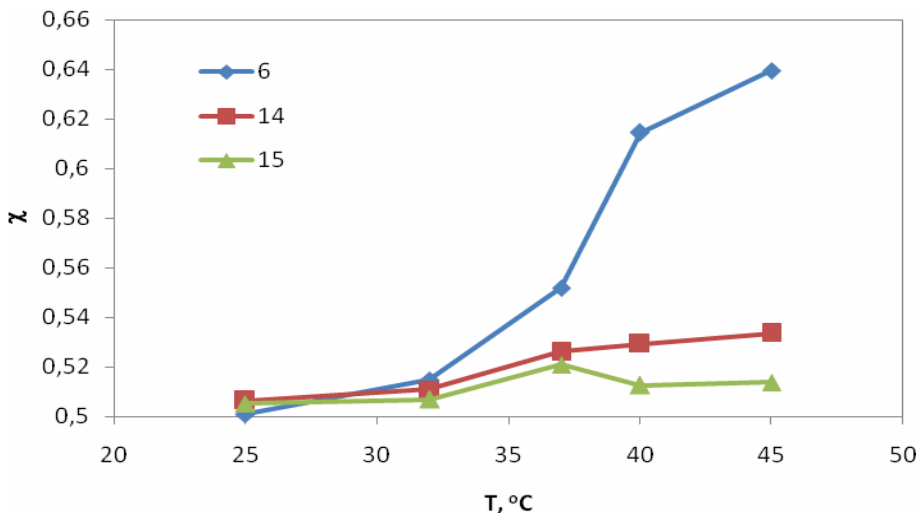

Figure 3.2: χ versus T curves for Samples 6 (1 % MMT), 14 (3 % MMT) and 15 (5 % MMT).

The results shown in these three figures indicate that the higher the temperature the lower is the swelling degree and the higher the interaction parameter. Because the NIPAAm is the main component, swelling degree decrease and the polymer - water interaction parameter increase with increasing temperature. However, the phase transition temperature (or LCST) was not changed by addition more MMT, ie., crosslinker into the gel. Its value is dependent on the type and concentration of comonomers and crosslinkers but not the crosslinker-content. The LCST for the present hydrogels is around the body temperature.

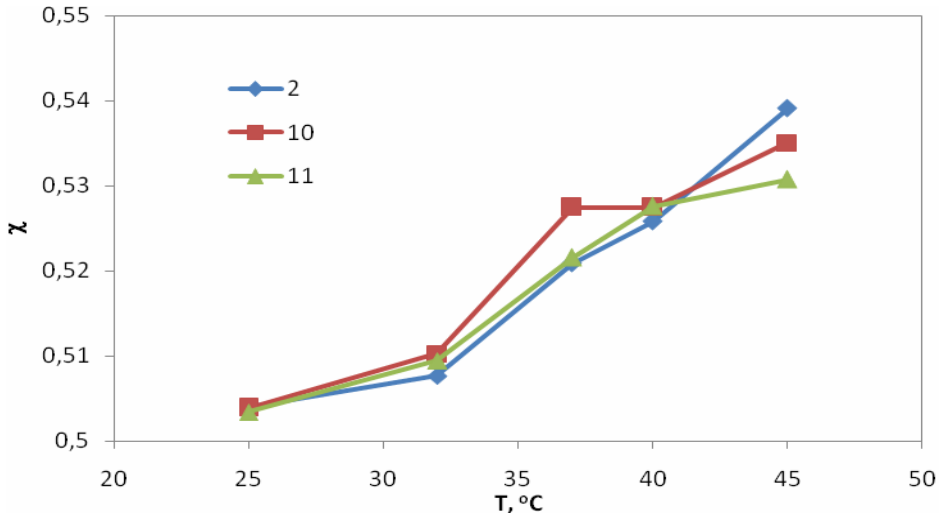

Figure 3.3: χ versus T curves for Samples 2 (1 % MMT), 10 (3 % MMT) and 11 (5 % MMT).

On the other hand, the Samples 5, 12, 13 and 6, 14, 15 synthesized at higher temperatures (T = 32˚C) and higher activator content (TEMED = $3.00x10^{-2}$ M) exhibited a clay content-dependent swelling degree and mechanical strength while Samples 2, 10, 11 showed clay content-independent mechanical and diffusion behaviours.

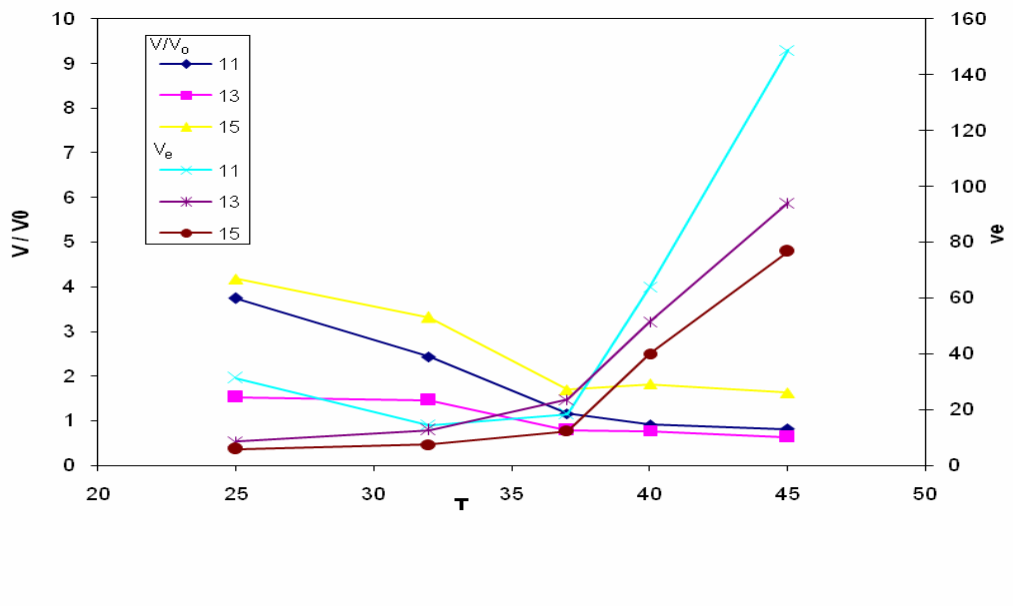

Figure 3.4: V/V_0 and v_e versus T curves for Samples 11 (5 % MMT), 13 (5 % MMT) and 15 (5 % MMT).

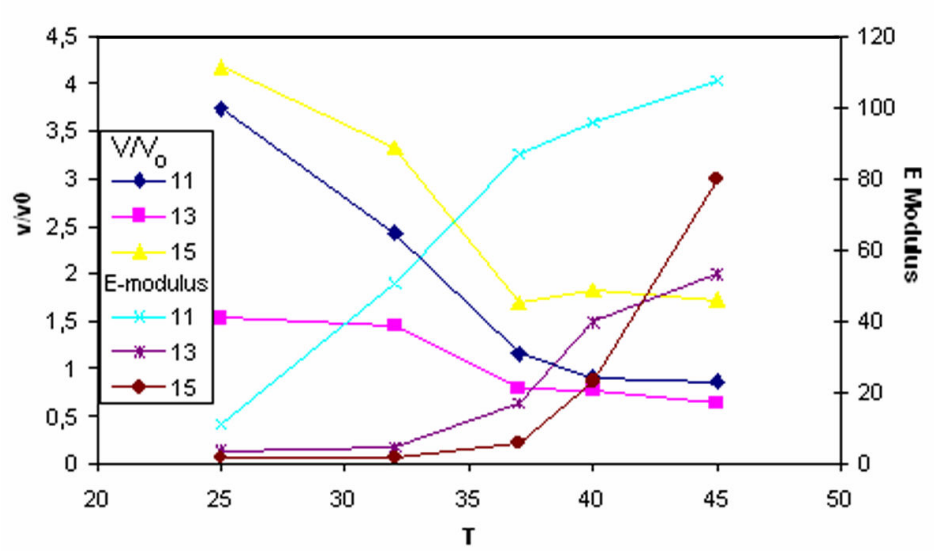

Figure 3.5: V/V_0 and E modulus versus T curves for Samples 11 (5 % MMT), 13 (5 % MMT) and 15 (5 % MMT).

These two graphs summarize the effect of reaction conditions such as $T_{reaction} > T_{room}$ (13), $T_{reaction} < T_{room}$ (11) and higher activator concentration (15) on the elastic modulus and crosslinking density, ie., swelling degree in the range of 25–45˚C for 5 % MMT of total monomer concentration. According to these experimental results,

- swelling degree increase with increase in the polymerization temperature and accelerator concentration whereas number of crosslinks per unit volume and elastic moduli of NIPAAm/MMT hydrogels decrease.

- in the case of the NIPAAm/MMT hydrogels synthesized by lower concentration of TEMED and at 10˚C (Sample 11, 5 % of MMT), swelling degree, crosslinking density and elastic modulus values are higher than the others.

Homogeneous gels have higher elastic moduli than the heterogeneous ones. The inhomogenity, being considered as only one of the factors decreasing mechanical strength, may be optimized or removed by the choice of synthesis method and temperature, comonomer and crosslinker structure.

In the present study, it has been observed that the mechanical performance and swelling degree of NIPAAm hydrogels could be improved by using Na^+-MMT as multi crosslinker and by synthesizing below the room temperature (T = 10˚C).

It is known that for both industrial and biomechanical applications, hydrogels with large water absorption capacity and favourable mechanical properties in the swollen state are required. Usually, an increase in the swelling is accompanied with a decrease in the mechanical properties. These properties can be modified by the type and concentration of crosslinking agent, by varying the preparation method and by chosing hydrophilic or hydrophobic monomers and crosslinkers.

In this work, both TEMED and its quaternary salt (cationic surfactant), QTEMED were used as accelerators. QTEMED were synthesized by Senkal et al **[21]**. **Table 3.3** and **Figure 3.6** show that the mechanical strength of the sample prepared by cationic surfactant QTEMED, containing long alkyl chains and hydrophobically modified is higher than that of the one synthesized using TEMED (T = 10˚C).

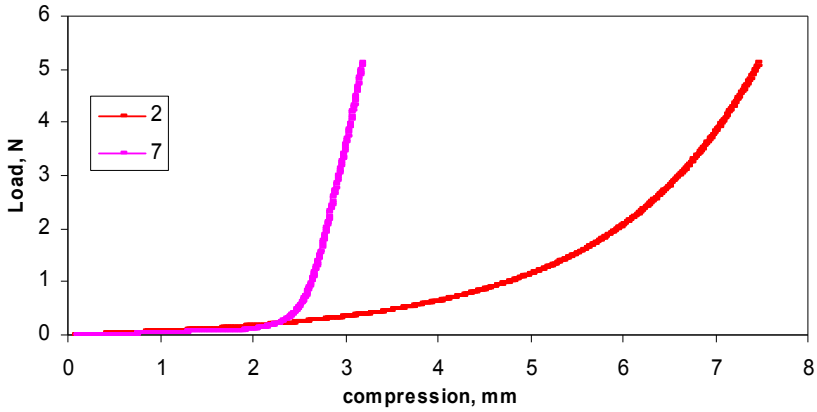

Figure 3.6: Load vs. compression curves for MMT/TEMED (1.50×10^{-2} M)/NIPAAm (0.7 M) (Sample 2) and MMT/QTEMED (1.50×10^{-2}M)/NIPAAm (0.7 M) (Sample 7)

4 CONCLUSION

NIPAAm / Na^+- MMT nanocomposite hydrogels with fixed concentration of NIPAAm (0.7 mol / L) and using three different concentration of Na^+- MMT (1.0, 3.0 and 5.0 % of monomer concentration, in weight %) were synthesized successfully in this thesis. From the foregoing discussions, some conclusions can be drawn as follows:

- Elastic moduli and crosslinking density of these nanocomposite hydrogels increased with an increase of MMT content and temperature.

- The mechanical measurements for the PNIPAAm hydrogels containing equal amounts of MMT indicated that the higher polymerization temperature and accelerator concentration result in the reduction of elastic modulus because of increasing heterogenity.

- For lower reaction temperature and accelerator concentration, both network parameters such as χ, ν_e, υ_{2s} and shear modulus G increased. It can be defined as clay content-independent mechanical and diffusion behaviour.

- The presence of clay platelets shifted to phase transition temperature from 32˚C (for conventional crosslinkers) to body temperature but it did not changed with the concentration of MMT.

- Hydrophobically modified accelerator, QTEMED increased the value of elastic modulus of NIPAAm/MMT hydrogels because of hydrophobic association.

REFERENCES

[1] Hu, Z., 2004. Nanostructed polymer gels, *Macromol. Symp.* **207**, 47–55.

[2] Gupta P., Vermani K. and Garg S., 2002. Hydrogels: from controlled release to pH-responsive drug delivery", *DDT*, **7**, No. 10, 569–571.

[3] Langer R., Peppas N.A., 2003. Advances in biomaterials, drug delivery, and bionanotechnology, *AIChE Journal,* **49**, No. 12, 2990–3006.

[4] Haraguchi K., Farnworth R., Ohbayashi A. and Takehisa T., 2003. Compositional effects on mechanical properties of nanocomposite hydrogels composed of poly(*N*,*N*-dimethylacrylamide) and clay, *Macromolecules,* **36**, 5732–5741.

[5] Lee W.F. and Chen Y.C., 2005. Effect of intercalated hydrotalcite on swelling and mechanical behavior for poly(acrylic acid-*co*-*N*-isopropylacrylamide) / hydrotalcite nanocomposite hydrogels, *Journal of Applied Polymer Science,* **98**, 1572–1580.

[6] Kopecek J. and Yang J., 2007. Review hydrogels as smart biomaterials, *Polymer International,* **56**, 1078–1098.

[7] Tanaka Y., Gong J.P. and Osada Y., 2005. Novel hydrogels with excellent mechanical performance, *Prog. Polym. Sci.,* **30**, 1–9.

[8] Haraguchi K. and Takehisa T., 2002. Nanocomposite hydrogels: A unique organic-inorganic network structure with extraordinary mechanical, optical, and swelling/deswelling properties, *Adv. Mat.,* **14**, No.16, 1120–1123.

[9] Bromberg L.E. and Ron E.S., 1998. Temperature-responsive gels and thermogelling polymer matrices for protein and peptide delivery, *Advanced Drug Delivery Reviews,* **31**, 197–221.

[10] Haraguchi K., Takehisa T. and Fan S., 2002. Effects of clay content on the properties of nanocomposite hydrogels composed of poly(*N*-isopropylacrylamide) and clay, *Macromolecules,* **35**, 10162–10171.

[11] Bignotti F., Sartore L., Penco M., Ramorino G. and Peroni I., 2004. Effect of montmorillonite on the properties of thermosensitive poly(*N* Isopropylacrylamide) composite hydrogels, *Journal of Applied Polymer Science*, **93**, 1964–1971.

[12] Lee W.F. and Fu Y.T., 2003. Effect of montmorillonite on the swelling behavior and drug-release behavior of nanocomposite hydrogels, *Journal of Applied Polymer Science*, **89**, 3652–3660.

[13] Lee W.F. and Jou L.L., 2004. Effect of the intercalation agent content of montmorillonite on the swelling behavior and drug release behavior of nanocomposite hydrogels, *Journal of Applied Polymer Science*, **94**, 74–82.

[14] www.azom.com

[15] Fischer H., 2003. Polymer nanocomposites: from fundamental research to specific applications, *Materials Science and Engineering C*, **23**, 763–772.

[16] Vaia R.A. and Wagnert H.D., 2004. Framework for nanocomposites, *Materials Today ISSN:1369 7021 © Elsevier Ltd*, 32–37.

[17] Skouri R., Schosseler J., Munch J.P. and Candau S.J., 1995. Swelling and elastic properties of polyelectrolyte gels, *Macromolecules*, **28,** 197–210.

[18] Emileh A., Vasheghani-Farahani E. and Imani M., 2007. Swelling behavior, mechanical properties and network parameters of pH- and temperature-sensitive hydrogels of poly((2-dimethyl amino) ethyl methacrylate-co-butyl methacrylate), *European Polymer Journal*, **43**, 1986–1995.

[19] Huglin M.B., Rehab M.M.A.-M. and Zakaria M.B., 1986. Thermodynamic interactions in copolymeric hydrogels, *Macromolecules*, **19**, No: 12, 2986–2991

[20] Schofield P., Cohen C. and Ober C.K., 1998. Synthesis and mechanical properties of semi-flexible polymer networks, *Polymer Gels and Networks*, **6,** 291–300.

[21] Erkal, D., Senkal, F., Sarac, A., 2007. *Macromol. Symp.*, **254**, 141.

APPENDIX

Table A. 1: Effect of Clay Content on the Mechanical Properties ($T_{swelling}$ = 32°C)

Sample	Composition	MMT %	E Modulus (kPa)	Compression % (for total load,5N)	Stress (kPa)
2	MMT + TEMED ($1.50x10^{-2}$M)	1	0.38	34.45	21.00
10	MMT + TEMED ($1.50x10^{-2}$M)	3	5.85	50.94	37.80
11	MMT + TEMED ($1.50x10^{-2}$M)	5	5.73	36.87	36.30

NIPAAm = 0.7 M;T = 10°C (under nitrogen atmosphere); t = 24 h

Table A. 2: Effect of Clay Content on the Network Parameters ($T_{swelling}$ = 32°C)

Sample	Composition	MMT %	G Modulus (kPa)	ν_e (mol/m^3)	χ
2	MMT + TEMED ($1.50x10^{-2}$M)	1	0.09	0.69	0.508
10	MMT + TEMED ($1.50x10^{-2}$M)	3	1.75	12.66	0.510
11	MMT + TEMED ($1.50x10^{-2}$M)	5	1.97	14.53	0.509

NIPAAm = 0.7 M;T = 10°C (under nitrogen atmosphere); t = 24 h

Table A. 3: Effect of Clay Content on the Mechanical Properties ($T_{swelling}$ = 37°C)

Sample	Composition	MMT %	E Modulus (kPa)	Compression % (for total load,5N)	Stress (kPa)
2	MMT + TEMED ($1.50x10^{-2}$M)	1	1.78	40.70	58.10
10	MMT + TEMED ($1.50x10^{-2}$M)	3	35.53	31.09	69.60
11	MMT + TEMED ($1.50x10^{-2}$M)	5	87.07	36.65	59.50

NIPAAm = 0.7 M;T = 10°C (under nitrogen atmosphere); t = 24 h

Table A. 4: Effect of Clay Content on the Network Parameters ($T_{swelling}$ = 37°C)

Sample	Composition	MMT %	G Modulus (kPa)	ν_e (mol/m^3)	χ
2	MMT + TEMED ($1.50x10^{-2}$M)	1	0.55	3.18	0.521
10	MMT + TEMED ($1.50x10^{-2}$M)	3	11.38	60.52	0.527
11	MMT + TEMED ($1.50x10^{-2}$M)	5	3.26	18.74	0.522

NIPAAm = 0.7 M;T = 10°C (under nitrogen atmosphere); t = 24 h

Table A. 5: Effect of Clay Content on the Mechanical Properties ($T_{swelling}$ = 40°C)

Sample	Composition	MMT %	E Modulus (kPa)	Compression % (for total load,5N)	Stress (kPa)
2	MMT + TEMED ($1.50x10^{-2}$M)	1	2.96	38.44	66.40
10	MMT + TEMED ($1.50x10^{-2}$M)	3	7.18	24.93	69.10
11	MMT + TEMED ($1.50x10^{-2}$M)	5	40.78	24.26	69.70

NIPAAm = 0.7 M;T = 10°C (under nitrogen atmosphere); t = 24 h

Table A. 6: Effect of Clay Content on the Network Parameters ($T_{swelling}$ = 40°C)

Sample	Composition	MMT %	G Modulus (kPa)	ν_e (mol/m^3)	χ
2	MMT + TEMED ($1.50x10^{-2}$M)	1	0.86	4.70	0.526
10	MMT + TEMED ($1.50x10^{-2}$M)	3	2.30	12.31	0.527
11	MMT + TEMED ($1.50x10^{-2}$M)	5	12.38	65.73	0.528

NIPAAm = 0.7 M;T = 10°C (under nitrogen atmosphere); t = 24 h

Table A. 7: Effect of Clay Content on the Mechanical Properties ($T_{swelling}$ = 45°C)

Sample	Composition	MMT %	E Modulus (kPa)	Compression % (for total load,5N)	Stress (kPa)
2	MMT + TEMED ($1.50x10^{-2}$M)	1	6.66	31.97	86.10
10	MMT + TEMED ($1.50x10^{-2}$M)	3	118.39	23.42	81.00
11	MMT + TEMED ($1.50x10^{-2}$M)	5	107.46	19.52	75.10

NIPAAm = 0.7 M;T = 10°C (under nitrogen atmosphere); t = 24 h

Table A. 8: Effect of Clay Content on the Network Parameters ($T_{swelling}$ = 45°C)

Sample	Composition	MMT %	G Modulus (kPa)	ν_e (mol/m^3)	χ
2	MMT + TEMED ($1.50x10^{-2}$M)	1	2.33	11.37	0.537
10	MMT + TEMED ($1.50x10^{-2}$M)	3	36.78	184.72	0.533
11	MMT + TEMED ($1.50x10^{-2}$M)	5	30.28	158.14	0.529

NIPAAm = 0.7 M;T = 10°C (under nitrogen atmosphere); t = 24 h

Table A. 9: Effect of Clay Content on the Mechanical Properties ($T_{swelling}$ = 25°C)

Sample	Composition	MMT %	E Modulus (kPa)	Compression % (for total load,5N)	Stress (kPa)
5	MMT + TEMED ($1.50x10^{-2}$M)	1	1.76	32.45	26.40
12	MMT + TEMED ($1.50x10^{-2}$M)	3	1.67	32.88	31.00
13	MMT + TEMED ($1.50x10^{-2}$M)	5	3.74	26.74	15.40

NIPAAm = 0.7 M; T = 32°C (under atmospheric oxygen); t = 48h

Table A. 10: Effect of Clay Content on the Network Parameters ($T_{swelling}$ = 25°C)

Sample	Composition	MMT %	G Modulus (kPa)	ν_e (mol/m^3)	χ
5	MMT + TEMED ($1.50x10^{-2}$M)	1	0.05	4.27	0.506
12	MMT + TEMED ($1.50x10^{-2}$M)	3	0.74	6.03	0.507
13	MMT + TEMED ($1.50x10^{-2}$M)	5	1.32	8.35	0.516

NIPAAm = 0.7 M;T = 32°C (under atmospheric oxygen); t = 48 h

Table A. 11: Effect of Clay Content on the Mechanical Properties ($T_{swelling}$ = 32°C)

Sample	Composition	MMT %	E Modulus (kPa)	Compression % (for total load,5N)	Stress (kPa)
5	MMT + TEMED ($1.50x10^{-2}$M)	1	1.33	33.91	44.40
12	MMT + TEMED ($1.50x10^{-2}$M)	3	1.10	42.32	48.00
13	MMT + TEMED ($1.50x10^{-2}$M)	5	4.76	21.43	12.70

NIPAAm = 0.7 M;T = 32°C (under atmospheric oxygen); t = 48 h

Table A. 12: Effect of Clay Content on the Network Parameters ($T_{swelling}$ = 32°C)

Sample	Composition	MMT %	G Modulus (kPa)	ν_e (mol/m^3)	χ
5	MMT + TEMED ($1.50x10^{-2}$M)	1	0.63	4.17	0.514
12	MMT + TEMED ($1.50x10^{-2}$M)	3	0.32	2.04	0.516
13	MMT + TEMED ($1.50x10^{-2}$M)	5	2.04	12.65	0.517

NIPAAm = 0.7 M;T = 32°C (under atmospheric oxygen); t = 48 h

Table A. 13: Effect of Clay Content on the Mechanical Properties ($T_{swelling}$ = 37°C)

Sample	Composition	MMT %	E Modulus (kPa)	Compression % (for total load,5N)	Stress (kPa)
5	MMT + TEMED ($1.50x10^{-2}$M)	1	18.97	20.18	107.80
12	MMT + TEMED ($1.50x10^{-2}$M)	3	36.52	24.70	94.00
13	MMT + TEMED ($1.50x10^{-2}$M)	5	16.86	16.79	19.20

NIPAAm = 0.7 M;T = 32°C (under atmospheric oxygen); t = 48 h

Table A. 14: Effect of Clay Content on the Network Parameters ($T_{swelling}$ = 37°C)

Sample	Composition	MMT %	G Modulus (kPa)	ν_e (mol/m^3)	χ
5	MMT + TEMED ($1.50x10^{-2}$M)	1	6.40	27.32	0.557
12	MMT + TEMED ($1.50x10^{-2}$M)	3	9.84	45.03	0.545
13	MMT + TEMED ($1.50x10^{-2}$M)	5	4.73	23.97	0.533

NIPAAm = 0.7 M;T = 32°C (under atmospheric oxygen); t = 48 h

Table A. 15: Effect of Clay Content on the Mechanical Properties ($T_{swelling}$ = 40°C)

Sample	Composition	MMT %	E Modulus (kPa)	Compression % (for total load,5N)	Stress (kPa)
5	MMT + TEMED ($1.50x10^{-2}$M)	1	6.00	14.72	134.30
12	MMT + TEMED ($1.50x10^{-2}$M)	3	23.12	21.77	97.80
13	MMT + TEMED ($1.50x10^{-2}$M)	5	39.61	12.43	19.50

NIPAAm = 0.7 M;T = 32°C (under atmospheric oxygen); t = 48 h

Table A. 16: Effect of Clay Content on the Network Parameters ($T_{swelling}$ = 40°C)

Sample	Composition	MMT %	G Modulus (kPa)	ν_e (mol/m^3)	χ
5	MMT + TEMED ($1.50x10^{-2}$M)	1	1.80	6.90	0.584
12	MMT + TEMED ($1.50x10^{-2}$M)	3	12.48	55.96	0.548
13	MMT + TEMED ($1.50x10^{-2}$M)	5	10.51	52.86	0.533

NIPAAm = 0.7 M;T = 32°C (under atmospheric oxygen); t = 48 h

Table A. 17: Effect of Clay Content on the Mechanical Properties ($T_{swelling}$ = 45°C)

Sample	Composition	MMT %	E Modulus (kPa)	Compression % (for total load,5N)	Stress (kPa)
5	MMT + TEMED ($1.50x10^{-2}$M)	1	115.14	10.58	167.20
12	MMT + TEMED ($1.50x10^{-2}$M)	3	24.68	20.22	107.30
13	MMT + TEMED ($1.50x10^{-2}$M)	5	53.31	9.85	22.00

NIPAAm = 0.7 M;T = 32°C (under atmospheric oxygen); t = 48 h

Table A. 18: Effect of Clay Content on the Network Parameters ($T_{swelling}$ = 45°C)

Sample	Composition	MMT %	G Modulus (kPa)	ν_e (mol/m^3)	χ
5	MMT + TEMED ($1.50x10^{-2}$M)	1	39.83	139.16	0.617
12	MMT + TEMED ($1.50x10^{-2}$M)	3	79.10	34.53	0.553
13	MMT + TEMED ($1.50x10^{-2}$M)	5	20.87	98.12	0.541

NIPAAm = 0.7 M;T = 32°C (under atmospheric oxygen); t = 48 h

Table A. 19: Effect of Clay Content on the Mechanical Properties ($T_{swelling}$ = 25°C)

Sample	Composition	MMT %	E Modulus (kPa)	Compression % (for total load,5N)	Stress (kPa)
6	MMT + TEMED ($3,00x10^{-2}$M)	1	0.33	25.12	1.00
14	MMT + TEMED ($3,00x10^{-2}$M)	3	0.78	39.03	27.60
15	MMT + TEMED ($3,00x10^{-2}$M)	5	1.67	37.04	25.40

NIPAAm = 0.7 M; T = 32°C (under atmospheric oxygen); t = 48 h

Table A. 20: Effect of Clay Content on the Network Parameters ($T_{swelling}$ = 25°C)

Sample	Composition	MMT %	G Modulus (kPa)	ν_e (mol/m^3)	χ
6	MMT + TEMED ($3,00x10^{-2}$M)	1	0.09	1.23	0.501
14	MMT + TEMED ($3,00x10^{-2}$M)	3	0.40	3.38	0.506
15	MMT + TEMED ($3,00x10^{-2}$M)	5	0.66	5.80	0.505

NIPAAm = 0.7 M;T = 32°C (under atmospheric oxygen); t = 48 h

Table A. 21: Effect of Clay Content on the Mechanical Properties ($T_{swelling}$ = 32°C)

Sample	Composition	MMT %	E Modulus (kPa)	Compression % (for total load,5N)	Stress, (kPa)
6	MMT + TEMED ($3{,}00x10^{-2}$M)	1	1.52	31.86	46.50
14	MMT + TEMED ($3{,}00x10^{-2}$M)	3	1.22	30.84	38.40
15	MMT + TEMED ($3{,}00x10^{-2}$M)	5	1.85	33.85	29.50

NIPAAm = 0.7 M; T = 32°C (under atmospheric oxygen); t = 48 h

Table A. 22: Effect of Clay Content on the Network Parameters ($T_{swelling}$ = 32°C)

Sample	Composition	MMT %	G Modulus (kPa)	ν_e (mol/m^3)	χ
6	MMT + TEMED ($3{,}00x10^{-2}$M)	1	0.72	4.70	0.515
14	MMT + TEMED ($3{,}00x10^{-2}$M)	3	0.38	2.70	0.511
15	MMT + TEMED ($3{,}00x10^{-2}$M)	5	0.92	7.49	0.507

NIPAAm = 0.7 M;T = 32°C (under atmospheric oxygen); t = 48 h

Table A. 23: Effect of Clay Content on the Mechanical Properties ($T_{swelling}$ = 37°C)

Sample	Composition	MMT %	E Modulus (kPa)	Compression % (for total load,5N)	Stress (kPa)
6	MMT + TEMED ($3{,}00x10^{-2}$M)	1	8.93	25.71	101.70
14	MMT + TEMED ($3{,}00x10^{-2}$M)	3	9.03	22.00	66.80
15	MMT + TEMED ($3{,}00x10^{-2}$M)	5	6.01	29.70	46.20

NIPAAm = 0.7 M;T = 32°C (under atmospheric oxygen); t = 48 h

Table A. 24: Effect of Clay Content on the Network Parameters ($T_{swelling}$ = 37°C)

Sample	Composition	MMT %	G Modulus (kPa)	ν_e (mol/m^3)	χ
6	MMT + TEMED ($3{,}00x10^{-2}$M)	1	2.70	11.87	0.552
14	MMT + TEMED ($3{,}00x10^{-2}$M)	3	2.34	12.73	0.526
15	MMT + TEMED ($3{,}00x10^{-2}$M)	5	1.93	12.61	0.514

NIPAAm = 0.7 M;T = 32°C (under atmospheric oxygen); t = 48 h

Table A. 25: Effect of Clay Content on the Mechanical Properties ($T_{swelling}$ = 40°C)

Sample	Composition	MMT %	E Modulus (kPa)	Compression % (for total load,5N)	Stress (kPa)
6	MMT + TEMED ($3{,}00x10^{-2}$M)	1	6.00	21.60	159.20
14	MMT + TEMED ($3{,}00x10^{-2}$M)	3	44.46	16.79	72.50
15	MMT + TEMED ($3{,}00x10^{-2}$M)	5	23.06	24.80	43.90

NIPAAm = 0.7 M;T = 32°C (under atmospheric oxygen); t = 48 h

Table A. 26: Effect of Clay Content on the Network Parameters ($T_{swelling}$ = 40°C)

Sample	Composition	MMT %	G Modulus (kPa)	ν_e (mol/m^3)	χ
6	MMT + TEMED ($3{,}00x10^{-2}$M)	1	1.66	5.83	0.614
14	MMT + TEMED ($3{,}00x10^{-2}$M)	3	15.36	80.08	0.529
15	MMT + TEMED ($3{,}00x10^{-2}$M)	5	6.13	41.06	0.513

NIPAAm = 0.7 M;T = 32°C (under atmospheric oxygen); t = 48 h

Table A. 27: Effect of Clay Content on the Mechanical Properties ($T_{swelling}$ = 45°C)

Sample	Composition	MMT %	E Modulus (kPa)	Compression % (for total load,5N)	Stress (kPa)
6	MMT + TEMED ($3{,}00x10^{-2}$M)	1	12.44	13.42	176.30
14	MMT + TEMED ($3{,}00x10^{-2}$M)	3	40.65	18.65	78.40
15	MMT + TEMED ($3{,}00x10^{-2}$M)	5	8.03	25.77	47.30

NIPAAm = 0.7 M;T = 32°C (under atmospheric oxygen); t = 48 h

Table A. 28: Effect of Clay Content on the Network Parameters ($T_{swelling}$ = 45°C)

Sample	Composition	MMT %	G Modulus (kPa)	ν_e (mol/m^3)	χ
6	MMT + TEMED ($3{,}00x10^{-2}$M)	1	3.75	12.75	0.629
14	MMT + TEMED ($3{,}00x10^{-2}$M)	3	10.23	52.21	0.531
15	MMT + TEMED ($3{,}00x10^{-2}$M)	5	5.40	35.47	0.514

NIPAAm = 0.7 M;T = 32°C (under atmospheric oxygen); t = 48 h

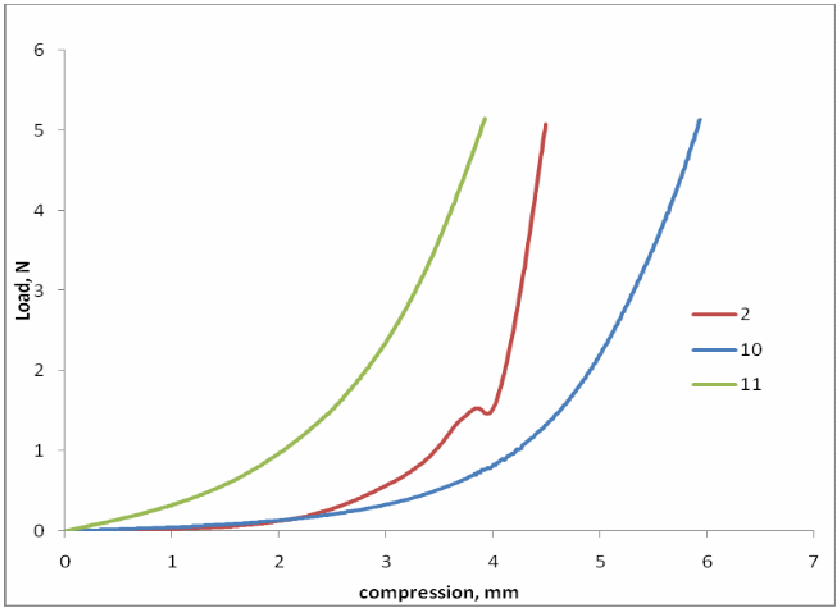

Figure A. 1: Measured force, F (N) as a function of compression (mm) for Samples 2, 10, 11 (T = 25˚C).

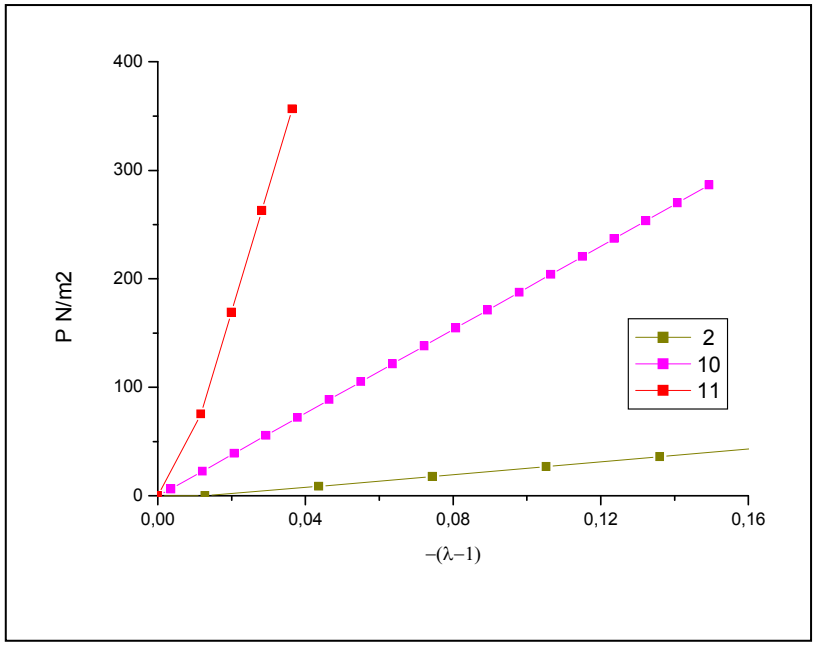

Figure A. 2: Compression stress-strain curves (Pressure (Pa) vs. -(λ – 1)) for Samples 2, 10, 11 (T = 25˚C)

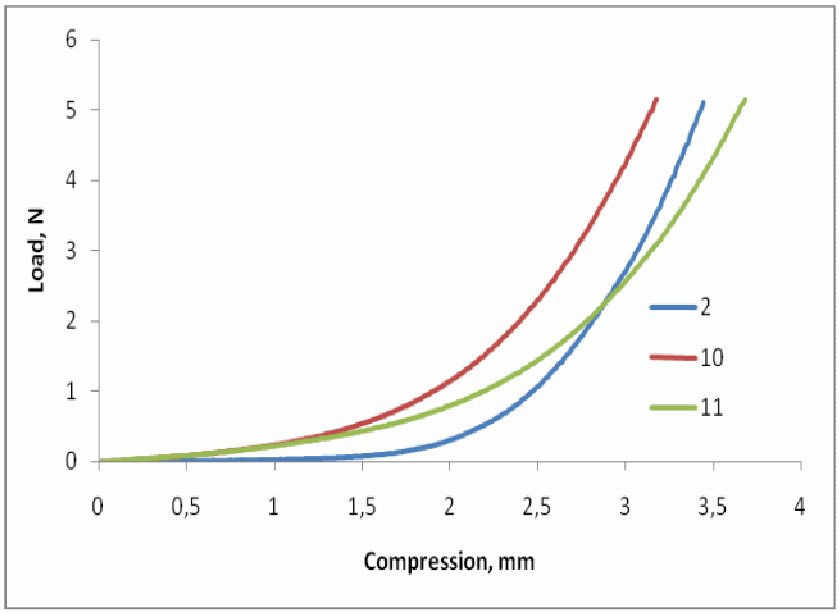

Figure A. 3: Measured force, F (N) as a function of compression (mm) for Samples 2, 10, 11 (T = 32˚C).

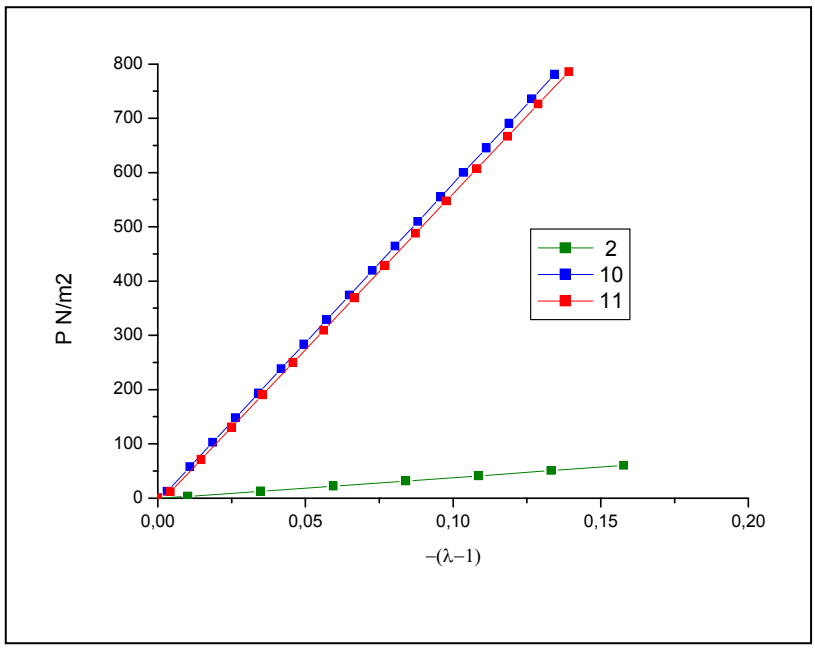

Figure A. 4: Compression stress-strain curves (Pressure (Pa) vs. -(λ – 1)) for Samples 2, 10, 11 (T = 32˚C)

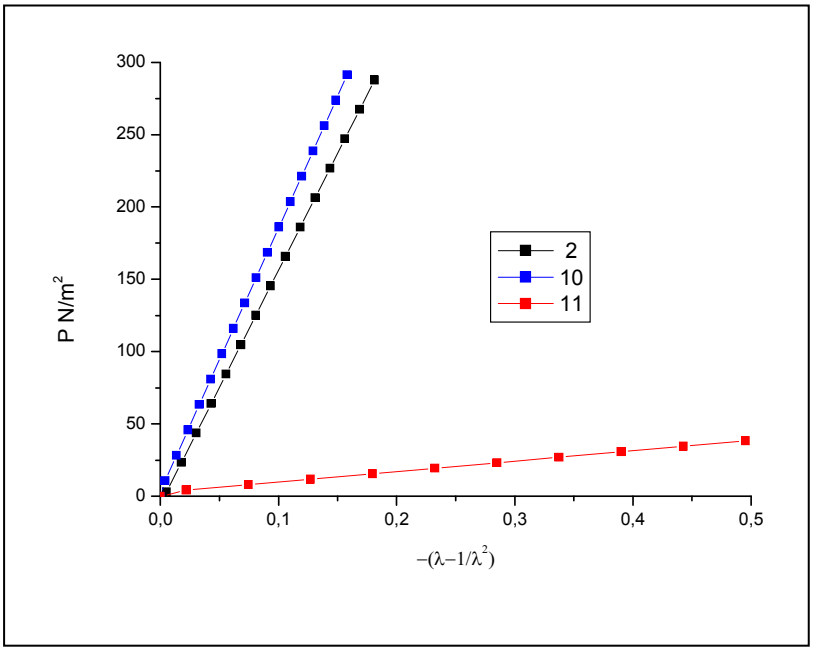

Figure A. 5: Compression stress-strain curves (Pressure (Pa) vs. $-(\lambda - \lambda^{-2})$) for Samples 2, 10, 11 (T = 32˚C)

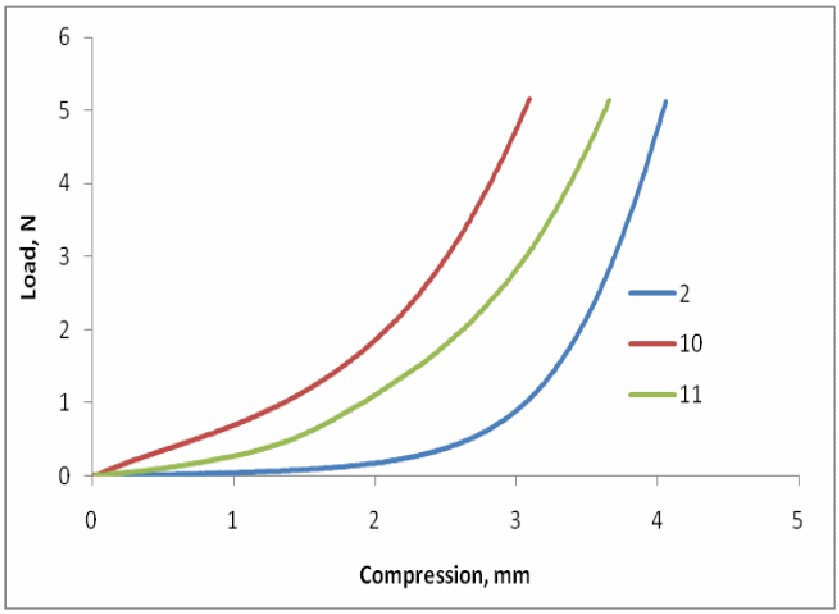

Figure A. 6: Measured force, F (N) as a function of compression (mm) for Samples 2, 10, 11 (T = 37˚C).

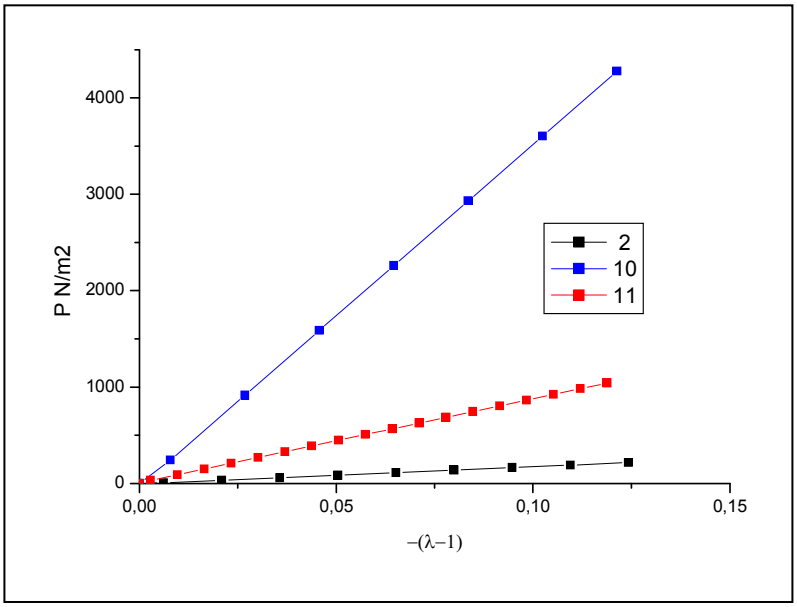

Figure A. 7: Compression stress-strain curves (Pressure (Pa) vs. -(λ – 1)) for Samples 2, 10, 11 (T = 37˚C)

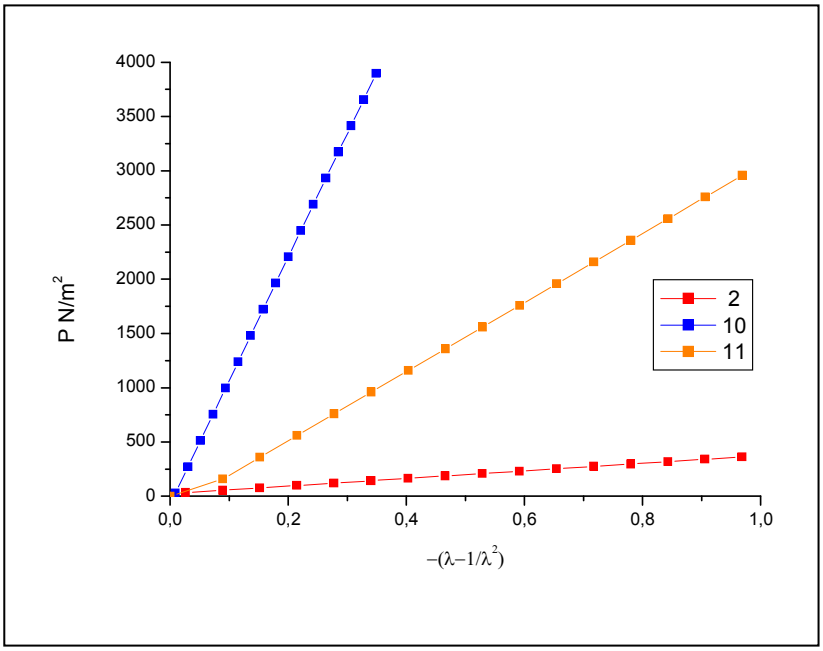

Figure A. 8: Compression stress-strain curves (Pressure (Pa) vs. -(λ – λ^{-2})) for Samples 2, 10, 11 (T = 37˚C)

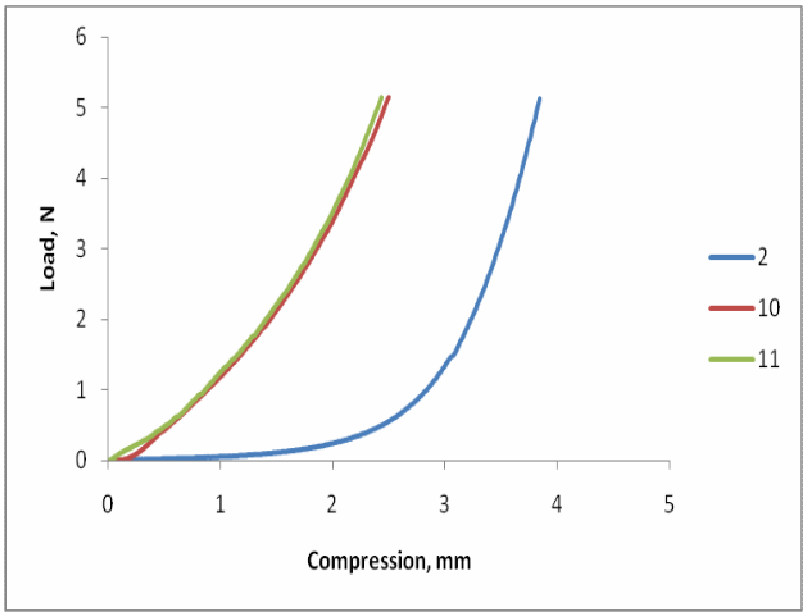

Figure A. 9: Measured force, F (N) as a function of compression (mm) for Samples 2, 10, 11 (T = 40˚C).

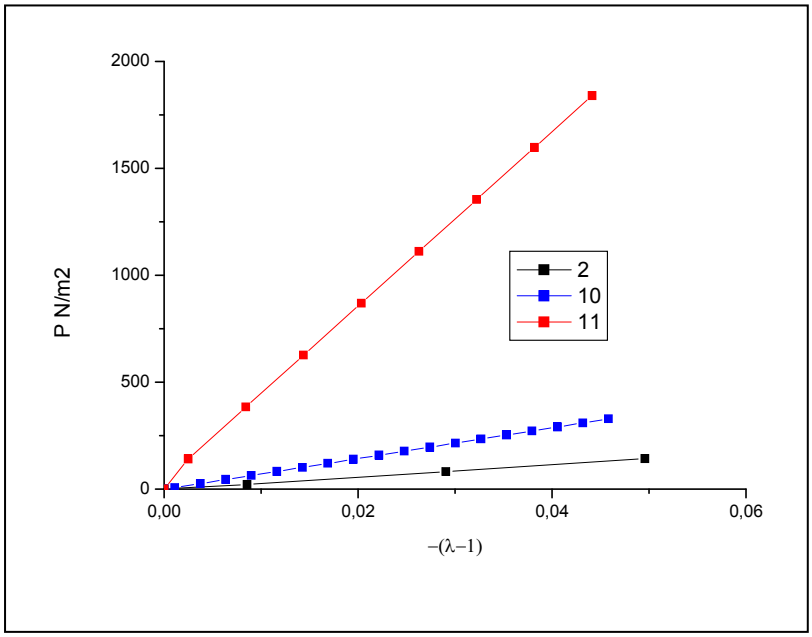

Figure A. 10: Compression stress-strain curves (Pressure (Pa) vs. -(λ – 1)) for Samples 2, 10, 11 (T = 40˚C)

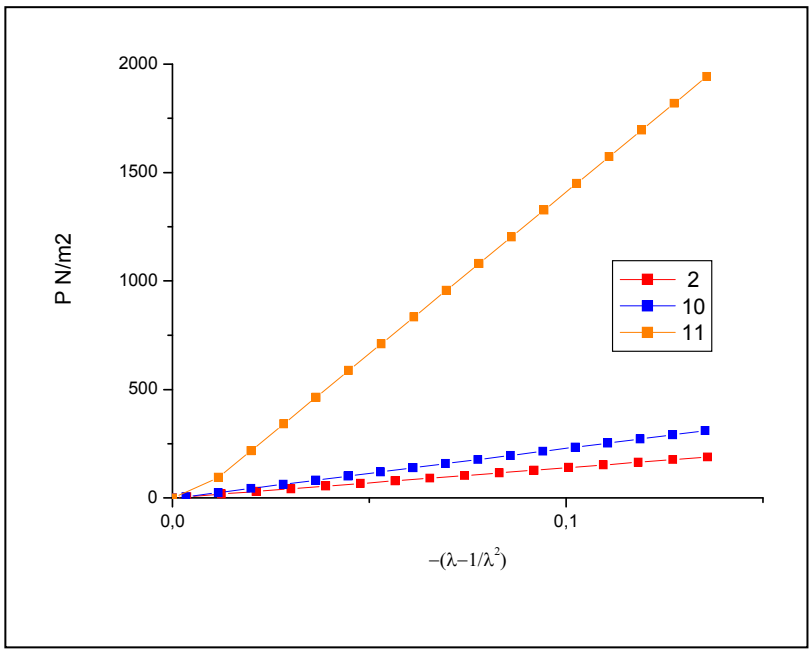

Figure A. 11: Compression stress-strain curves (Pressure (Pa) vs. $-(\lambda - \lambda^{-2})$) for Samples 2, 10, 11 (T = 40˚C)

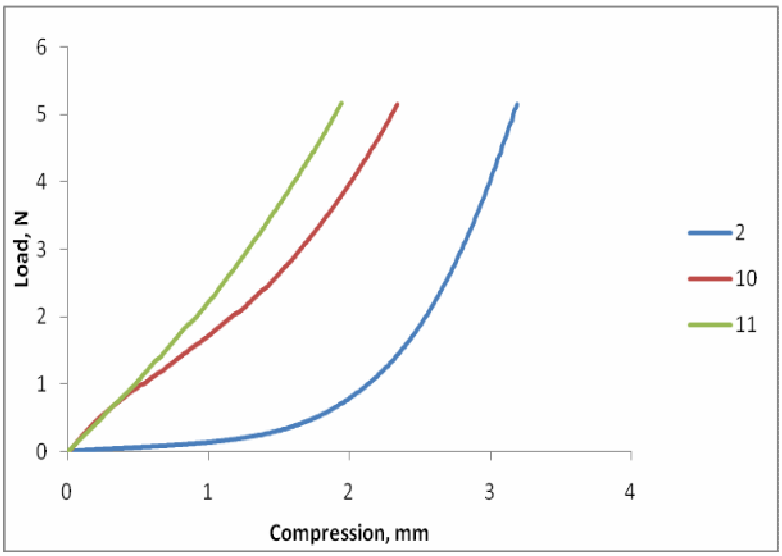

Figure A. 12: Measured force, F (N) as a function of compression (mm) for Samples 2, 10, 11 (T = 45˚C)

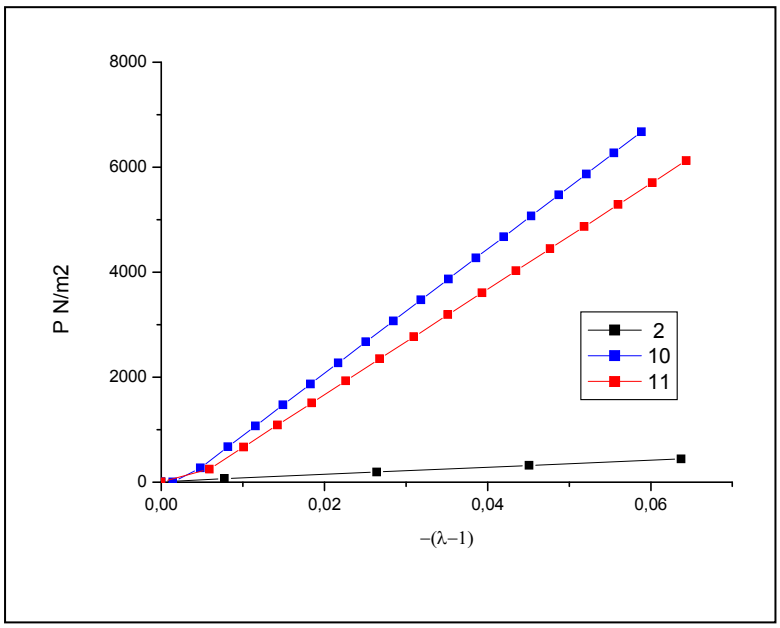

Figure A. 13: Compression stress-strain curves (Pressure (Pa) vs. -(λ – 1)) for Samples 2, 10, 11 (T = 45˚C)

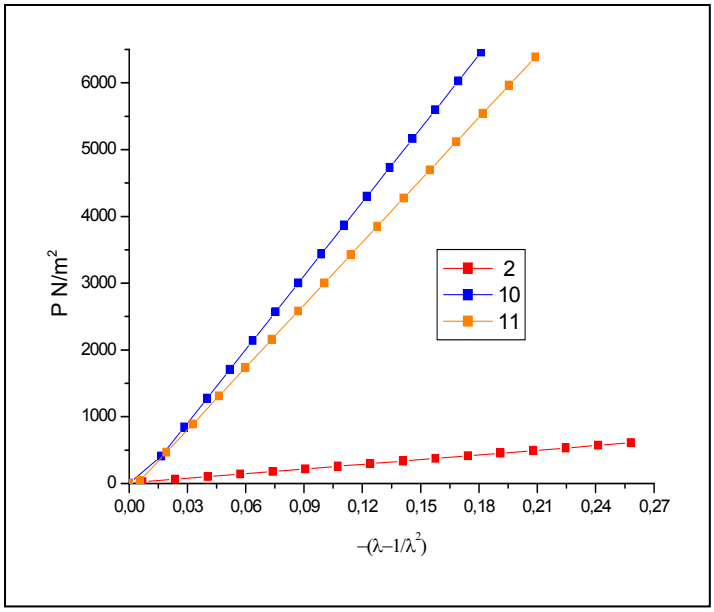

Figure A. 14: Compression stress-strain curves (Pressure (Pa) vs. -(λ – λ^{-2})) for Samples 2, 10, 11 (T = 45˚C)

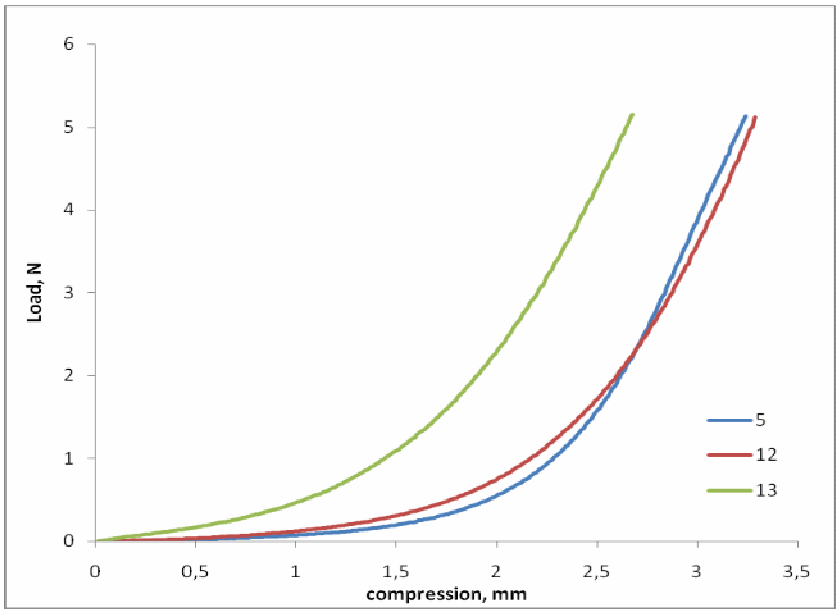

Figure A. 15: Measured force, F (N) as a function of compression (mm) for Samples 5, 12, 13 (T = 25˚C)

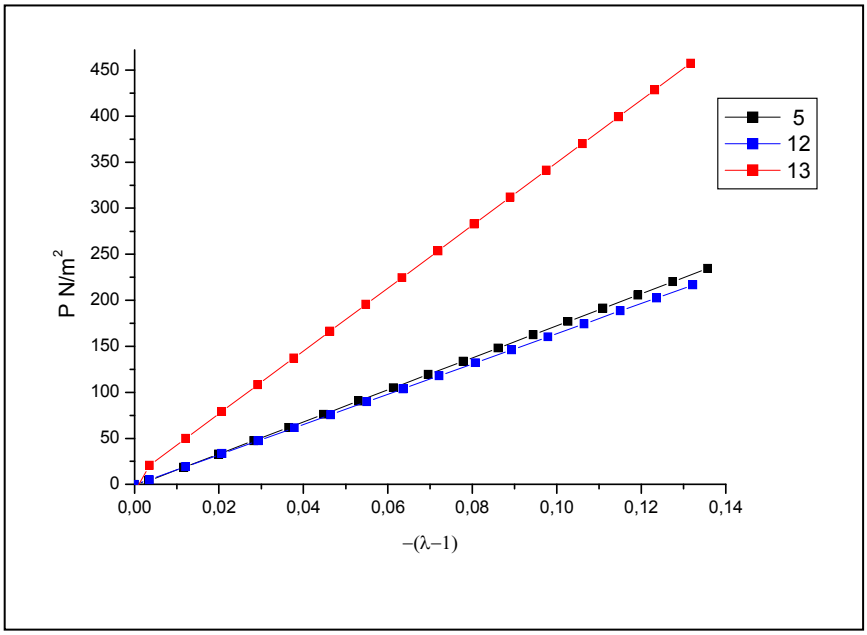

Figure A. 16: Compression stress-strain curves (Pressure (Pa) vs. -(λ – 1) for Samples 5, 12, 13 (T = 25˚C)

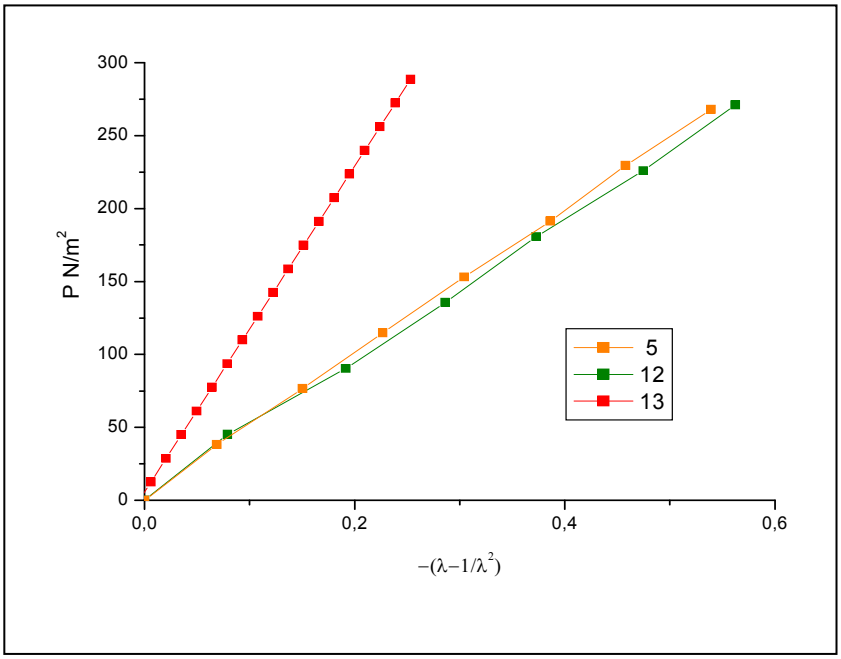

Figure A. 17: Compression stress-strain curves (Pressure (Pa) vs. $-(\lambda - \lambda^{-2})$) for Samples 5, 12, 13 (T = 25˚C)

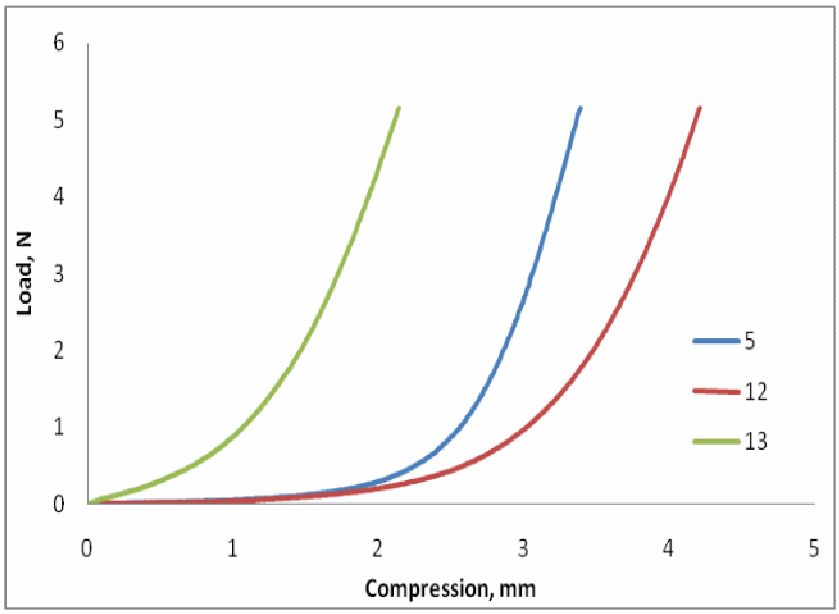

Figure A. 18: Measured force, F (N) as a function of compression (mm) for Samples 5, 12, 13 (T = 32˚C)

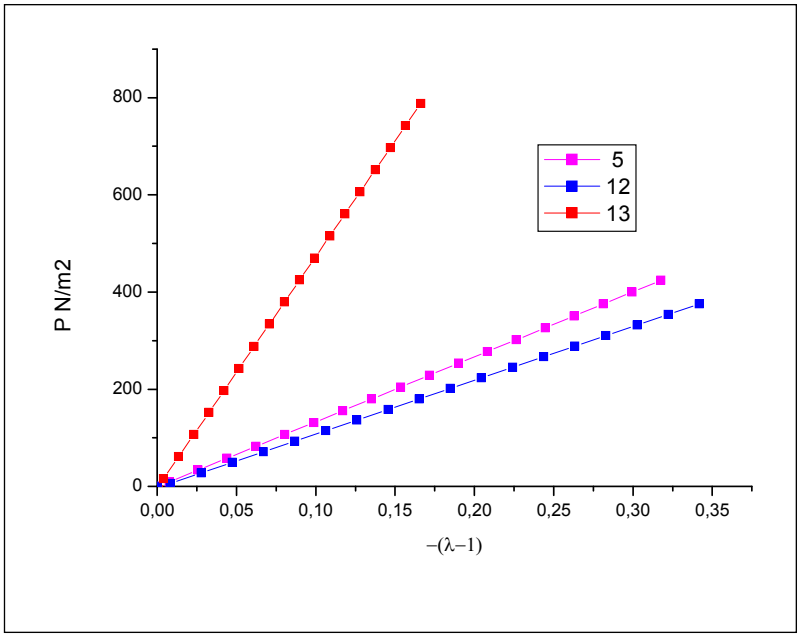

Figure A. 19: Compression stress-strain curves (Pressure (Pa) vs. -(λ – 1)) for Samples 5, 12, 13 (T = 32˚C)

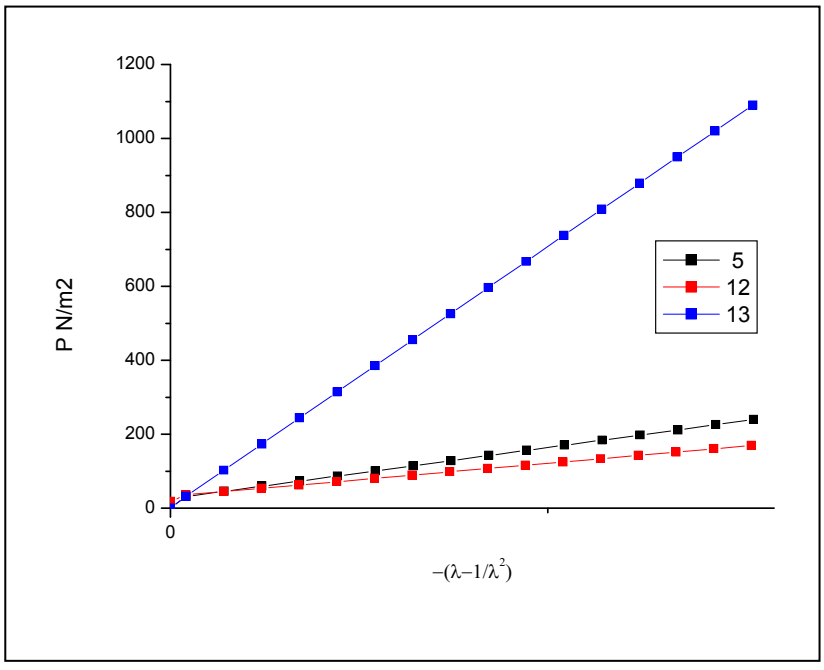

Figure A. 20: Compression stress-strain curves (Pressure (Pa) vs. -(λ – λ^{-2})) for Samples 5, 12, 13 (T = 32˚C)

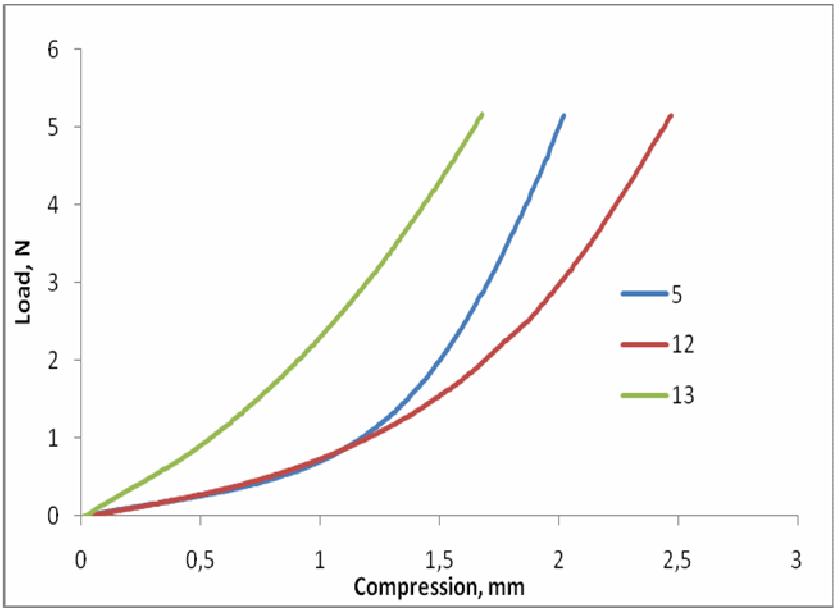

Figure A. 21: Measured force, F (N) as a function of compression (mm) for Samples 5, 12, 13 (T = 37˚C)

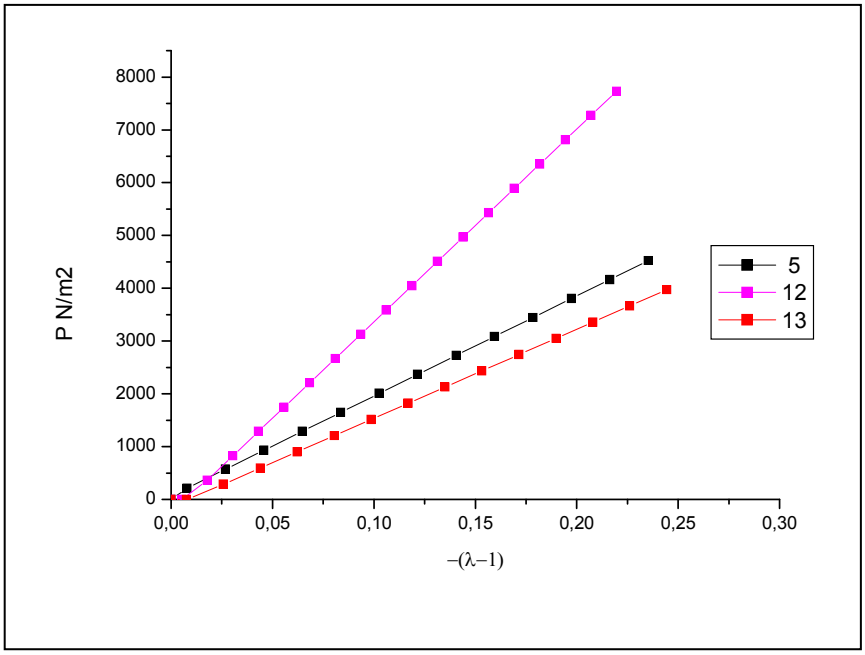

Figure A. 22: Compression stress-strain curves (Pressure (Pa) vs. -(λ – 1)) for Samples 5, 12, 13 (T = 37˚C)

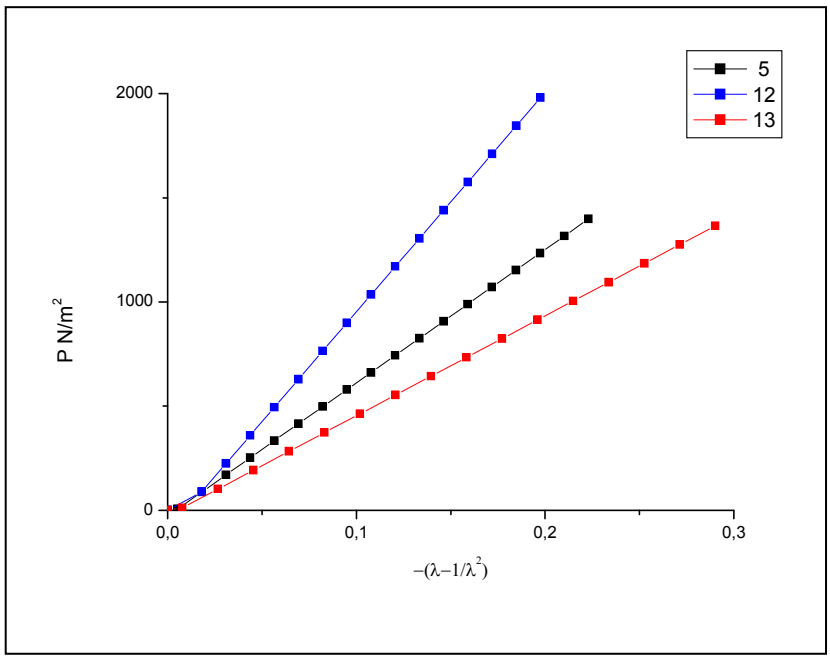

Figure A. 23: Compression stress-strain curves (Pressure (Pa) vs. $-(\lambda - \lambda^{-2})$) for Samples 5, 12, 13 (T = 37˚C)

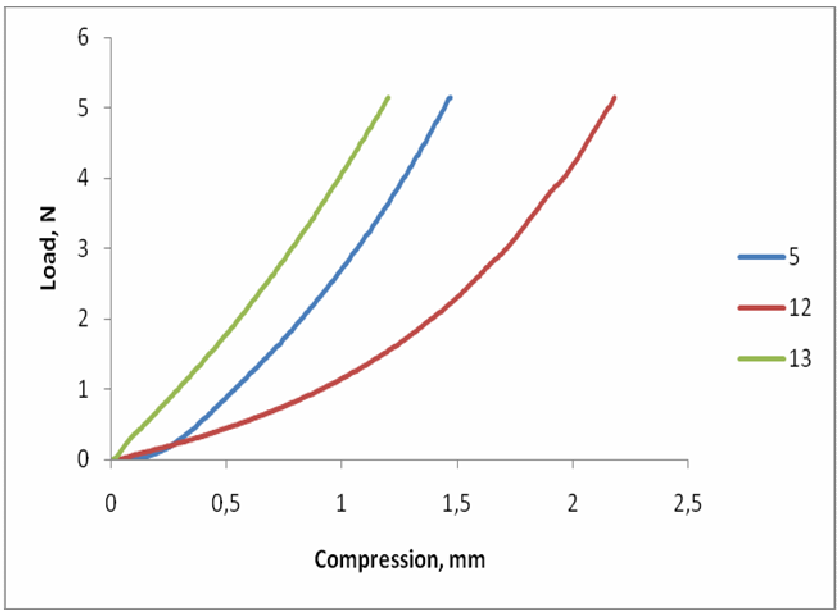

Figure A. 24: Measured force, F (N) as a function of compression (mm) for Samples 5, 12, 13 (T = 40˚C)

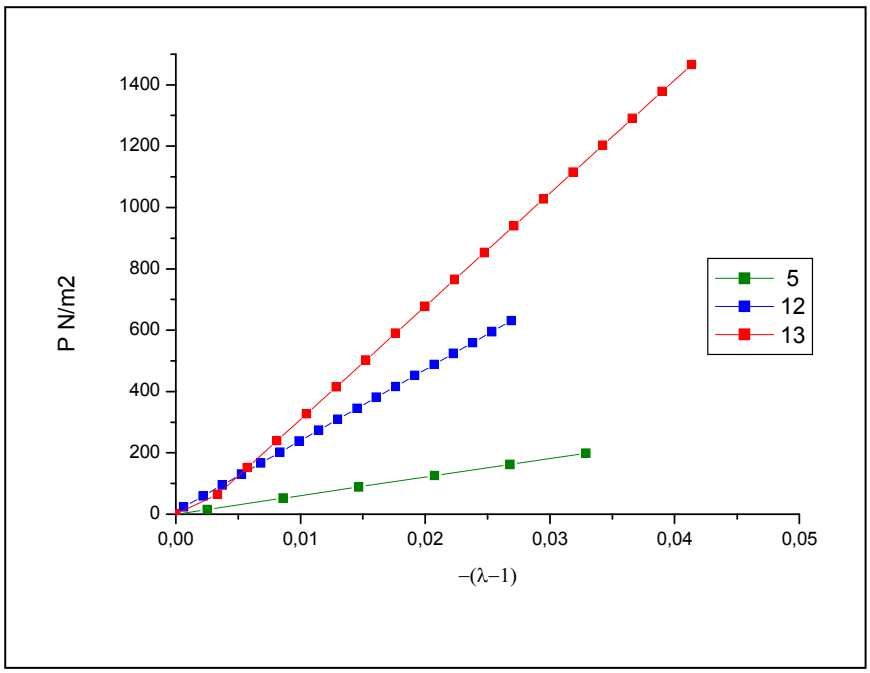

Figure A. 25: Compression stress-strain curves (Pressure (Pa) vs. -(λ – 1)) for Samples 5, 12, 13 (T = 40˚C)

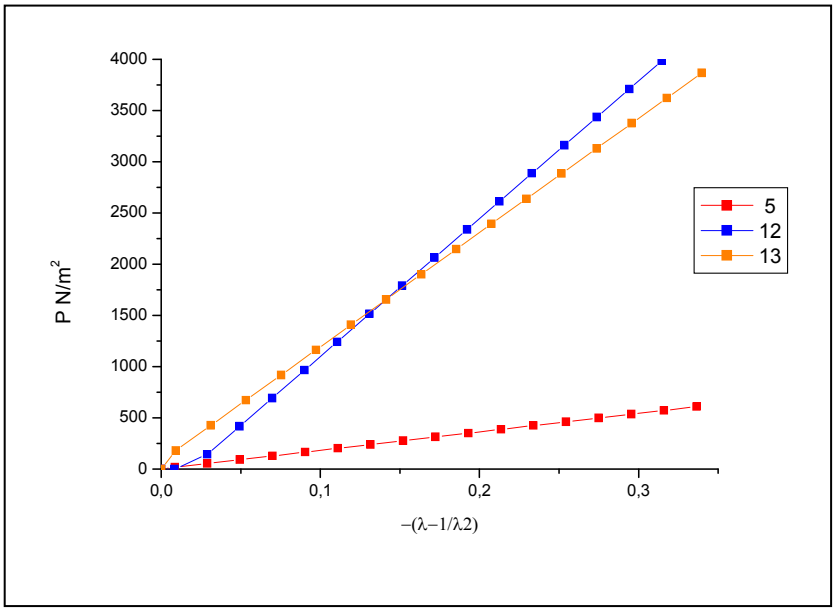

Figure A. 26: Compression stress-strain curves (Pressure (Pa) vs. -(λ – λ^{-2})) for Samples 5, 12, 13 (T = 40˚C)

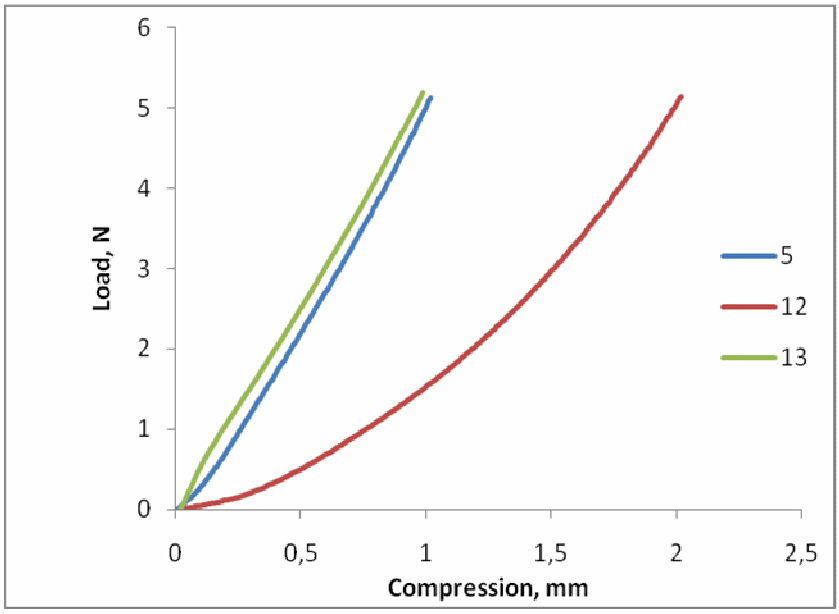

Figure A. 27: Measured force, F (N) as a function of compression (mm) for Samples 5, 12, 13 (T = 45˚C)

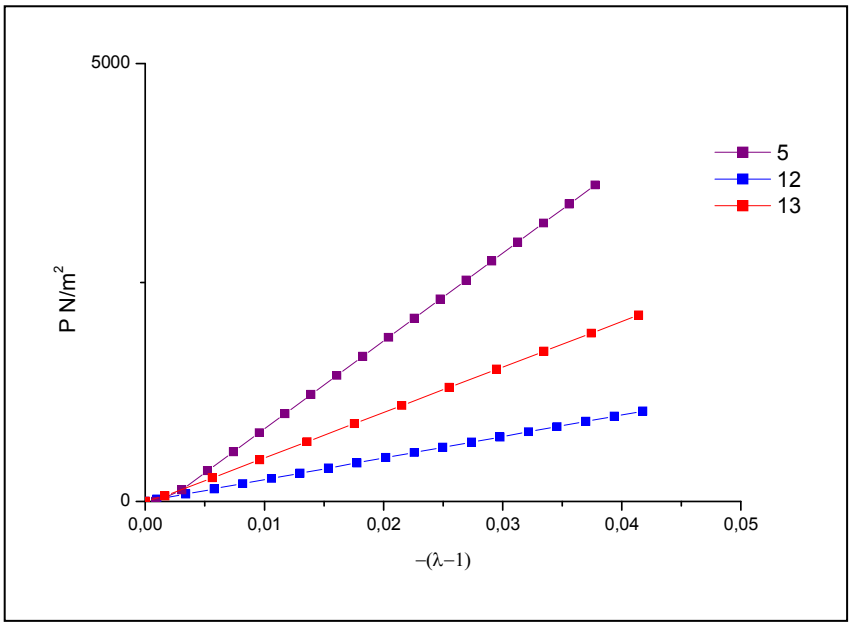

Figure A. 28: Compression stress-strain curves (Pressure (Pa) vs. -(λ – 1) for Samples 5, 12, 13 (T = 45˚C)

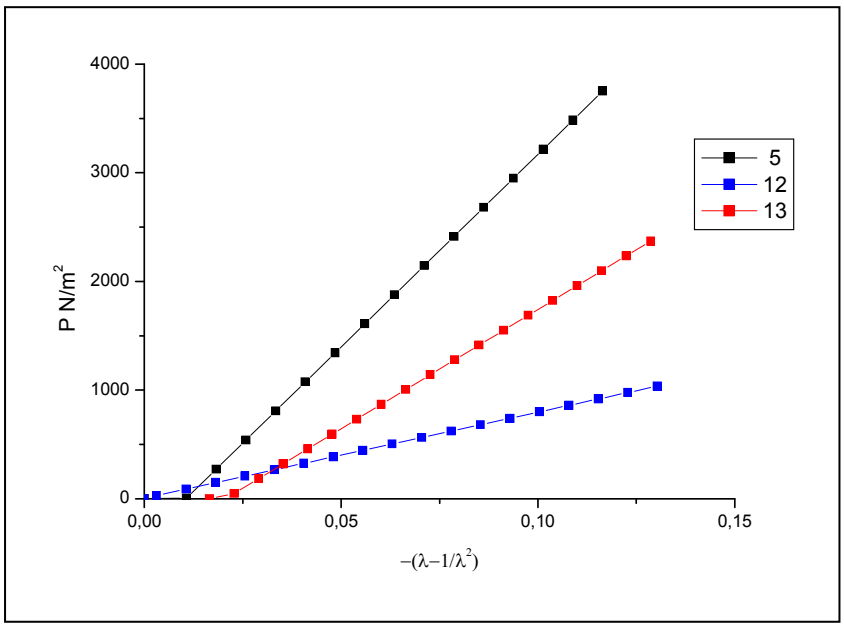

Figure A. 29: Compression stress-strain curves (Pressure (Pa) vs. $-(\lambda - \lambda^{-2})$) for Samples 5, 12, 13 (T = 45˚C)

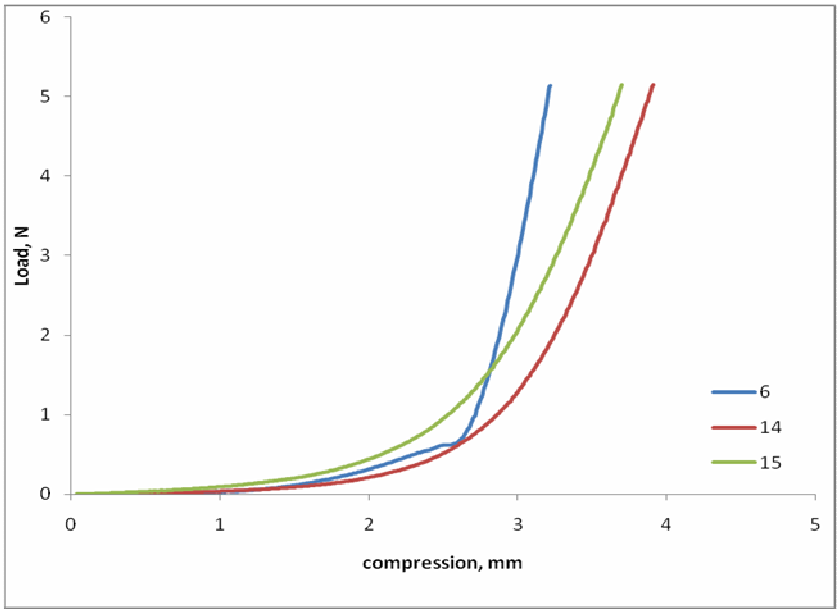

Figure A. 30: Measured force, F (N) as a function of compression (mm) for Samples 6, 14, 15 (T = 25˚C)

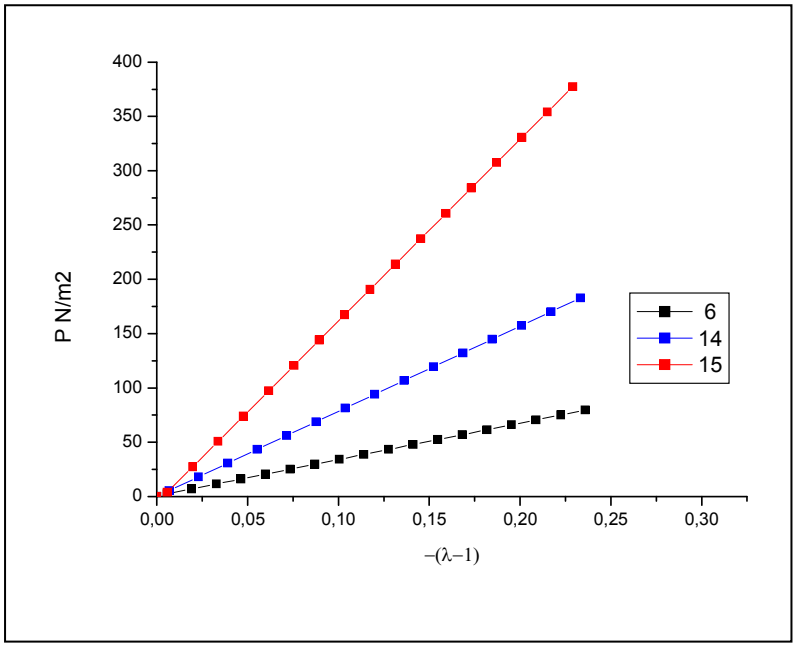

Figure A. 31: Compression stress-strain curves (Pressure (Pa) vs. -(λ – 1)) for Samples 6, 14, 15 (T = 25˚C)

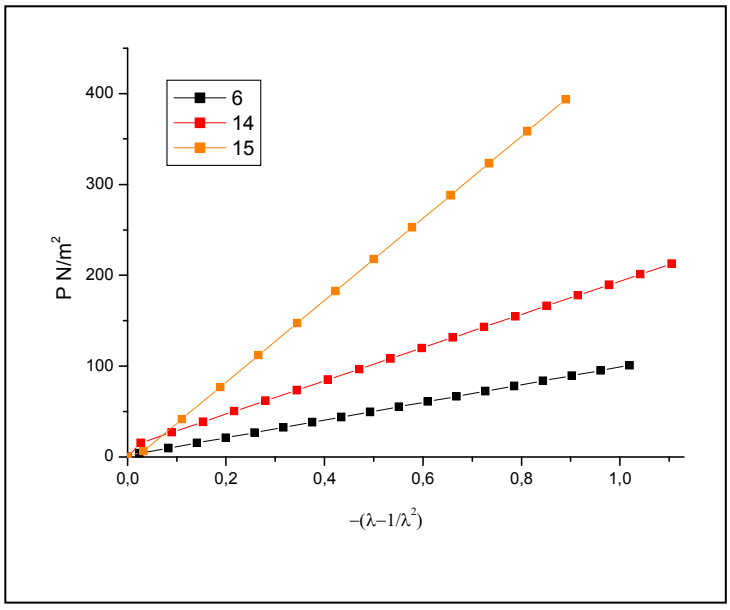

Figure A. 32: Compression stress-strain curves (Pressure (Pa) vs. -(λ – λ^{-2})) for Samples 6, 14, 15 (T = 25˚C)

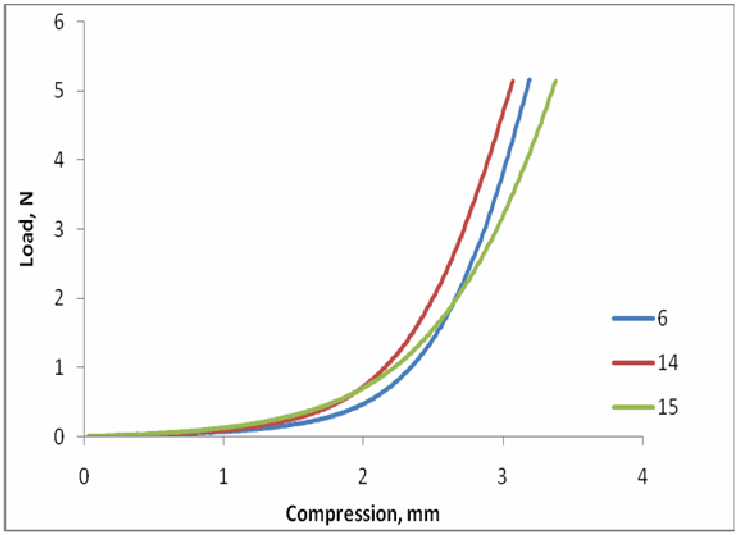

Figure A. 33: Measured force, F (N) as a function of compression (mm) for Samples 6, 14, 15 (T = 32˚C)

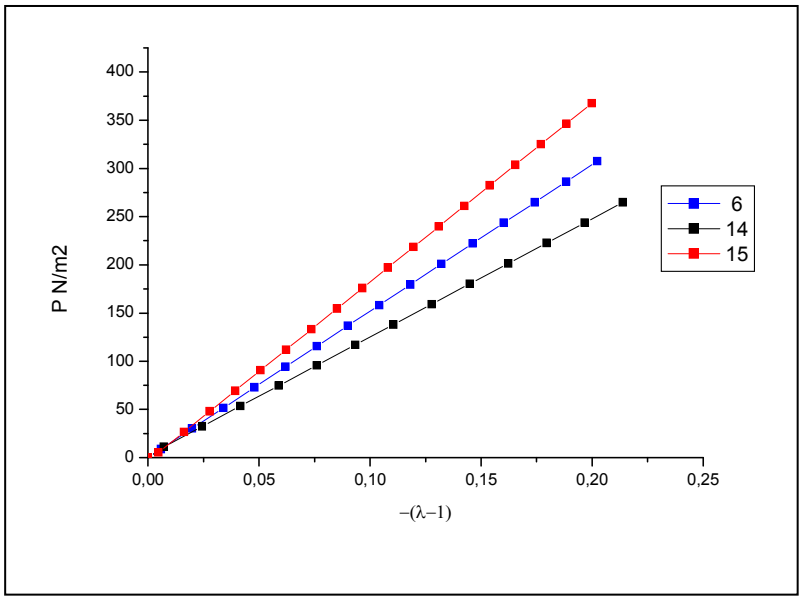

Figure A. 34: Compression stress-strain curves (Pressure (Pa) vs. -(λ – 1)) for Samples 6, 14, 15 (T = 32˚C)

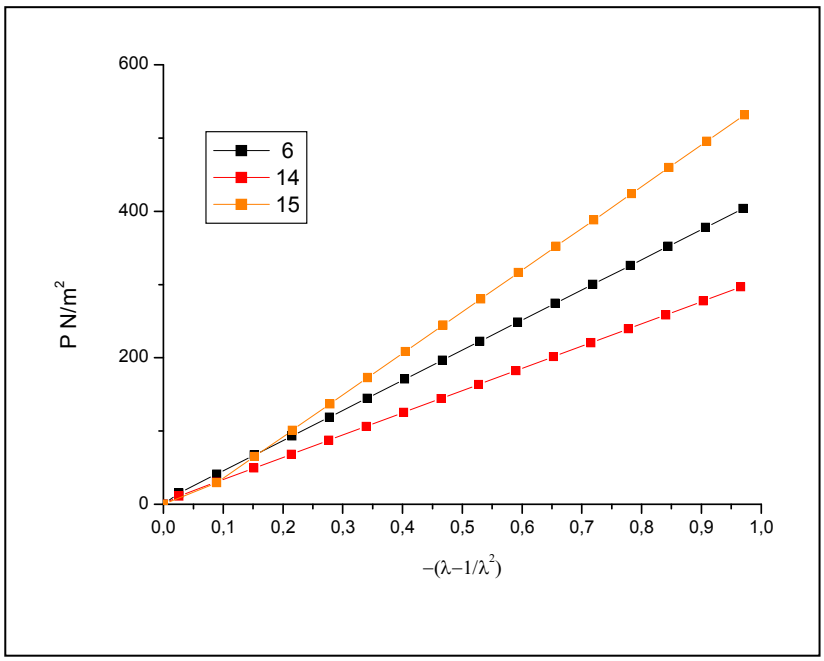

Figure A. 35: Compression stress-strain curves (Pressure (Pa) vs. $-(\lambda - \lambda^{-2})$) for Samples 6, 14, 15 (T = 32˚C)

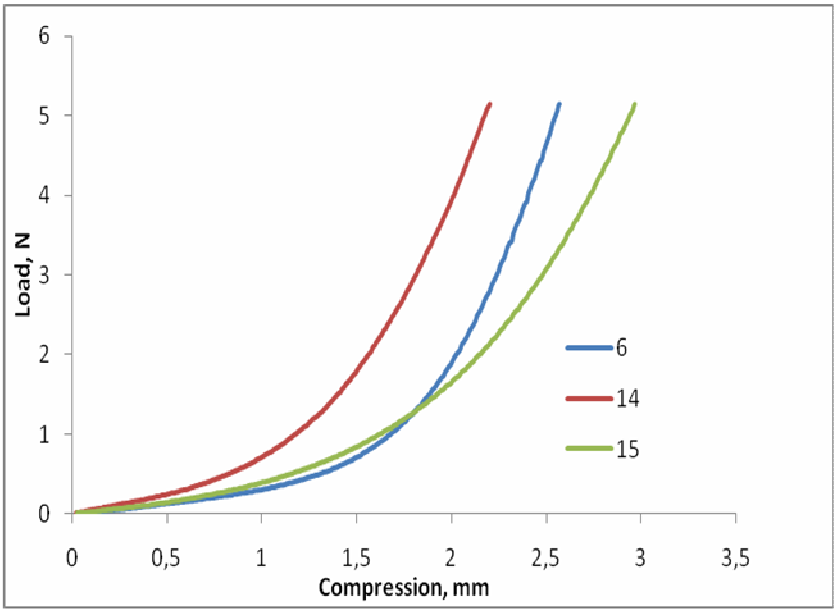

Figure A. 36: Measured force, F (N) as a function of compression (mm) for Samples 6, 14, 15 (T = 37˚C)

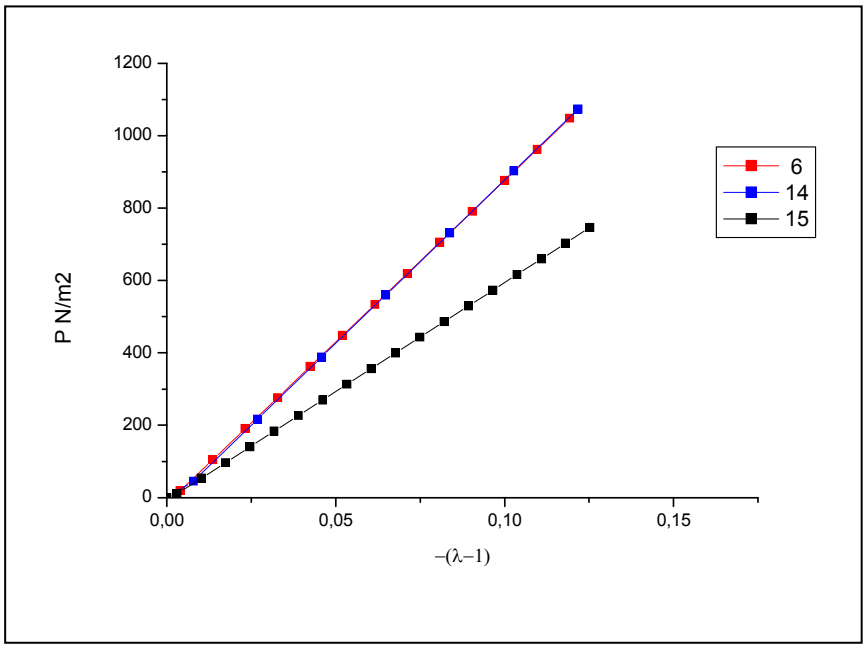

Figure A. 37: Compression stress-strain curves (Pressure (Pa) vs. -(λ – 1)) for Samples 6, 14, 15 (T = 37˚C)

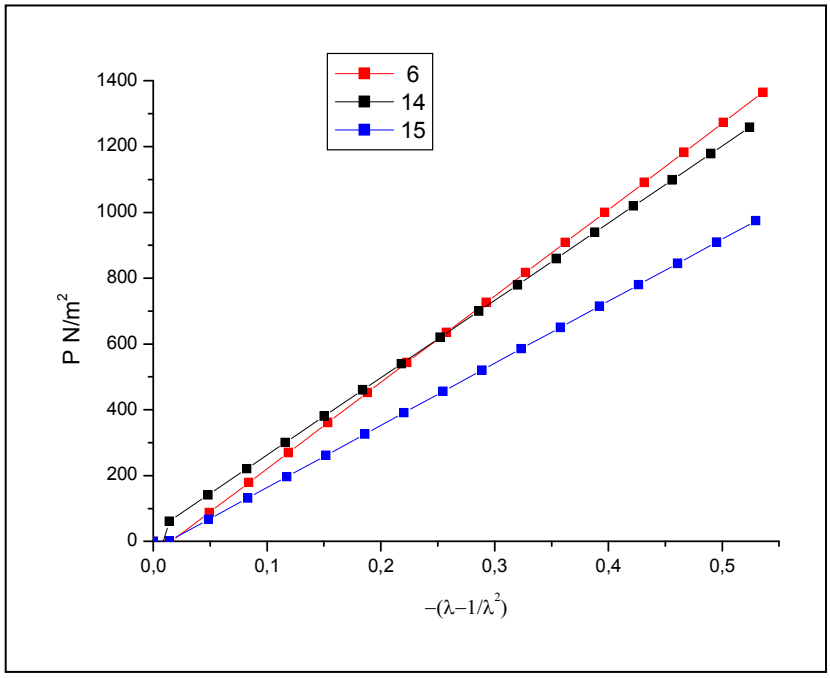

Figure A. 38: Compression stress-strain curves (Pressure (Pa) vs. -(λ – λ^{-2})) for Samples 6, 14, 15 (T = 37˚C)

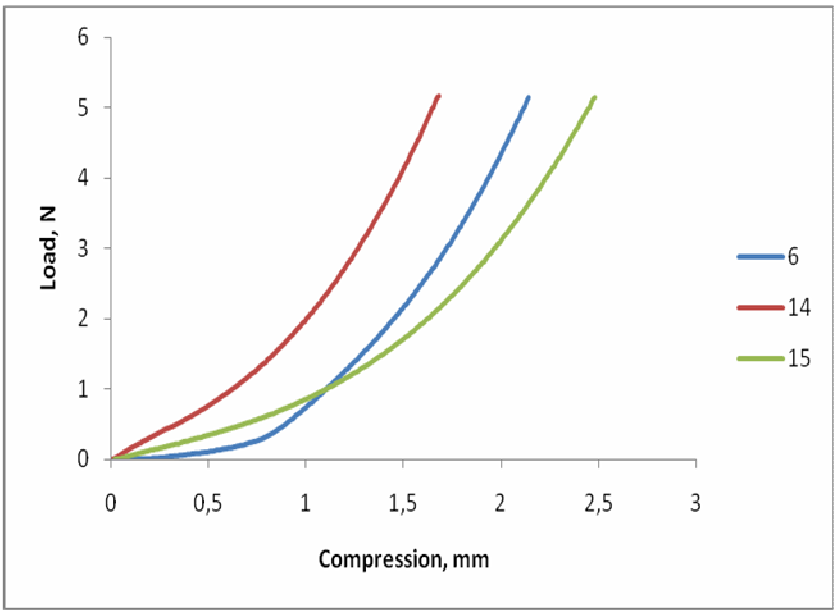

Figure A. 39: Measured force, F (N) as a function of compression (mm) for Samples 6, 14, 15 (T = 40˚C)

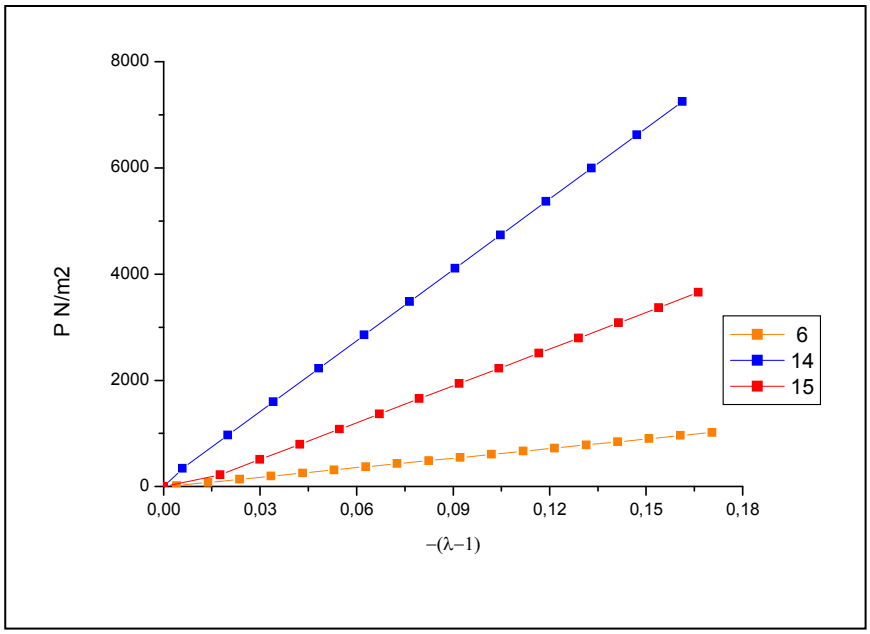

Figure A. 40: Compression stress-strain curves (Pressure (Pa) vs. -(λ – 1)) for Samples 6, 14, 15 (T = 40˚C)

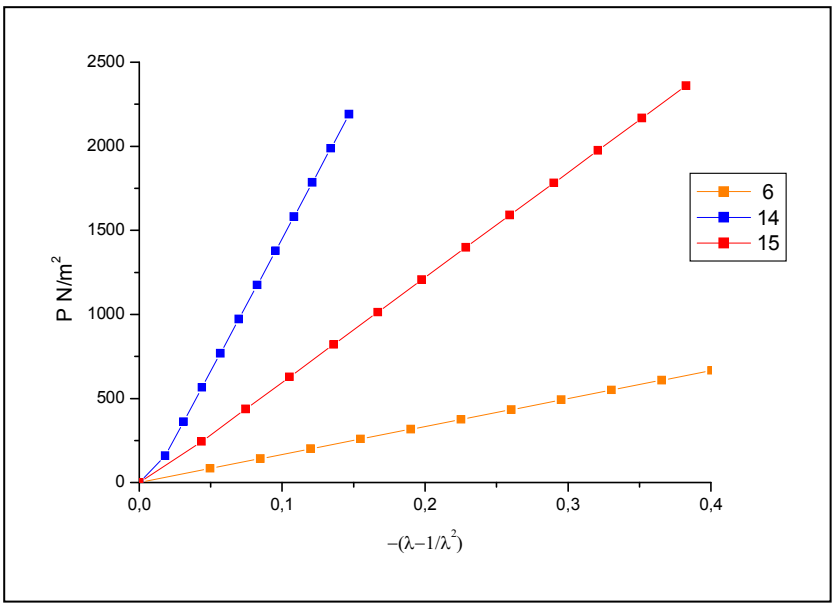

Figure A. 41: Compression stress-strain curves (Pressure (Pa) vs. $-(\lambda - \lambda^{-2})$) for Samples 6, 14, 15 (T = 40˚C)

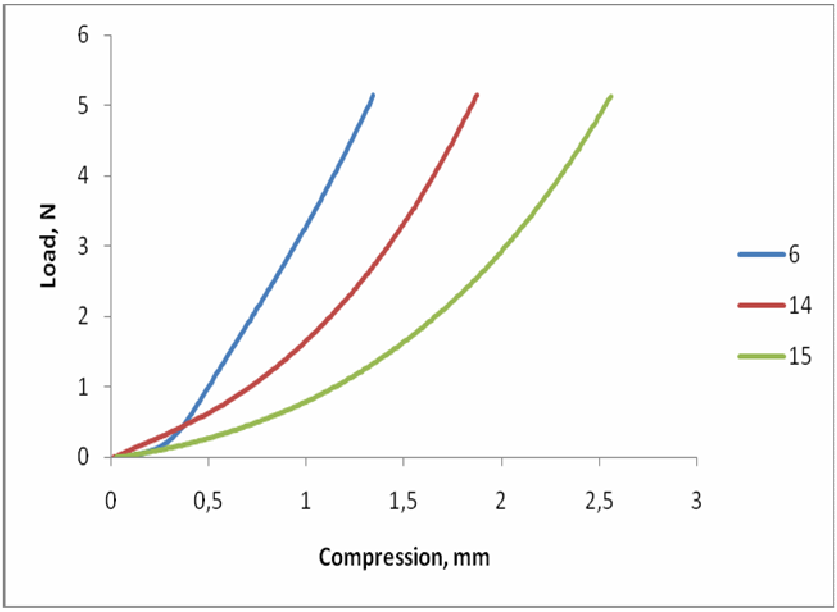

Figure A. 42: Measured force, F (N) as a function of compression (mm) for Samples 6, 14, 15 (T = 45˚C)

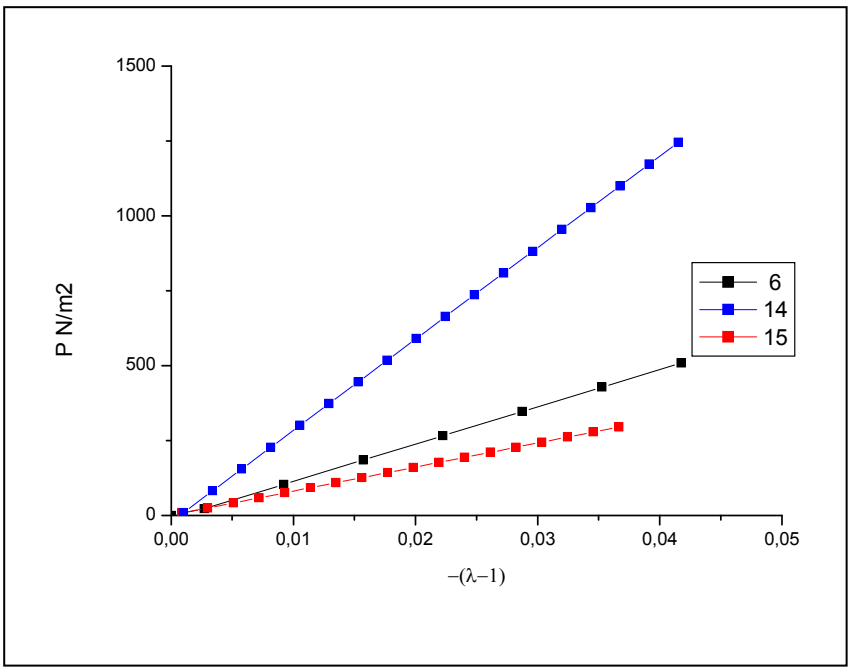

Figure A. 43: Compression stress-strain curves (Pressure (Pa) vs. -(λ – 1)) (for Samples 6, 14, 15 (T = 45˚C)

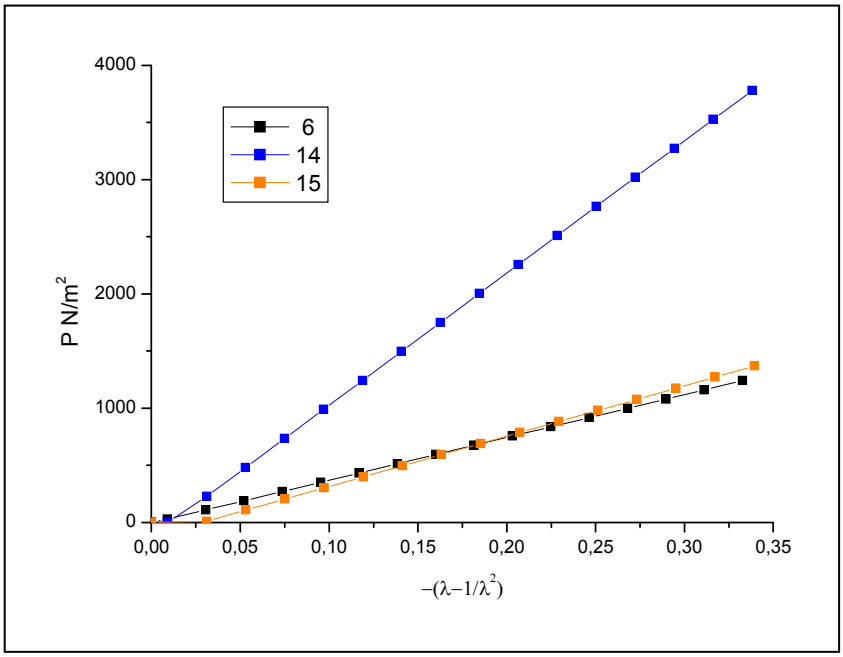

Figure A. 44: Compression stress-strain curves (Pressure (Pa) vs. -(λ – λ^{-2})) for Samples 6, 14, 15 (T = 45˚C)

CURRICULUM VITAE

I was born in Edirne in 11.01.1982. I graduated from Edirne Anatolian High School and Chemistry Department of İstanbul University. I attended the symposium and the scientific course given below;

- **D. Topuz, A. T. Gökçeören, B. F. Şenkal and C. Erbil**, "Effects of Accelerator Type on the Network Parameters and Swelling Properties of Poly(N-isopropylacrylamide) /Montmorillonite Nanocomposite Hydrogels", PAT2007, 24–28 October 2007, Shangai-China.

- Institut d' Etudes Scientifiques de Cargèse, "morphogenesis through the interplay of nonlinear chemical instabilities and elastic active media", 2-14 July 2007, Corsica-France